Nanofiltration of Brewery Wastewater for Agricultural Reuse

MSc Thesis

Julia van Witzenburg

TU Delft

Nanofiltration of Brewery Wastewater for Agricultural Reuse

MSc Thesis

Julia van Witzenburg
6063632

Supervisory Team:

Dr. Ir. Begüm Tanis	TU Delft (Supervisor)	Assessment Committee
Dr. Ir. Ralph Lindeboom	TU Delft (Supervisor)	
Toon van den Heuvel	Waterschap De Dommel (Advisor)	
Michiel Roest	The Biomakerij (Advisor)	

Project Duration:	February 2025 – November 2025
Faculty:	Department of Water Management, Faculty of Civil Engineering and Geosciences, Delft University of Technology (TU Delft)

Acknowledgements

I would like to express my sincere gratitude to my supervisors, friends, and family for their invaluable support throughout this thesis project. This work would not have been possible without your guidance and encouragement.

First, my deepest thanks to my TU Delft supervisors, Begüm Tanis and Ralph Lindeboom, for their continuous guidance and constructive feedback. Their expertise and encouragement have been fundamental in shaping this research.

I am also grateful for the collaboration with TU Delft, Waterschap De Dommel, and the Biomakerij. Special thanks to Toon Heuvel from Waterschap De Dommel for offering valuable insights from a waterboard perspective, and to Michiel Roost for sharing his knowledge of the treatment system, assisting with sample collection, and facilitating connections with the Biomakerij and Koningshoeven Abbey. Your support was essential in the success of this thesis.

My sincere thanks also to NX Filtration for providing experimental materials and expert advice. As well as the TU Delft laboratory staff for providing the resources necessary to complete my experiments and collect samples.

To my friends and colleagues at TU Delft, thank you for your inspiring academic curiosity and drive. A special thanks to Guille, for always being there for me throughout this program, even if it meant traveling to Hengelo to pick up equipment.

To my friends around the world, I am forever grateful for your presence across the different chapters of my life. Though living in many places means being far from loved ones, I have learned that home is made by the people you return to, not the place itself. I am incredibly lucky to have so many homes to visit, call, and carry with me wherever I go.

To my van Witzenburg family, I am so grateful to have gotten to know you better these past two years in the Netherlands. I am especially grateful to Oma and Opa for always welcoming me into your home with kindness and delicious meals whenever I needed peaceful retrieve from university. To my Aunt and Grandma back in the U.S., thank you for your calls and letters, each one a reminder of your love and encouragement that always brightened my day.

Most of all, thank you to my Mom, Dad, Lucas, and Clementine, for your unwavering love and belief in me, even when I doubted myself. Lucas, thank you for the long calls and laughter, I am so fortunate to be your sister. To my parents, who have guided me through every step of life, served as inspiring role models, and raised me to be adventurous, driven, and compassionate in a world that often lacks kindness, I can never thank you enough.

Abstract

With global water scarcity and demand continuing to rise, alternative water sources are being explored for agricultural irrigation. The brewery industry, among the largest industrial water consumers, generates wastewater typically characterized by high biological oxygen demand (BOD) and chemical oxygen demand (COD) due to organic compounds, as well as total suspended solids (TSS) and nutrients such as phosphorous and nitrogen species. It can also have high sodium concentrations and microbial contaminants such as *E. coli* that serves as an indicator of fecal contamination. This thesis evaluates the application of nanofiltration (NF) as a tertiary treatment for brewery to assess its potential for agricultural reuse in accordance with Dutch and EU water reuse regulations, *Regulation 2020/741*.

The relevant reuse standards were first identified to establish target water quality limits. Then six brewery wastewater samples were collected at different time points to characterize influent variability. Physical, chemical and biological parameters were analyzed, including particle size distribution (PSD), TSS, ion concentrations, alkalinity, total organic carbon (TOC), and *E. coli* as an indicator pathogen of fecal contamination. The results found maximum particle sizes that could cause pore blocking of polymeric membrane fibers and particle load to be a risk for fouling propensity, leading to the investigation of sand filtration as a pretreatment. Comparison of the measured results to the reuse standards identified sodium, sulfate, nitrate, ammonium, and *E. coli* concentrations were found to exceed their respective thresholds, 120 mg/L, 100 mg/L, 10 mg/L, 1.5 mg/L and 10 CFU/ 100mL, confirming the need for tertiary treatment before being reused for irrigation.

Two nanofiltration membranes, a 0.9 nm ceramic Inopor membrane and a polymeric NX Filtration dNF80 membrane, were experimentally assessed. Experiments were performed at 2 and 4 bars, using both direct and sand filtered influents, including a prolonged fouling test, to evaluate permeability, flux stability, and removal efficiency.

The polymeric membrane achieved higher removal efficiencies of TOC (81% ± 3%) removal and 7 – 55% higher removal efficiency of multivalent ions (phosphate, sulfate, Ca^{2+} and Mg^{2+}). The ceramic membrane showed more consistent biological removal efficiencies, with all but one fouling test qualifying for class A reuse and 6 – 60% higher removal efficiency for most monovalent ions (Cl^-, NO^-_2, Br^-, NO_3^-, Na^+, NH^+_4, and K^-). During the fouling tests, the polymeric membrane recovered 93 - 96% of 5 L over four hours, while the ceramic membrane achieved 15 – 16% recovery of 2 L over 24 hours. The polymeric membrane showed higher fouling sensitivity, while the ceramic membrane had higher stability. Sand filtration pretreatment improved flux stability for both membranes, and higher pressure increased polymeric permeability but did not affect the ceramic membrane.

While the complexity of differences in membrane composition, material, and geometry prevented definitive identification of individual exclusion mechanisms, the findings provide valuable insight into how these factors collectively influence nanofiltration performance. Overall, NF effectively bridges the gap between brewery wastewater and agricultural reuse regulations. The polymeric membrane offers higher organic and multivalent ion removal and higher flux but greater fouling propensity. Whereas the ceramic membrane has a higher resistance to fouling and lower but stable flux. Sodium, nitrate, and ammonium, remain the key limitations for reuse.

1 Contents

List of figures

List of Tables

List of Abbreviations

AD	Anaerobic Digestion
AVG	Average
BOD	Biological Oxygen Demand
CA	Citric Acid cleaning
CFU	Colony-forming Unit
CFV	Cross-flow Velocity
CLF	Cake Layer Formation
COD	Chemical Oxygen Demand
CPB	Complete Pore Blocking
CW	Constructed Wetland
DAF	Dissolved Air Flotation
DOM	Dissolved Organic Matter
EC	Electrical Conductivity
ED	Electrodialysis
Flush	Forward Flush
GAC	Granular Activated Carbon
GS	Gas Separation
HRAP	High Rate Algal Pond
IC	Ion Chromatography
LRV	Log Removal Value
Max	Maximum Value
MBR	Membrane Bioreactor
MD	Membrane Distillation
MF	Microfiltration
Min	Minimum Value
MNR	Metabolic Network Reactor
MWCO	Molecular Weight Cut-off
NF	Nanofiltration
NOM	Nonorganic Micropollutants
NTU	Nephelometric Turbidity Unit
PAC	Powdered Activated Carbon
PEI	Polyetherimide
PEM	Proton Exchange Membrane
Perm	Permeability after treatment
PES	Polyethersulfone
PFP	Primary Facultative Pond
PSD	Particle Size Distribution
PV	Pervaporation
PVDF	Polyvinylidene
RIVM	Rijksinstituut voor Volksgezondheid en Milieu
RO	Reverse Osmosis
S	Settled Samples

SA_m	Membrane Surface Area
SF	Sand Filtration
SPB	Standard Pore Blocking
SVI	Sludge Volume Index
TMP	Transmembrane Pressure
TN	Total Nitrogen
TOC	Total Organic Carbon
TSS	Total Suspended Solids
UF	Ultrafiltration
US	Unsettled Samples

1 Introduction

1.1 Relevance

As the impact of climate change intensifies globally, a key consequence is increasing water scarcity. This fear is even prevalent in countries such as the Netherlands, where a shortage of fresh water seemed unimaginable a few years ago (van Leerdam et al., 2023). To combat the extreme droughts that impact many countries during the summer months, limited water consumption and increasing circularity must be further considered to ensure water demands are still met. The agricultural industry is the world's largest freshwater consumer, consuming 70% of the world's freshwater supply (Ritchie et al., 2018). This agricultural industry includes grains such as barley that are grown to produce beer.

The beer brewing industry is constantly growing, producing 188 billion liters of beer worldwide in 2023 [3]. The process of brewing beer consumes a large amount of water with the main consumption processes being the cleaning, bottling, and fermentation stages. For every one liter of beer, three to ten liters of wastewater are produced [4].

In addition to the beer brewing industry consuming large volumes of fresh water, the significant amount of wastewater also poses an environmental threat. Brewery wastewater has very high concentrations of organic matter and nutrients, that could have harmful environmental impacts if not discarded and treated properly [5]. The high organic matter levels create high biological and chemical oxygen demands within the water, thus resulting in oxygen depletion within the aquatic ecosystems that the wastewater is disposed of in. Additional environmental risks are due to the high nutrient levels increasing plant growth leading to eutrophication [6–8].

As such, the pursuit of water reuse and sustainable management within breweries represents both an environmental necessity and an opportunity for innovation.

1.2 Wastewater Source Introduction

The wastewater used for this thesis is sourced from a Trappist Monk brewery that recognizes the large environmental footprint from the brewery industry and hopes to reduce its impact and aim for water circularity. In collaboration with Waterschap De Dommel an on-site wastewater treatment plant named 'the Biomakerij' was installed in 2018.

The Biomakerij has a maximum capacity of 438 m^3/day and occupies 847 m^2 on the property [9]. However, the typical daily capacity of the plant is roughly 143 m^3/day seven days a week. The treatment plant currently consists of a Metabolic Network Reactor (MNR) reactor, phosphate precipitation, dissolved air flotation (DAF), microfiltration and a belt press [10].

The treatment plant functions by utilizing the roots of the plants and netting in the tanks coated with microbial biofilm to treat the wastewater [4]. Currently the treatment plant's effluent does not meet legal reuse standards.

With reuse standards not met, the filtrate is sent to the Tilburg wastewater treatment plant, with a disposal fee per cubic meter discarded. This practice is a waste of resources by disposing of water that has already undergone partial treatment. Incorporating an additional tertiary treatment to the existing treatment system will create sufficient effluent water quality for reuse and reduce the demand on freshwater sources.

1.3 Water Reuse Introduction

Many tertiary wastewater treatment methods are currently being explored for the reclamation and reuse of brewery wastewater, including zeolites, activated carbon, multi-media filters, and membranes [11]. For the Biomakerij, membrane-based treatment is the most suitable option due to its ability to produce high quality permeate, small spatial footprint, and relatively low operating costs [12,13].

Within membranes there is a large variety of treatment options firstly differentiated by their driving mechanisms. This thesis will focus on pressure-driven membranes [14]. Pressure-driven membrane technologies are classified into four categories differentiated by their pore size, microfiltration (MF), ultrafiltration (UF), nanofiltration (NF), and reverse osmosis (RO), gas separation (GS), Pervaporation [14]. Microfiltration has the largest pore size range and reverse osmosis has the smallest pore sizes impacting what particles are filtered out of the permeate. Smaller pore sizes have a higher contaminant removal efficiency, in turn an increased risk of clogged necessitating a pretreatment. Further explanation of membrane properties and behavior can be seen in Membrane Technologies in the following literature review [14].

Producing potable water from wastewater often requires reverse osmosis to meet all drinking water quality requirements [15–17]. Typically, ultrafiltration is used as a pretreatment method for reverse osmosis, this additional step increases energy consumption and reduces permeate recovery, thus increasing the costs [14,15,18]. Direct nanofiltration is a cost-effective alternative that still produces a permeate with sufficient water quality for many reuse purposes [14,15,18–22]. For these reasons, the experimental research conducted during this thesis will focus on assessing the performance of multiple nanofiltration membranes on treating brewery wastewater.

In 2021 the Biomakerij partnered with Semilla IPStar bv. and Waterschap de Dommel on a pilot study implementing nanofiltration on-site as a tertiary treatment step. While the treatment method proved successful in achieving the desired water quality, large particles in the feed quickly clogged the membrane rendering prolonged usage infeasible. This limitation led to the conclusion that direct nanofiltration was not a sustainable long-term tertiary treatment method, and future research was ended.

Since the initial pilot, both nanofiltration technology and the on-site biological treatment have improved. To further mitigate the risk of immediate clogging a detailed water quality analysis will be conducted, and minimal pretreatment methods will be investigated. These technological improvements, water quality precautions combined with successful permeate water quality results from the past pilot are the foundation of the present study. The research will explore impacts of various nanofiltration membranes and membrane properties, to determine the feasibility of implementing the design for a prolonged duration.

1.4 Objective

The goal of this thesis is to test multiple membranes on pre-treated brewery wastewater to determine which membrane and membrane properties are most effective and determine if and how the reclaimed water can be reused. This will be done by answering the following research question.

Research Question:

To what extent could the application of nanofiltration as a tertiary treatment improve the potential of treated brewery wastewater for agricultural reuse?

Sub-questions:

1. What is the current gap between the key water quality performance indicators of brewery wastewater and agricultural reuse requirements, and what removal efficiencies are required to bridge this gap?
2. What influence do nanofiltration membrane properties (material, pore size, etc.) have on the most relevant water quality parameters?
3. How do ceramic and polymeric nanofiltration membranes differ in their treatment performance and suitability for brewery wastewater reuse?
4. Which membrane characteristics enable the treated water to meet the reuse water quality standards?

1.5 Definitions

Prior to beginning this report some critical words must be defined:

Brewery Wastewater – In this thesis the term "brewery wastewater" refers to the influent water samples used for experimentation and the water treated on-site at the Biomakerij. The term "wastewater" is used as opposed to "process water" because the influent originates from a variety of industrial and domestic sources, not exclusively from the brewery. The "brewery wastewater" consists mostly of brewery process water, but also includes effluents from a bakery, chocolate and cheese production, industrial cleaning, and two infrequently used toilets. Given this diverse composition, but brewery process water as the majority contributor, the influent will be referred to as "brewery wastewater" throughout the thesis.

Tertiary Treatment – The proposed water treatment method will be referred to as a "tertiary treatment" rather than a "polishing step". This is due to the scale of the proposed treatment being larger than a traditional polishing step.

Capacity – This refers to the volume of water treated.

Recovery – This is in reference to the volume of permeate produced relative to the feed volume.

Removal Efficiency – This is the difference between feed concentrations compared to permeate concentrations in percentage.

Shedding – This term refers to the loss of biofilm along the roots and netting in the MNR tank.

Sloughing – This is one of the biofilm detachment mechanisms, indicating the loss of particulate matter from fouling along a membrane surface due to fluid shear force.

Biofilm Detachment – This is the detachment of biofilm as a result of erosion or sloughing

Water matrix - refers to an aqueous solution composed of water and any other particles, ions, etc. within the solution.

Direct Filtration – The experiments used the influent without any sand filtration pretreatment.

E. coli – A biological contaminant used as an indicator of fecal matter contamination in wastewater.

1.6 Research Approach

This report approaches the research question and sub-questions in four sections following the introduction. Section two reviews relevant literature to provide context for hypothesizing experimental results, identifying tertiary treatment methods, brewery wastewater characteristics, water reuse regulations and the wastewater source used in this study. Section three describes the experimental methodology designed to attain results to the research questions, including influent samples, membrane selection, experimental setups, analytical methods, and the preliminary Modelling system. Section four presents the results, detailing preliminary water quality analyses, brewery treatment experiments regarding flux, chemical, and biological outcomes, a comparison of membrane results, and the pretreatment method results. The final section concludes with answers to the research question and sub-questions, followed by recommendations for further research, general membrane reuse applications, and site-specific considerations.

2 Theoretical Background and Literature Review

2.1 Wastewater Reuse Methods Considered

As the threat of a global water shortage continues to grow and water quality regulations are becoming increasingly stringent, scientists and researchers are trying to find ways to best remove pollutants from water. These methods can be used on both fresh and reclaimed water, however for the purpose of this study the wastewater applications will be focused on. All methods discussed both in this section and the following pretreatment section can be used as tertiary treatment methods and within water treatment chains.

2.2 Membrane Technologies

A membrane is defined as "a barrier to separate two phases and able to restrict the transport of various components in a selective manner" [14]. There are many different qualities and characteristics that can be used to classify membranes ranging from separation driving forces, material, geometry, pore size, etc. The first characteristic to be discussed is the membrane's driving force. This is the phenomenon in which the membrane is able to separate into two phases, and these range from pressure-driven, concentration-gradient-driven, temperature-driven, and electrical-potential-driven. Table 2.1 below shows the different driving mechanisms and examples of how they are implemented.

Table 2.1 Membrane Driving Forces

Driving force	Driving force theory	Implementation examples
Pressure-driven	Difference in pressure in the system allows the permeate to pass through the membrane [15].	Reverse osmosis (RO), nanofiltration (NF), ultrafiltration (UF), microfiltration (MF), gas separation (GS). Pervaporation (PV) requires partial pressure.
Concentration-Gradient-Driven	The solution allows the permeate to pass through the membrane from a high concentration to a low concentration [23].	Dialyses

Temperature-Driven	A hydrophobic membrane separates two different solutions at different temperatures creating a difference in vapor pressure allowing molecules to pass through the membrane from a higher vapor pressure to a lower vapor pressure [24].	Membrane distillation (MD)
Electrical-Potential-Driven	The membranes separates two solutions of different charges creating a difference in electrical potential that allows ions to pass through the membrane [25].	Electrodialysis (ED)

Summary of the fundamental membrane transport driving forces, their underlying physical principles, and common implementation examples in separation processes.

2.2.1 Pressure-driven Membranes

This thesis will only focus on pressure-driven membranes due to their efficacy on removing a large variety of micropollutants and their ease of implementation. Within the pressure-driven membranes gas separation was not considered due to the feed being a liquid rather than a gas and pervaporation was not proposed as a result of its high cost and short lifespan of the membrane [26,27].

The four main types of pressure-driven membrane technologies considered were microfiltration (MF), ultrafiltration (UF), nanofiltration (NF), and reverse osmosis (RO), each distinguished by progressively smaller pore sizes [25]. There are also alternative types of membranes that are driven by temperature and concentrations; however, this study will only explore pressure-driven membranes. Figure 2.1 shows the pore size ranges of each type of membrane. For this thesis, nanofiltration was selected as it provides a balance between cost and energy efficiency, all while still producing a reusable permeate.

Membrane operations are based on how the feed water passes through the membrane. There are two membrane operation modes, cross-flow and dead-end, which can be seen in . Dead-end filtration directs the feed perpendicularly to the membrane surface, allowing all feedwater to pass through the membrane, with all solids and contaminants larger than the pore size retained on the membrane surface. These retained solids create a cake layer over time and increase the resistance to the membrane and lead to faster membrane fouling.

This method simplifies the treatment process and is mostly used for feeds with low solid content, for laboratory, and medical filtration [12,15].

In cross-flow filtration the feed flows tangentially across the membrane, visualized in Figure 2.2. Allowing a portion of the feedwater to pass through the membrane, called the permeate, while the remaining feedwater continues to flow parallel to the surface taking away the particles larger than the pore size. This slows down the buildup of the cake layer, helps maintain a more stable flux over time, and reduces membrane fouling compared to dead-end filtration [14,18,20,28]. In some industrial systems the concentrate is partially recirculated to increase overall water recovery, although this can also increase the concentration of retained solutes thus the potential for fouling and need for more frequent and intense cleaning [15,18,20]. Due to cross-flow filtrations ability to handle higher feed loads and operate for longer period, it is often used in large-scale nanofiltration and reverse osmosis [15].

For laboratory testing, cross-flow filtration was selected to reduce the volume of wastewater needed to be transported to campus for testing. However, if the membrane system were to be installed on-site, the membrane operation would be dead-end as the permeate is redirected to reuse and the concentrate disposed of. This will impact on the longevity of the membrane, and additional cleaning will be needed as opposed to the lab tests.

Nanofiltration is increasing in popularity for industrial wastewater to achieve water reuse for industrial purposes because of its ability to retain multivalent ions and contaminants similar to RO but also allow the partial permeation of monovalent ions [29]. Allowing this partial permeation the osmotic pressure of the membrane is lowered resulting in a lower pressure gradient, thus requiring less energy than RO [15,29–31]. This lower pressure gradient also produces higher fluxes than that of RO due to the slightly more rigidity of the membrane coupled with the lower pressure gradient. These characteristics result in lower operating costs and maintenance costs than seen by RO while simultaneously producing a larger volume of permeate [12,41].

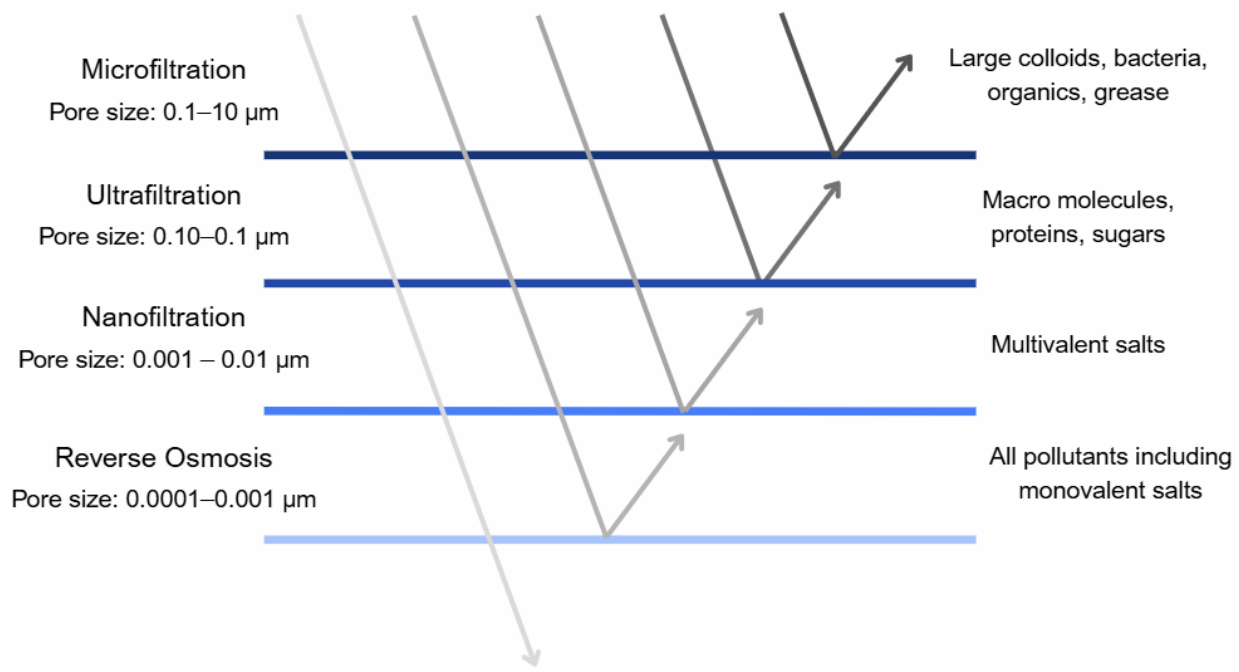

Figure 2.1 Pressure-Driven Membrane Pore Size Range Categories

Schematic representation of relative pore size ranges and contaminant removal targets of MF, UF, NF, and RO membranes. Adapted from [11,14,32].

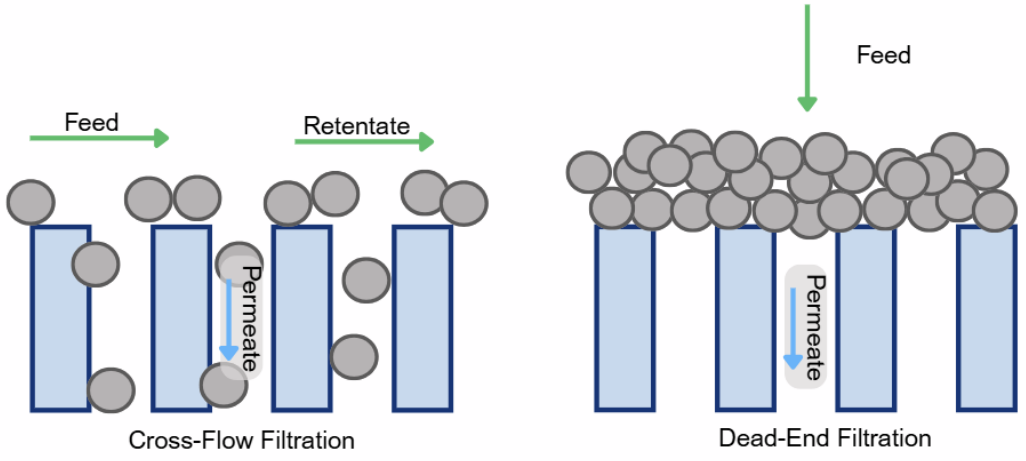

Figure 2.2 Cross-Flow and Dead-end Filtration Schematic

Schematic showing the difference between cross-flow filtration, where feed moves tangentially across the membrane reducing fouling. Dead-end filtration, feed flows perpendicular to the membrane surface resulting in rapid cake layer formation. [14,15,20]

2.2.2 Materials and Properties of Nanofiltration

As previously mentioned, nanofiltration has a pore size range of 0.001 – 0.01 µm and a molecular weight cut-off (MWCO) between 200 to 1000 Da [32]. Nanofiltration membranes are available in many different geometries, including hollowfiber, spiral wound, plate-frame and tubular (Figure 2.3) [33].

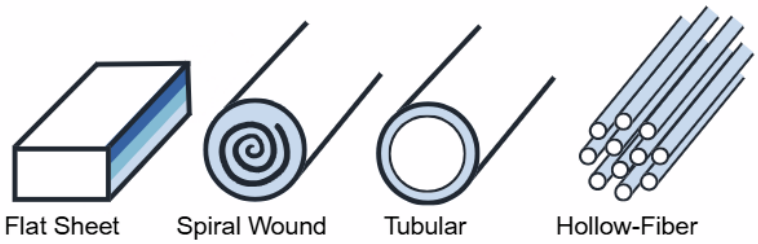

Figure 2.3 Nanofiltration Geometries Schematic

Schematic representation of common nanofiltration membrane geometries, including flat sheet, spiral wound, tubular, and hollow fiber. Adapted from [34].

An ideal membrane maximizes surface area in a compact structure, minimize resistance to tangential flow to reduce energy consumption, maintain a uniform velocity distribution, generate turbulence at the concentrate discharge to limit fouling, be easily cleaned and maintained, and remain low cost [15,20,31,35]. Table 2.2 below summarizes the differing performance characteristics of each of the nanofiltration geometries [33].

For this thesis, two membrane geometries were selected: hollow fiber and tubular. The hollow fiber membrane was selected for its lower pressure requirements, thus reducing energy consumption [18,20,36]. The tubular membrane was chosen for its low membrane fouling propensity and ease of cleaning, minimizing the on-site maintenance [18,20].

Table 2.2 Membrane Characteristics

Characteristics	Spiral wound	Hollow fiber	Tubular	Plate and frame
Packing density [m^2/m^3]	800	6000	70	500
Required feed flow [m^3/m^2-s]	0.25-0.50	~0.005	1.0-5.0	0.25-0.50

Feed pressure [psi]	43-85	1.4-4.3	28-43	43-85
Membrane fouling Propensity	High	High	Low	Moderate
Ease of cleaning	Poor to good	Poor	Excellent	Good
Feed stream filtration requires	10-25µm filtration	5-10 µm filtration	Not required	10-25µm filtration

Summary of key characteristics of common nanofiltration membrane geometries, including typical packing density, feed flow requirements, operating pressure, fouling propensity, and ease of cleaning. [33]

Nanofiltration membranes are typically made from polymeric materials such as polyethersulfone (PES) with proton exchange membrane (PEM) coatings, polyetherimide (PEI), or polyvinylidene fluoride (PVDF) [37]. More recently, ceramic membranes have been developed for nanofiltration. Ceramic membranes have proven to be successful in the past with ultra and microfiltration [38]. Typically, faster fouling and more irreversible fouling is seen on polymeric membranes as opposed to ceramic membranes [39]. Ceramic membranes are more stable and reliable and better for intermittent treatment. However, ceramic membranes show a greater variation in ion rejection based on the membrane surface charge and produce less permeate [40]. A large portion of ion rejection rates are dependent on the ion composition within the feed water; this study will compare both polymeric and ceramic membranes experimentally.

Additional variations between membranes include coatings, membrane operation, operation mode, surface area, MWCO, ion retention rates, and surface charge. The hypothesized answer to sub question two is, the MWCO will greatly influence the removal of removal of high BOD, COD, TSS, *E. coli*, and some nutrients and ion concentrations that the existing treatment system does not remove.

Currently, The Biomakerij is unable to remove the BOD, COD, TSS, *E. coli*, and some ion concentrations from the wastewater in order to attain agricultural reuse quality. Nanofiltration will remove BOD, COD, TSS, *E. coli*, and some of the concerning ions in order to reach reuse water quality [8,11,12,24,41].

The membrane coatings and surface charge will be most impactful in removing the remaining contaminants that have a smaller particle size that fit through the membrane pores. Coatings can influence hydrophilicity, improve performance, reduce fouling, and enhance durability [42]. The membrane operation as previously mentioned refers to cross-flow and dead-end filtration relative to the flow path of the concentrate and feed stream. Operation mode is the direction of the feed flow relative to the membrane surface, those options are inside out or outside in, referring to the direction at which the feed flow passes through the membrane. For inside out the influent flow through the bore, and the permeate is sent to the outside of the shell [14,18,20,43]. While outside in the influent is sent from the shell and the permeate is inside the bore or lumen for hollow fiber [14,18,20,43].

The surface area of a membrane is directly correlated with the volume of permeate produced, the larger the surface area the more permeate is made. The molecular weight cut-off (MWCO) is the "molecular weight of the organic tracer that is 90% retained by the membrane, determined by drawing the organic tracer retention as a function of the tracer molecular weight" [44]. The retention rates are influenced by a myriad of factors including salt concentration, fixed membrane charge, membrane coating, co-ion valence, and the counter-ion valence [45]. Lastly, the fixed surface charge, influenced by the material and coating, impact the Donnan exclusion. Donnan exclusion is how the ion interactions and equilibrium behave with the charged membrane surface [29,46].

2.2.2.1 Membrane Fouling

Membrane fouling is one of the main drawbacks of membrane treatment that are inevitable. As particles and contaminants are removed from the permeate as the feed passes through the membrane the removed particles are deposited in and on the membrane surface. There is reversible and irreversible fouling. For reversible fouling the deposited particles can easily be removed from the membrane surface, reducing the system pressure, by back washing, or chemical cleaning [15,17,47,48]. Irreversible fouling occurs over time as the membrane is used and cleaning results in a decrease in flux over time [49]. The mechanisms which cause irreversible fouling are chemisorption and pore plugging, which is the chemical bond forming between a particle and the membrane surface and the physical bonding of particles blocking pores [49]. Irreversible fouling increases the chemical cleaning agent and energy consumption, reduces the membrane lifespan, and lowers the production of permeate [50,51].

Membrane fouling is dependent on many things within the system, from the membrane characteristics (geometry, surface charge, pore size, material hydrophilicity), the feed influent (the water matrix, pH, concentration of contaminants), and the operating conditions (temperature, cross-flow velocity, and transmembrane pressure) [15,17,50]. Fouling can be

reduced by pretreating the feed and adapting the operating conditions and membrane surface to be optimized for the influent water [15]. Fouling can be removed through physical cleaning or chemical cleaning. Physical cleaning includes backwash, forward flush, or using electrical methods, however backwash cannot be used for RO and NF. Chemical cleaning methods require the use of chemical cleaning agents to aid in the removal of foulants. Typically, the chemical agent used is intended to target a specific type of fouling occurring [52].

There are four types of membrane fouling, particulate fouling, organic and inorganic fouling, scaling, and biofouling, [16]. Particulate fouling or colloidal is the deposition of suspended solids, colloids, and other particles on the membrane resulting in the creation of a cake layer [15,53]. Organic/ inorganic fouling is the result of dissolved organic matter, often times natural organic matter (NOM), which has chemical components that result in them being difficult to degrade and ultimately adhere to the membrane surface, which is greatly impacted by the membrane surface charge [15,53]. Scaling is the formation of an impermeable layer on the surface of the membrane from precipitation of insoluble minerals in a supersaturated solution [15]. Biofouling is a result of bacteria and microorganisms adhering to the membrane surface resulting in growth of the organisms as they metabolize the nutrients in the feed water [15,53–56]. An additional membrane surface behavior that can occur as a result of biofouling is detachment. Detachment is when biofilm disconnects from the membrane surface as a result of two mechanisms, either particle size erosion or sloughing [57]. Particle size erosion causes small sized particles to detach as a result of particles in the influent eroding the particles and biofilm on the membrane surface [57]. Sloughing is the detachment of larger pieces of biofilm and the cake layer detaching due to fluid shear force [54–59]. Both of these mechanisms limit the biofilm growth and creates steady-state fouling resistance [54–59].

While these four categories describe the types of foulants and their general behavior, Hermia's model provides a theoretical framework for understanding the mechanisms by which fouling occurs. The model identifies four main fouling mechanisms: A. complete pore blocking (CPB), B. intermediate pore blocking (PPB), C. cake layer formation (CLF), and D. standard pore blocking (SPB), and [15,50,52,53]. Hermia's model is the most commonly accepted list of fouling mechanisms; however, it assumes that all pores are symmetrical and parallel, all foulants are uniform spheres, and the total filter resistance is constant [52]. The fouling mechanisms can be seen in Figure 2.4. Complete pore blocking is when a particle completely blocks and plugs a pore forming only one layer on the membrane surface pore [15,52,53]. Intermediate pore blocking is similar to complete pore blocking, but the particles can be deposited on top of previously accumulated particles. Cake filtration is the result of multiple layers of foulants covering the membrane surface, increasing the

membrane resistance as the cake layer thickness increases pore [15,52,53]. Lastly, standard pore blocking is a result of foulants only being within the pores and not on the surface, decreasing the diameter of the pore [15,52,53].

While Hermia's model discusses the fouling mechanisms in terms of impact on the membrane surface with its influence on the pores, fouling mechanisms can also occur at the membrane inlet. For membrane geometries with relatively smaller inlet inner diameters compared to the particle influent volume, resulting in the plugging of entire fibers of the membrane and can lead to a cake layer forming at the influent inlet. For hollow fiber membranes this type of fouling is referred to as fiber-inlet plugging, where particles block the influent from entering the lumen, which is the inside of the fiber [14,18]. This blockage can result in an increase in system pressure and decrease the flux [14,18]. Similar to CPB and CLF, fiber-inlet plugging can be reduced be prefiltering the influent [18].

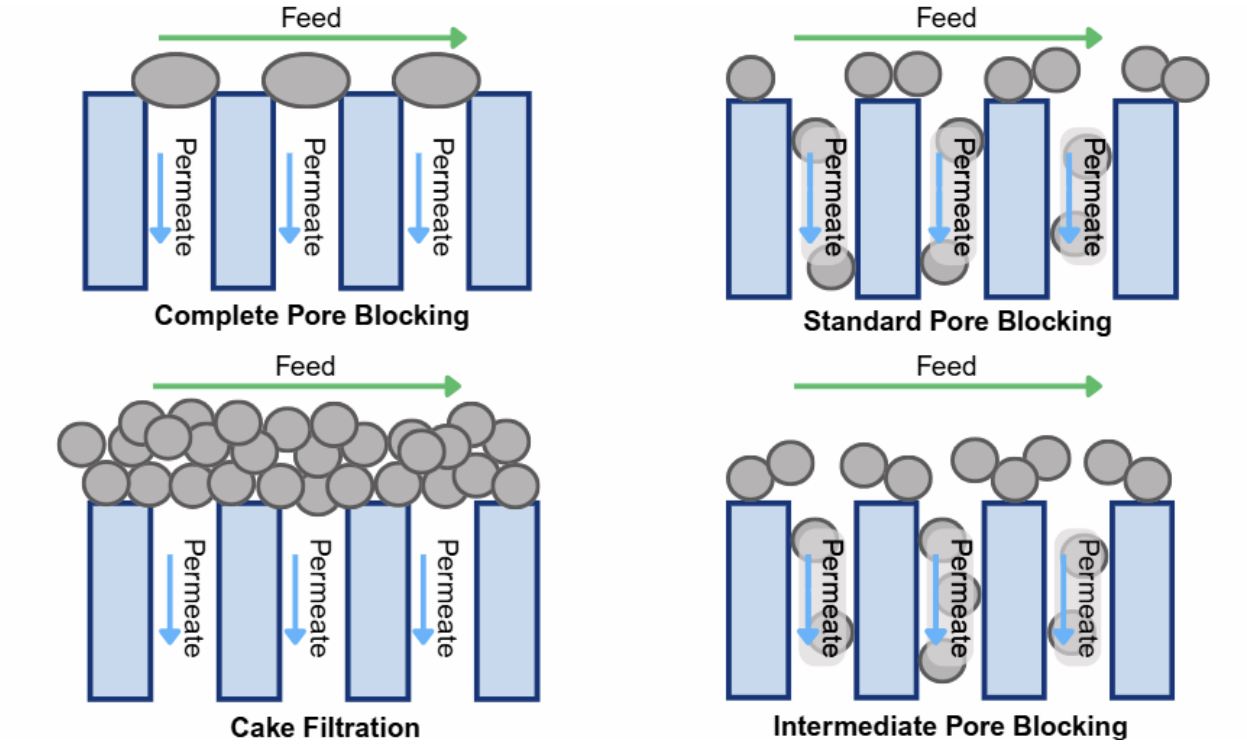

Figure 2.4 Simplified Diagram of Fouling Mechanisms [52]

Schematic representation of the four different types of fouling mechanisms from Hermia's model, CPB, SPB, IPB, and CF. the arrows indicate feed and permeate flow, the blue rectangles are the membrane walls, and the grey particles represent the accumulation and behavior of foulants associated with each mechanism [18,52].

2.2.2.2 Nanofiltration Exclusion Mechanisms

Nanofiltration exclusion mechanisms can be influenced by many aspects of the membrane system including the micropollutant and membrane parameters, operation parameters, and feed water quality characteristics or water matrix.

The micropollutant and membrane parameters that make up nanofiltration exclusion mechanisms are, steric hindrance, electrostatic interaction (Donnan exclusion), and dielectric exclusion. The steric hinderance is the range of particle sizes within the feed water, which are influenced by the membrane molecular weight cut-off and pore size and distribution. If the molecule is larger than the pore size then it is rejected, and the smaller particles more likely remain in the permeate [29]. Electrostatic interactions is influenced by the membrane charge or zeta-potential and is impacted by the pKa of the micropollutants. The ions in the solution and polarization charges on the surface of the membrane are repelled [29,30]. Within electrostatic interactions is the previously mentioned Donnan exclusion mechanism which allows ions of opposite charge to that of the surface will be retained by the membrane or same charge will be repelled. Dielectric exclusion is from the

interaction between ions with bound electric charged induced by ions at membrane interfaces with different dielectric constants [60]. Hydrophilic interactions are a part of dielectric interactions impacted by the hydrophilicity of the membrane and the log K_{ow} and dipole moments of the micropollutants [30].

The mechanisms listed above are based on the water matrix of the feed and the characteristics of the membrane. The water matrix refers to a solution of water and any other particles, ions, etc. within the solution [61]. These mechanism interactions within the system can be changed if there are any changes in the feed pH, DOM content, or ionic strength of the water. At a lower pH the membrane surface typically maintains a negative charge for Donnan exclusion, while at a higher alkaline pH the membrane surface is positive [29,52,53]. Similarly with high influent DOM content coupled with high pH the negatively charged DOM will more likely be retained by the positively charge membrane surface [25,29].

In addition to the physical mechanisms occurring between the feed pollutants and membrane surface, there are many operational parameters in the system that can influence how these mechanisms behave. These operational changes can be the cross-flow velocity, impacting the time for these mechanisms to occur, and the system pressure impacting the pressure gradient [25].

In summary, membrane technology provides a modular and controllable means of separating dissolved and suspended contaminants in industrial wastewaters. The choice of membrane type is strongly influenced by feedwater composition, target contaminants, and operational objectives. This indicates that for the Biomakerij wastewater, a membrane with moderate molecular weight cut-off (MWCO) may balance the ion retention and permeate flux, enabling effective removal of organics and multivalent ions without excessive energy demand or fouling propensity. Although monovalent ions such as sodium and chloride have low nanofiltration removal efficiencies, this partial passage can partial passage can be advantageous for maintaining osmotic balance and reducing concentrate salinity.

This conclusion is further supported by the compositional analysis of brewery wastewater discussed in Section 2.4, where the specific characteristics of brewery wastewater justify the use of nanofiltration with moderate selectivity and high material robustness.

2.3 Other Wastewater Reuse Technologies

2.3.1 Zeolites

Zeolites, crystalline porous materials composed of aluminosilicates, function as molecular sieves and are ideal for ion exchange and adsorption (Figure 2.5) [62]. Zeolites are used for wastewater treatment to adsorb inorganic and organic pollutants in the water that can be

harmful for humans and nature if not treated properly. This treatment process can be used when the wastewater is intended for reuse and also when discharging into external bodies of water. When the zeolites are added to the wastewater and removed, the contaminants remain adhered to the zeolite's surface, thus removing them from the wastewater [16].

The use of zeolite treatment as a tertiary treatment for brewery wastewater was applied in a project in Xanthi Greece. The project found that zeolites in addition to constructed wetlands achieved effective ion and ammonium removal [64]. At the Biomakerij, however, the existing biological treatment plant already targets phosphate and many of the ions removed by zeolites. The required tertiary treatment must focus on disinfection and solids removal in a side stream system to allow for reuse. Zeolites could still be considered as an additional treatment step for monovalent ion-exchange if potable water were desired.

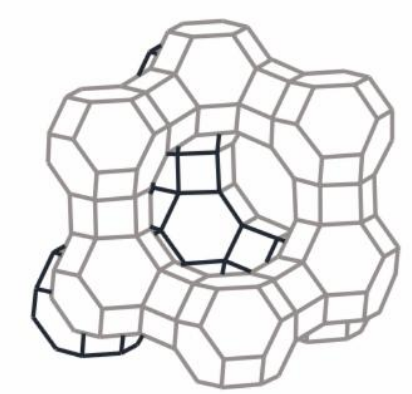

Figure 2.5 Zeolite Structure Schematic

Schematic representation of a zeolite crystalline framework illustrating the interconnected microporous structure [65].

2.3.2 Activated Carbon

Activated carbon treatment operates similarly to zeolites, as it is a highly porous structure with a large surface area that is used to adsorb ions and organic matter [66]. Powdered activated carbon (PAC), is derived from many sources and can only be used once before disposal, whereas granular activated carbon (GAC) can be regenerated. Activated carbon, like zeolites, are added to the water and when removed the contaminants on the surface of the particles are removed from the water. This treatment application is quick and effective in removing pollutants from water [67,68].

A recent study demonstrated that PAC from pumpkin seeds, when coupled with electrocoagulation, successfully treated brewery wastewater [69]. While the results are

promising, the Biomakerij's existing biological treatment would require significant additional infrastructure to integrate this process. Moreover, both PAC and GAC require large spatial footprints and investments, making them not ideal for the site.

2.3.3 Multimedia Filter

A multimedia filter functions like a sand filter but uses three or more media layers of varying densities, such as gravel, silica stone, zeolites, and activated carbon, to remove a range of particle sizes and provide different adsorption surfaces (Figure 2.6). Treatment with the filter is then followed by periodic backwashing for cleaning [18]. Studies applying multimedia filters to brewery wastewater have proved reductions in TSS, BOD and COD [70]. However, results are typically less successful than that of membrane filtration, and complete disinfection is not achieved making them an unsuitable tertiary treatment method to use the reclaimed water for all irrigation methods on food crops.

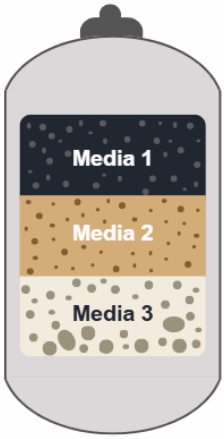

Figure 2.6 Multimedia Structure Schematic

Schematic representation of a multimedia filtration unit showing the stratified arrangement of granular media layers with decreasing grain size from top to bottom [20].

2.3.4 Pretreatment Methods Considered

To prolong membrane longevity and performance and improve system robustness, pretreatment options were evaluated to address the primary fouling risks identified in prior studies. Pretreatment plays a crucial role in removing suspended solids, colloids and bacteria which can accelerate and worsen membrane fouling. This selection of pretreatment steps for this study considered both the expected feedwater composition at the Biomakerij and operation simplicity required for implementation at a small-scale brewery. Two approaches were considered: sand filtration and chemical precipitation,

based on their ability to mitigate specific fouling risks observed in previous pilot studies, including high particle loads and elevated alkalinity.

2.3.4.1 Sand Filtration

The results of the previous pilot raised concerns about the impact the size of particles in the treated wastewater have on the membrane which led to the investigation of slow sand filtration as a compact, low-maintenance pretreatment option. Filtration is defined as "the removal of solid particles from a suspension by passage of the suspension through a porous medium" [18]. Slow sand filtration was selected over rapid sand filtration due to its simpler operation and lack of backwashing requirements. Instead, a biological layer (Schmutzdecke) forms on the sand surface, and maintenance consists of scraping away 1 – 2 cm when head loss occurs. A typical filter bed consists of 1.25 m of silica sand with a grain size of 0.15 – 0.35 mm over a 0.3 – 0.6 m gravel layer [71,72].

2.3.4.2 Precipitation

Alkalinity is defined as water's buffering capacity against pH changes. Elevated alkalinity is identified as a potential risk to the selected polymeric membrane. As water hardness is one of the contributing factors to alkalinity, chemical precipitation was considered to reduce this. Chemical precipitation is defined as the "addition of chemicals to bring about removal of specific constituents through solid-phase precipitation", which can result in the water to be softened [18]. Two dosing options were evaluated: calcium carbonate, initiating precipitation at pH 8 - 9, and phosphoric acid, that targets ion imbalances to form struvite at pH 10.5 -11 [73,74]. The implementation of precipitation and the final chemical choice were determined based on initial water quality results and preliminary testing.

2.4 Brewery Wastewater Characteristics and Nanofiltration Treatment

2.4.1 Brewery Wastewater

The beer brewing process has five main stages: (1) malting, (2) wort production, (3) fermentation and maturation, (4) filtration, and (5) beer bottling. Each stage of treatment requires substantial volumes of water [75]. The water source typically used at breweries is carefully selected to achieve certain water quality parameters for taste. Often times brewery locations are selected by the ground water quality, and wells are constructed on-site to provide the water for the brewery. In 2014 the specific water consumption was 3 cubic meters of water needed per hectoliter of beer produced [12,13,76].

The large water consumption during beer production results in the generation of similarly large volumes of wastewater, on average producing 0.6 cubic meters of wastewater per hectoliter of beer produced [76]. Brewery wastewater is typically characterized as having

high biological (BOD), and chemical oxygen demands (COD) due to the organic compounds, along with elevated total suspended solids (TSS) and nutrients such as phosphorus and nitrogen compounds [12,77–79]. If inadequately treated, this wastewater can place a strain on municipal treatment facilities or cause significant harm to nearby aquatic ecosystems [4]. Ranges of common contaminant concentrations in brewery wastewater in Table 2.3, alongside their possible nanofiltration removal efficiency based on literature. If nanofiltration treatment reaches the removal efficiencies listed in the table below the gap in key water quality performance indicators, such as COD/BOD, TSS, ions, and *E. coli*, will be bridged to qualify for reuse.

Therefore, pretreatment before disposal is a frequent practice, with aerobic and anaerobic biological processes being the most common approaches. The Biomakerij uses aerobic biological treatment which results in high removal efficiencies of COD, nutrients, and organic compounds. However, its disadvantages are the high energy consumption, large special footprint, and effluent production with biodegradable impurities that are difficult to remove [12]. Further details on the Biomakerij's existing treatment plant system and resulting water quality follow in Section 2.6.1 "The Biomakerij".

Past studies have found significant levels of bacteria in brewery wastewater ranging from 1300 CFU/100mL to 19,100 CFU/mL. This water quality measurement is a key indicator of "recent" fecal contamination within the wastewater, thus being representative of other pathogenic bacteria [5,77,80]. Presence of fecal matter within a water source is the main cause of waterborne diseases. Direct exposure to *E. coli* can result in vomiting and diarrhea, however the presence of *E. coli* leads to the possibility of more severe waterborne diseases [80–83]. The usage of water contaminated with waterborne pathogens from fecal matter causes diarrhoeal disease, that is the third-leading cause of death for children under the age of five [84].

The sodium concentration of brewery wastewater ranges greatly across different breweries, typically dependent on the cleaning chemicals used. The concentrations range from 0.17 mg/L to 1400 mg/L [41,85,86]. Sodium levels can also be of concern when using reclaimed brewery wastewater for irrigation [87,88]. Over time the sodium accumulates in the soil which can deteriorate the soil's hydro-physical properties and contaminate ground water [87–89]. However, other studies have found that some crops have a higher salt tolerance, and certain fungi can be added to the soil to reduce the sodium accumulation [86].

Table 2.3 Brewery Wastewater Quality Characteristics

Water Quality Characteristic	Typical Brewery Wastewater Concentration Ranges	Expected Nanofiltration Removal Efficiencies*
BOD	5- 5,000 mg/L[90]	76.90% [41,91]
COD	300 – 9,000 mg/L[79,90]	92% ± 9% [41,91–93]
TSS	150-3,800 mg/L[79,90]	95% ± 4% [91,93,94]
Sodium	0 – 1,400 mg/L [41,85,86]	39% ± 24% [41,92,95]
Fluoride	0 – 50 mg/L [96]	60% ± 38% [95,97,98]
Chloride	50 – 250 mg/L [41]	45% ± 32% [41,92,95]
Nitrite	0-0.24 mg/L [79,85]	68% ± 7% [99,100]
Nitrate	1 -34 mg/L [79,85]	63% ± 13% [92,99,101]
Ammonium	0 - 13 mg/L [5,79]	28% ± 28% [41,92,95]
Phosphate	8 – 98 mg/L [85]	42% ± 2% [90,95]
Sulfate	30 -33 mg/L [85]	62% ± 17% [92,95]
E. coli	1,300 – 19,000 CFU/ 100mL [41,85,86]	99% ± 0% [102,103]

* The removal efficiencies are from a range of all nanofiltration membranes and membrane characteristics

Most water quality characteristics have a large range of concentrations and removal efficiencies, so these are greatly dependent on the source and membrane used.

Typical concentration ranges of key brewery wastewater constituents and their corresponding expected removal efficiencies by nanofiltration, based on reported literature values.

2.4.2 Brewery Wastewater Tertiary Treatment Studies

This section will review some previous studies that applied nanofiltration as a tertiary treatment of brewery wastewater. The findings and methods of these studies aided in the design of this experiment.

Implementation of nanofiltration as a tertiary treatment for pre-treated brewery wastewater began in the early 2000s. A study in Malle, Belgium tested four NF membranes on wastewater collected from different points in the brewing process and intended to use the reclaimed water as cooling water. The different feed waters were from biologically treated wastewater, bottle rinsing water, rinsing water from the beer reservoir, and rinsing water from the brewing room. The results showed that the only biologically treated wastewater produced permeate of acceptable quality with sufficient COD, Na^+, and Cl^- removal [41]. However, all membranes experienced a 10-40% flux decline during the three-hour treatment period.

A more recent study conducted in Montreal, Canada in 2020 compared membrane distillation (MD), NF, and RO membranes for treating brewery wastewater pre-treated with a membrane bioreactor (MBR). The results showed a significant decline in flux occurred for both the NF and RO treatment during the 80-hour treatment period, but when a pretreatment method was added prior to the MBR the decline in flux was not as severe. MD was ultimately proposed as the most effective option at this site, but because of its high energy consumption it was not considered for this thesis [85].

A study conducted in France in 2023 researched the valorization of phenolic compounds from brewery wastewater at varying pH conditions using UF and NF [50]. In the brewing process, malt and hops have significant concentrations of phenolic compounds, which are high in antioxidants that can be reused in a range of industrial applications. This study explored recovering phenolic compounds and alkaline substances, to display both the environmental and economic benefits of brewery wastewater reclamation. The results of the study showed that a higher pH of the feedwater resulted in a lower fouling propensity. Another result of the study showed the predominant flux-limiting mechanisms were cake layer formation, pore blocking, and osmotic pressure. The study concluded that direct nanofiltration of alkaline brewery wastewater is promising for recovery of phenolic compounds.

The most recent study of the previously discussed applications applied reverse osmosis and nanofiltration on wine and brewery wastewater in Italy. The study explored the multiple uses of RO and NF membrane within the wastewater industry and during the production process. The study found that in order for membrane implementation to successfully outweigh the risks of fouling and energy costs, the membranes must be tailored to the feed water matrix [104].

In addition, to studies measuring the improved water quality of brewery wastewater after tertiary treatment, other studies have explored the benefits of using the tertiarily treated wastewater on crops. A study conducted in 2018 in South Africa investigated the use of

treated brewery effluent as a nutrient source for irrigating crops. In this study, the effluent was first treated with anaerobic digestion (AD) and was followed by different tertiary treatment methods to determine the best for crop irrigation. Six different irrigation sources were compared for cabbage irrigation: direct usage of effluent after AD, effluent from AD with primary-facultative-pond (PFP), post-treatment, effluent from AD with high-rate-algal-pond (HRAP) post-treatment, post-treatment, effluent from AD with constructed-wetland (CW) post-treatment, tap water, and tap water with a nutrient-solution [87]. The intention of this study was to find the irrigation source that resulted in better crop production without causing soil deterioration. The study found that the effluent from AD and the effluent from AD with PFP post-treatment resulted in cabbage crops that grew much larger than those irrigated with only tap water, but not as big as those irrigated with tap water and a nutrient solution. The soil after treatment showed significantly higher sodium concentrations after three months of irrigation with the reclaimed water, but the soil's hydro-physical properties were not deteriorated [87]. Further investigation needs to be conducted into the long-term impacts of sodium in the soil.

The composition of brewery effluents is therefore variable but typically characterized by elevated organic load, residual sugars, and moderate salinity. Understanding this composition is crucial in selecting a membrane system that can effectively target these parameters. The high organic load implies a risk of fouling and physical stress emphasizing the benefit of mechanically strong and chemically resistant materials to ensure system robustness. Consistent with the considerations outlined in Section 2.2, a nanofiltration membrane with a moderate MWCO is expected to achieve the best balance between water quality improvement, flux stability, and energy demand for brewery wastewater treatment.

2.5 Water Regulations

Wastewater reuse regulations vary widely depending on the country and the intended application of the reclaimed water. In breweries, reclaimed water has been explored for use in bottle washing and irrigation [5,13,77]. In the Netherlands, irrigation reuse is largely dependent on the *E. coli* concentrations, which determine the reuse class of the treated water and the required monitoring frequency [105]. The reuse classes are summarized in Figure 2.7 below. The Netherlands uses the Class A-D regulation system to only refer to the *E. coli* concentration of the sample. However, the European commission also includes and regulates the concentrations of BOD_5, TSS, Turbidity, *legionella*, and intestinal nematodes to reach Class A reuse. Based on the European Commission, the regulations must be met in at least 90% of all the samples collected [106]. The additional European commission regulations can be seen in Table 2.4, only regarding Class A reuse, there are no regulations regarding these additional parameters for Classes B-D [106]. The *legionella* regulation is

only applicable if there is a risk of aerosolization in greenhouses, which could be applicable due to the MNR greenhouse. The intestinal nematodes also serves as an indicator of fecal contamination and is also applicable only if the site chooses to irrigate nearby pastureland [106].

The *E. coli* regulations of the Netherlands and European Commission remain the same. As previously mentioned in Section 2.4.1, *E. coli* regulations and measurements serve as an indicator of fecal contamination in the water source [80–82]. *E. coli* does not pose a critical health risk alone. However, it does provide an indication that there could be other pathogens in the water from fecal waste that pose a much larger threat [80–82]. This risk stresses the importance of abiding by these regulations for *E. coli* when considering wastewater reuse. Using nanofiltration as a tertiary treatment step can effectively remove bacterial pathogens, thereby substantially mitigating this health risk [107].

In addition to microbial standards, in 2023 RIVM released legal limits for ions of concern for reuse purposes, which are shown in Table 2.5 below [108]. Potable water reuse would fall under drinking water regulations for Tilburg, but this is not the intended purpose of the current thesis and would require additional treatment steps.

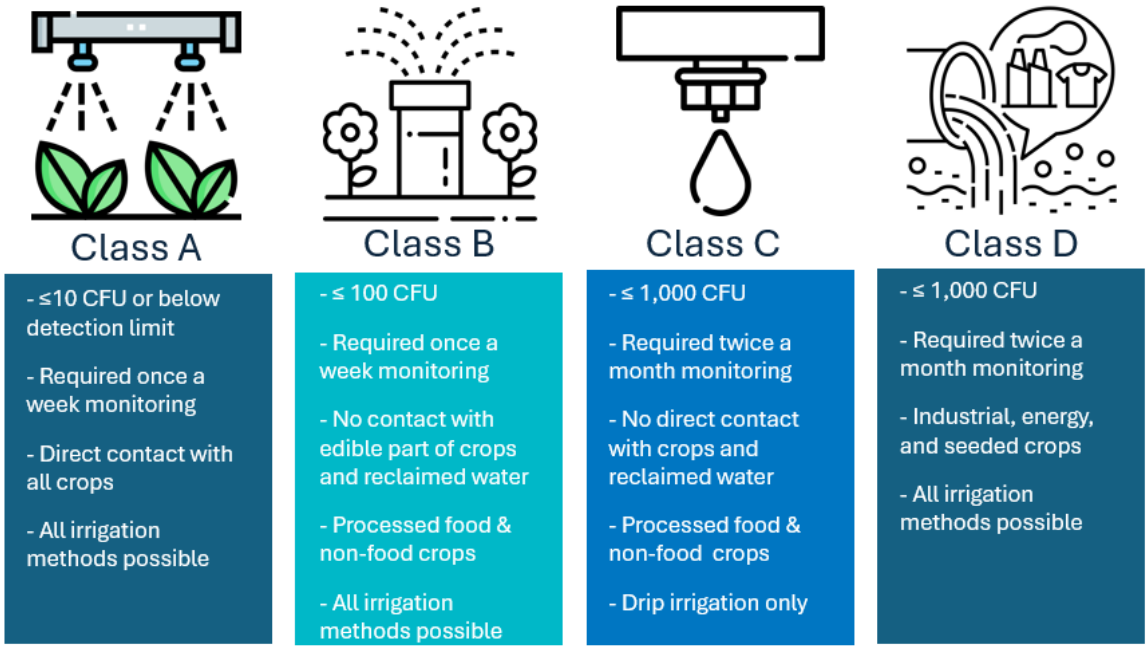

Figure 2.7 Biological Reuse Restrictions

Summary of biological water reuse classifications and corresponding microbial quality requirements for reclaimed water, showing allowable applications and monitoring frequencies [105].

Table 2.4 Additional Required Reuse Concentrations for Class A Reuse

Contaminant	Legal Concentration Limit	Measurement Frequency Required
BOD_5 [mg/L]	≤ 10	Weekly
TSS [mg/L]	≤ 10	Weekly
Turbidity [NTU]	≤ 5	Continuous
Legionella [CFU/L] *	<1,000	Weekly
Intestinal Nematodes [egg/L] **	≤1	Bi-monthly

Additional water quality requirements and monitoring frequencies for Class A reclaimed water [105,108].

Table 2.5 Netherlands Chemical Concentration Regulations

Contaminant	Legal Concentration Limit	Necessary Removal Efficiency for to Reach Reuse Limit**
Fluoride [mg/L]	1.5	94%
Chloride [mg/L]	100	33%
Nitrite [mg/L]	1	*
Nitrate [mg/L]	10	43%
Phosphate [mg/L]	1	98%
Sulfate [mg/L]	100	*
Sodium [mg/L]	120	83%
Ammonium [mg/L]	1.5	77%

*Average expected influent concentration is already below the reuse limit
** The average ion concentration was used from Table 2.3
Summary of Dutch regulatory limits for chemical parameters in reclaimed water and the corresponding removal efficiencies for the average expected concentrations to meet reuse standards [105,108].

2.6 Brewery Wastewater Water Source

2.6.1 The Biomakerij

The wastewater used during this thesis is sourced primarily from brewery production as well as many additional industrial sources as a result of the wide variety of facilities on the property. The broad range in sources results in wastewater of equally diverse composition, all of which is processed in the on-site treatment plant named The Biomakerij. Domestic sewage is directed into two separate tanks within the MNR greenhouse treatment facility. The Biomakerij has created what is typically an unattractive wastewater treatment plant into a tropical greenhouse, particularly vibrant during springtime (Figure 2.9). The industrial wastewater on-site originates from beer brewing, cheese production, chemical cleaning operations, and two toilets within the brewery remain connected to the industrial treatment line.

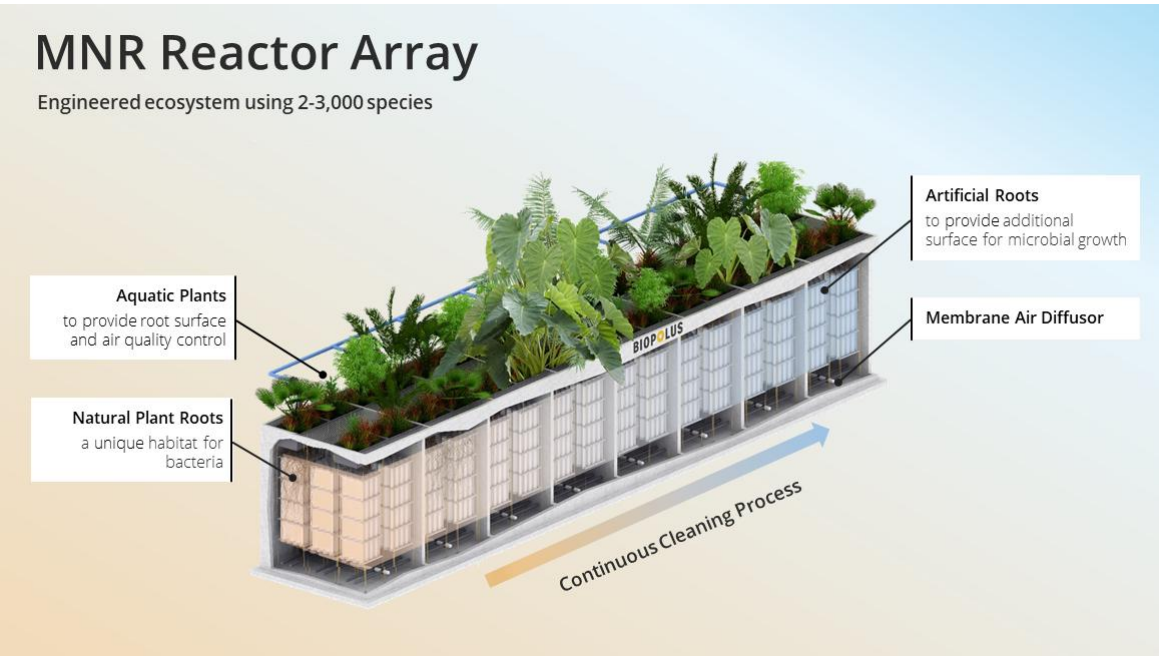

Figure 2.8 Biomakerij MNR System

Schematic representation of the Biomakerij Metabolic Network Reactor (MNR) system, illustrating the integration of aquatic plants, artificial roots, and membrane aerations for biological wastewater treatment [9].

Figure 2.9 MNR System Blooming

Photograph of the Biomakerij MNR system during plant blooming, showing the integration of vegetation within the greenhouse treatment environment.

The treatment process begins in an equalization tank where preliminary water quality measurements are taken. From there the water is pumped to the MNR greenhouse reactors, where iron chloride or iron sulfate is dosed to spark phosphate precipitation.

Figure 2.8 depicts the components of an MNR system. The metabolic network reactor (MNR) is an aerobic, biofilm-based treatment and is the core of the current process. Biofilm develops along the roots of the plants above the reactors, with additional netting installed to increase surface area which directly increases the amount of biofilm. Microbial communities within the biofilm metabolize nutrients in the wastewater [4]. Within the MNR tanks there is also a dissolved air flotation unit (DAF), where polymers are added as flocculants to bind smaller particles.

This MNR system is based on this biofilm growth on the netting in the reactor. This growth is dependent on four main forces that allow this biofilm to grow, which are electrostatic interactions, covalent bond formation, hydrophilic interactions, and partial covalent bond formation [15]. The electrostatic interactions represent the need for a positive surface charge as nearly all microorganisms are negatively charged. The covalent bonds are formed with the surface being adhered to. The hydrophilic properties of the surface and the microorganism ideally with the surface and biofilm having hydrophilic tendencies to remove

the water molecules separating the biofilm from the surface. Lastly, are the partial covalent bonds further holding the film to the netting surface between the biofilm and the hydroxyl groups on the surfaces [15].

The forces along the surface combine to be a delicate balance that also relies on the nutrients within the system to continue to promote the growth of the biofilm. The biofilm coupled with the aerobic properties results in nitrification as the microorganisms metabolize ammonium to nitrite and then nitrite to nitrate, thus being limited by the inorganic nitrogen concentration [9,109]. The microorganisms in the system require a balanced ratio of biological oxygen demand (BOD), nitrogen (N), and phosphorus (P) of 100:5:1 [110]. The influent typically has comparatively high BOD levels and nitrogen concentrations below the desired ratio. However, the brewery wastewater typically has high concentrations of organically bound nitrogen, which is a much lengthier process to make it usable in the nitrification process [111]. As a result, nitrogen is dosed to achieve a more balanced ratio. The dosage of nitrogen along with the constantly fluctuating water quality result in a very delicate system that results in overflows. Typically, the overflow of the system begins with nitrogen levels being unusually low resulting in the shedding of the biofilm, followed by excessive nitrogen dosage to compensate [112,113]. However, at this point the biofilm did not have enough nitrogen in the nutrient balance to maintain its bonds to the surface resulting in it being shed into the water. This causes large particles to accumulate in the system while not being balanced and ultimately resulting in an overflow.

In the MNR tanks either $FeSO_4$ to $FeCl_2$ are dosed as coagulants to reduce the phosphate concentration of the brewery wastewater. During the initial portion of this project $FeSO_4$ was the coagulant dosed, which result in high sulfate concentrations in the system. If the system is not well aerated and the sulfate concentration is high, then sulfate reducing bacteria is able to grow which converts the sulfate into hydrogen sulfide gas (H_2S) [114–116]. H_2S is a toxic, highly flammable, corrosive and explosive gas that can pose a life-threatening risk if the concentration are high enough [117]. This production of H_2S within the MNR greenhouse has occasionally exceeded safe limits, thus preventing anyone from entering the facility until safe levels are reached. The coagulant was changed to $FeCl_2$ before the final sample was collected for this thesis.

After the MNR system the treated water is sent to a 10 µm drum microfilter, which often shows visible signs of iron flocs (Figure 2.10). In the final stage of treatment all remaining sludge is dewatered using a belt press, this is the only stage where domestic and industrial waste streams are treated with the same equipment.

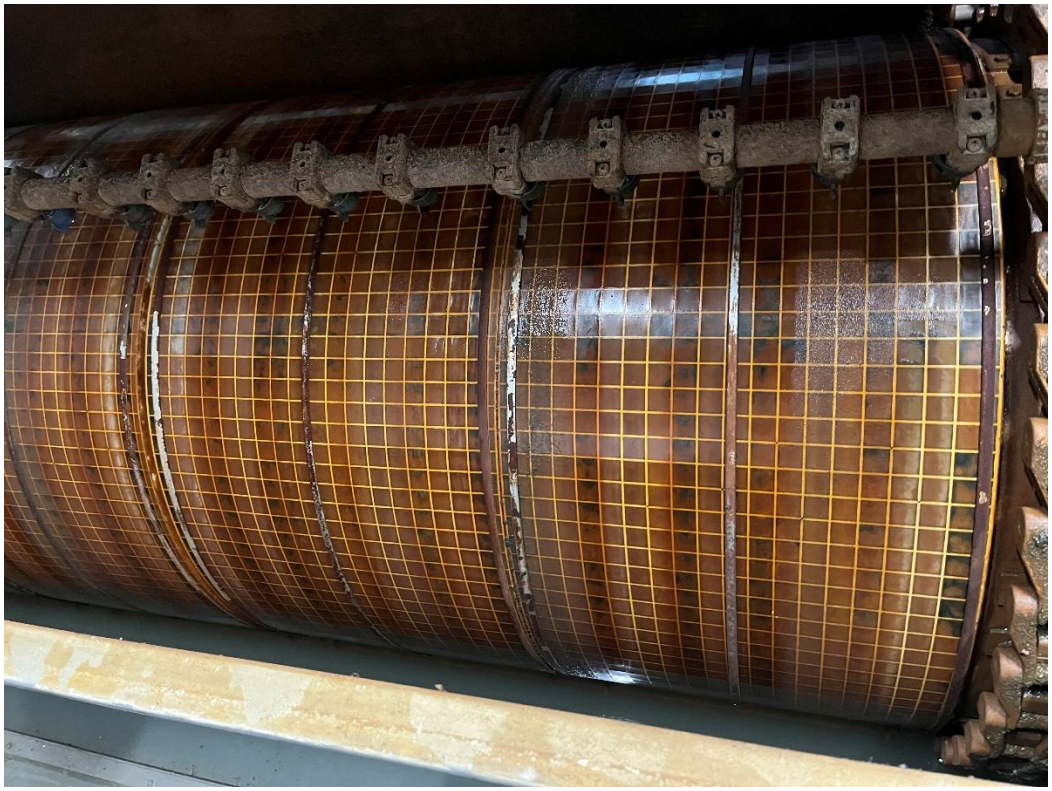

Figure 2.10 Iron Flocs on Drum Filter

Accumulation of iron flocs on the surface of the drum filter within the Biomakerij treatment system.

On-site water quality is monitored using Hach kits, with all results stored in a long-term database. This dataset reveals patterns such as variations linked to specific beer production cycles, staff holidays, and system overflows. While variations in water quality were anticipated, the extent proves to be greater than expected, inhibiting the use of this data for a full proof model. Thus, a preliminary water quality analysis phase is necessary before designing any membrane experiments. The aim of this step was to identify contaminants requiring removal to meet legal reuse limits and determine whether pretreatment would be needed to avoid a rapid decline in flux.

Since the opening of the Biomakerij there has been a struggle to reach the Abbey's goals of achieving water recirculation. There have been extensive studies conducted in an attempt to pinpoint the cause of the water quality failures. The hypothesis of all past studies have been that there is a nutrient imbalance within the system, after identifying large changes in contaminant concentration from day to day and tank to tank [10,118,119]. This in turn is prohibiting the MNR system from reaching its full treatment ability and effluent water quality. Each of these reports noted the irregularities in the system and identified parts that were more efficient than others and provided solutions to best combat these issues. Given the large variety of facilities on the property a variation of water quality is expected but this is a

rather extreme case. Based on the variations in the water quality from the data repository, coupled with the previous study results the membrane tertiary treatment proposed will have to be a versatile and robust system that can still perform under many conditions.

When the MNR system is functioning properly its impact on the water quality parameters can be seen in Table 2.6. This shows the difference between raw brewery wastewater as opposed to the MNR treated wastewater used as the influent for the experiments conducted in this thesis.

Table 2.6 MNR Influence on Brewery Wastewater Quality

Water Quality Parameter	Influence of MNR Treatment on Concentration of Parameter	MNR Process That Influence on Quality Parameters
COD	Decrease	Heterotrophic oxidation and biodegradation of organic matter [13,78,120]
BOD	Decrease	Biological oxidation of biodegradable organics [78,120]
TOC	Decrease	Conversion of organic carbon to CO_2 and biomass through microbial metabolism [13,120]
TSS	Decrease	Biomass aggregation and settling, Sludge separation and floc formation [13,120]
Ammonium	Decrease	Nitrification by autotrophic bacteria [120]
Nitrite	Fluctuates	Intermediate of nitrification and denitrification [120]
Nitrate	Increase	Product of nitrification [120]
Total Nitrogen	Decrease	Sequential ammonification to nitrification [120]
Phosphate	Decrease	Microbial uptake for growth and chemical precipitation [78,120]

Sulfate	This should be decreased, unless iron sulfate is dosed, then it increases.	Biological sulfate reduction in anoxic zones, forming H_2S [13,115]
Chloride	Remains mostly unaffected, unless iron chloride is dosed then concentration increases.	Conservative ion, only affected by dosing [78,120]
Alkalinity	Fluctuates	Consumed during nitrification and regenerated during denitrification [120]
E. coli	Decreased	Biological competition and settling [13]

Summary of the influence the MNR treatment system has on key brewery wastewater quality parameters and the corresponding biological and chemical processes responsible for these changes.

2.6.2 Pilot Study Results

The EU-funded Next Gen Pilot project was a collaboration between the Biomakerij, Semilla IPStar bv., and Waterschap de Dommel as an extension of the project that constructed the MNR on-site. The pilot evaluated and implemented a treatment train comprised of electrodialysis, MNR, the direct nanofiltration, reverse osmosis stage one, and reverse osmosis stage two, with all membrane concentrates recirculated (Figure 2.11).

Prior to implementation, a model was developed to assess the alkalinity, pH, electrical conductivity (EC), temperature, flow rate, carbonate, phosphate, and sulfate concentrations for three scenarios. When the treatment system was conducted on-site, treatment was successful when done as a batch reaction allowing the influent to settle completely and then be sent for treatment. However, when integrated directly into the existing treatment line, the nanofiltration membrane was quickly clogged, halting production. Consequently, further membrane research was discontinued, and the system was not permanently implemented.

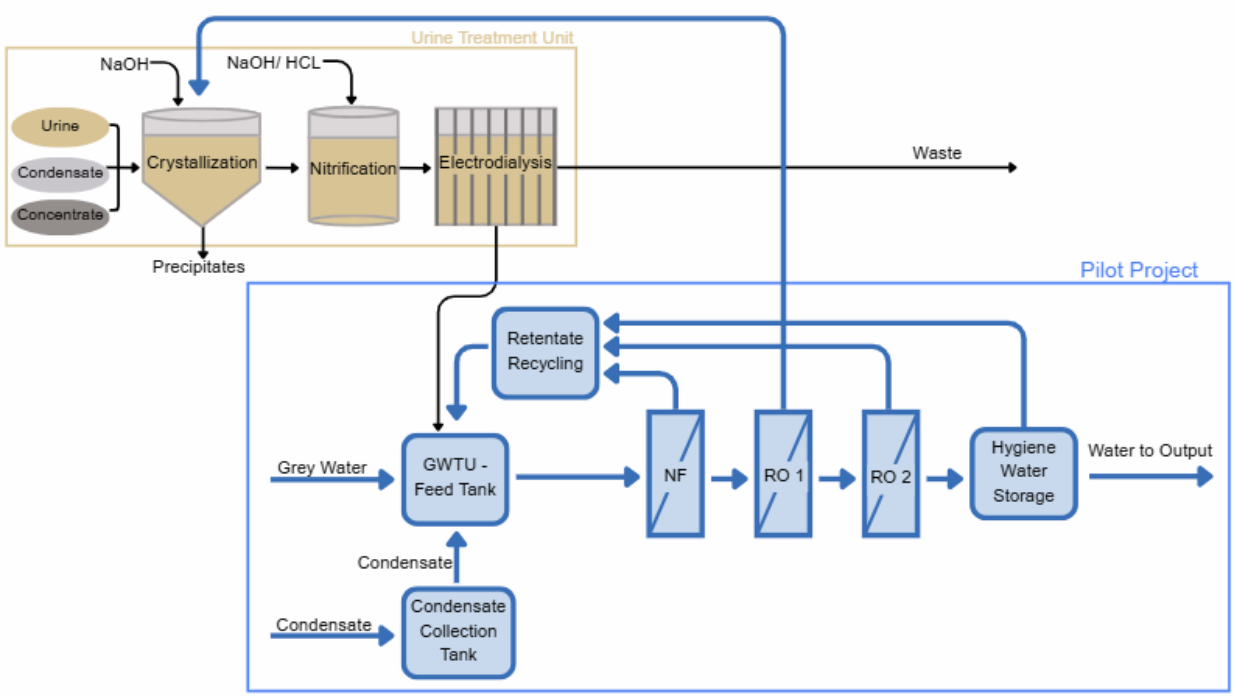

Figure 2.11 Pilot Project Experimental Diagram

Schematic diagram of the pilot project experimentational system, showing the integrated nanofiltration and reverse osmosis systems for wastewater reuse [45].

Based on the reviewed technologies, wastewater characteristics, regulations and specific composition of the Biomakerij effluent, nanofiltration was selected as the most suitable and sustainable tertiary treatment method, combining high selectivity with practical implementation at small scale.

3 Materials and Methods

3.1 Influent Source and Sampling Scheme

The experimental work was divided into three main phases: (1) water quality assessment, (2) pretreatment methods, and (3) membrane treatment. The initial intention was to use the water quality results to guide the selection of membranes for laboratory testing. However, due to time and resource constraints, the influence of the water quality assessment on the membrane selection was more limited than originally planned.

Water quality analyses were conducted immediately after sample collection. In total, six samples were collected. Table 3.1 provides an overview of the samples along with relevant information about the Biomakerij processes at the time of collection.

Table 3.1 MNR System Operating Conditions and Implications During Each Sample Collection

Sample #	Volume Collected [L]	Treatment Plant Condition at Time of Sample Collection	Potential Impact of Unstable Conditions on Membrane Performance
1	10	Alcohol free beer being brewed, should see high total nitrogen (TN)	Higher TN results in more negative ions in the feedwater, which can impact the Donnan effect and increase concentration polarization [99,121].
2	10	Completed brewing alcohol-free beer. Previously high TN will result in high ammonium levels	Ammonium typically has a higher NF removal rating resulting in lower permeate TN concentrations [99].
3	10	System overflowed and bypassed the drum filter, large particle sizes	Could clog/block the membrane pores and polymeric fibers if particles are large enough [28,122].

4	10	Scaling caused blockage of pipes three days prior, most likely high sample alkalinity.	Scaling caused by supersaturation could cause blockages within the system [123,124].
5	10	Scaling caused blockage of pipes four days prior, most likely high sample alkalinity.	Scaling caused by supersaturation could cause blockages within the system [123,124].
6	80	- Iron dosage was changed from $FeSO_4$ to $FeCl_2$ - The chemicals used in the brewery are better monitored and used more sparingly	- Sulfate has a higher typical removal efficiency from NF than chloride, can cause membrane oxidation [73,74]. New NF membrane properties could result in a higher Cl^- removal than past projects for the polymeric membrane [127]. - Using less of the cleaning chemicals will result in a lower alkalinity, thus less membrane scaling [128].

Operating conditions of the MNR system during each sample collection and the corresponding implications of unstable influent characteristics on nanofiltration performance.

Samples 1-3 were collected with the sole purpose of conducting a water quality assessment, but all samples water quality was measured. Samples 4 and 5 were collected on the same day, but Sample 4 was set aside 1 day prior to collecting Sample 5. These 20 L samples were intended for all laboratory membrane tests, with the volume based on preliminary permeability tests with the ceramic membrane. However, once the polymeric lab setup became available, it was evident that a much larger water volume was required. As a result, 80 L of Sample 6 was collected at a later stage. The first five samples were collected in jerry cans and transported by bike and train, while Sample 6 was transported by car due to its large volume.

During the period between each of these collections, the Biomakerij experienced several operational changes. At the time of Sample 3, there were large system overflows on-site. Before Samples 4 and 5, excessive use of softening chemicals in the brewery were identified

and a monitor was installed to limit this. The excessive chemicals in the wastewater caused the water to be supersaturated resulting in large scaling in the pipes causing a blockage that required mechanical removal. Prior to Sample 6 collection the treatment plant changed the iron dosing chemical compound. Combined with the inherent fluctuations in water quality from the batch brewing process, these factors mean that the findings in this thesis only apply to the water quality measured in the collected samples and may not reflect all future variations.

Sample 6 was collected in nine separate jerry cans, which showed noticeable differences in coloration between the first and last container. To normalize the sample, all jerry cans were combined in a large vessel and mixed. Unfortunately, during mixing, a valve on the large tank was accidentally opened, and approximately 35 L of the sample was lost, limiting the number of experiments possible.

Once the samples were collected the volume was divided into two containers of equal volume for measurements. One of the sample containers was for the unsettled sample measurements, which was shaken before any measurements or testing was done. The second batch of that sample was left to settle for five days, and the water was taken off the top of the container to prevent particle disruption for quality measurements.

The following water quality parameters were measured to determine key contaminant concentrations in the water samples:

1. Particle size distribution
2. Ion composition
3. Total organic carbon
4. Total suspended solids
5. *E. coli* concentrations
6. Alkalinity

Each parameter was selected to provide insight into the suitability of the wastewater for membrane treatment.

3.2 Selected Membranes

This section outlines the rationale behind the membranes selected for this thesis. The main goal when selecting the membranes for experimentation was to remove the high BOD, COD, TSS, bacteria, nutrients, and ions in order to achieve a permeate that is classified as Class A for water reuse, while also being economically efficient. To reach the economic efficiency only nanofiltration membranes were considered due to reverse osmosis's high energy consumption and operation costs. The current treatment system efficiently removes large

BOD, COD, and TSS concentrations; however, the reuse limits are not met in the effluent, so a further reduction is needed. The DAF aeration system is intended to reduce the bacterial compositions, but further treatment is needed to reach the concentration levels needed for reuse. The nanofiltration should lower these water quality characteristics to a level that is can be reclaimed. The contaminants that may remain a concern after nanofiltration are ion concentrations of ions with molecular sizes smaller than that of the pores and not complete disinfection. The ions of concern that are not removed by the membrane can be targeted with the membrane coating and surface charge.

The two membranes chosen for this experiment are the Inopor 0.9 nm ceramic membrane and the dNF80 NX Filtration polymeric membrane. For clarity they will be referred to as the ceramic membrane and polymeric membrane, respectively, for the remainder of the thesis. Both were chosen based on their accessibility and suitability for the experimental objectives.

The ceramic membrane was selected for its high durability as opposed to polymeric options. The available size was limited to a lab-scale module, but its 0.9 nm pore size was considered sufficient to produce permeate of adequate quality. The membrane size was limited by laboratory availability but was sufficient to conduct controlled comparative brewery treatment under varying operating conditions. The polymeric NX Filtration dNF80 membrane was chosen based on its successful application in similar studies [32,129]. Of the two NX Filtration nanofiltration options, the dNF80 with a MWCO of 80 Da, was preferred because the larger pore size results in less clogging that was experienced in the previous pilot.

3.2.1 Characterization of the Selected Membranes

As previously mentioned, the following experiments will explore the impact of the Inopor 0.9 nm ceramic membrane and an NX Filtration dNF80 polymeric membrane on pre-treated brewery wastewater.

Table 3.2 summarizes the specifications of both membranes. The ceramic membrane is 10 cm long, has an outer diameter of 10mm, and an inner diameter of 7mm. The total membrane surface area is 22 cm^2. The manufacturer recommends three pre-mixed cleaning detergents from Ecolab, tailored to specific fouling scenarios. However, these pre-mixed detergents were not recommended for the polymeric membrane, so they were not used in this experimental procedure. In order to standardize the cleaning method across both membranes different chemical reagents were explored. Multiple studies have found NaOH, NaOCl, and citric acid to be the best chemical cleaning reagents for ceramic [38,130–132]. Ultimately the selected cleaning agent with be based on initial water quality results and initial membrane testing. To further hypothesize the results based on the specific membrane characteristics, the ceramic membrane will likely have larger removal efficiencies due to its smaller pore size, but the polymeric membrane will produce a larger

volume of permeate due to its larger surface area. Both membranes are operated with cross-flow filtration.

Table 3.2 Selected Membrane Characteristics

Membrane Characteristic	Inopor Ceramic	NX Filtration dNF80
Module length [mm]	100	300
Outer diameter [mm]	10	25
Inner diameter [mm]	7	0.7 (fiber inner diameter)
Membrane surface area [cm^2]	22	650 [133]
Cross-flow velocity at 2 bar [m/s]	0.65	0.36
Cross-flow velocity at 4 bar [m/s]	1.1	0.36
Membrane housing	PVC	PVC-U Transparent
Membrane material	TiO_2	Modified PolyEtherSulfone (PES)
MWCO [Da]	450	800
Pore size [nm]	0.9	< 2
pH range	1-12	1-13
Max. system pressure [bar]	10	10
Max. TMP pressure [bar]	10	6
Potting material	N/A	Epoxy resin

Characteristics of the selected nanofiltration membranes used in this study, comparing the Inopor ceramic membrane and the NX Filtration dNF80 polymeric membrane.

The NX dNF80 polymeric membrane is made of modified polyethersulfone (PES). The membrane is a pilot scale module measuring 300 mm long, with an outer diameter of 25 mm, and each hollow fiber tube has an inner diameter of 7 mm [134]. The inner diameter of the hollow fiber tubes are the constraining factor when it comes to large particles clogging the membrane. The total membrane surface area is 650 cm^2, which is nearly thirty times greater than that of the ceramic membrane [135]. Consequently, the expected permeate volume is much higher. To ensure comparability, the experimental procedures for both membranes were designed to account for this size difference. Additionally, both membranes have a

contact angle less than 90 degrees, so they are hydrophilic, but the ceramic membrane is more hydrophilic than the polymeric membrane [37,39,40,53,136,137].

The material and structural characteristics of the selected membranes directly influence the dominant mechanisms of pressure-driven membranes. The ceramic tubular membrane along with its TiO2 coating, provides high rigidity, chemical stability, and strong hydrophilicity, resulting in a lower fouling propensity and stable flux under elevated transmembrane pressures [94,130,137]. Whereas, the polymeric membrane has a flexible structure and high surface area leading to higher flux, but its smaller fiber diameters and has a less hydrophilic surface chemistry which can result in higher fouling propensity [40,59,138]. These differences in surface chemistry, pore size, and geometry affect hydraulic resistance, fouling behavior, and removal efficiencies under pressure-driven conditions [20,41].

3.3 Experimental Setups

The overall objective of the experimental setups is to evaluate the nanofiltration performance of the two different membranes on their ability to treat brewery wastewater and produce a permeate that is sufficient for reuse quality. The setup is designed to simulate industrially feasible operating conditions for future implementation while maintaining lab-scale control, allowing for a comparison between membrane performance in terms of flux, fouling propensity, and permeate quality [11,12,41,85,139].

Based on the fundamental principles of pressure-driven membrane processes, where a hydraulic pressure gradient across a semi-permeable barrier forces smaller solutes to pass through the membrane, producing a permeate with a reduced contaminant concentration [18,20]. The rate of permeate flow or flux is dependent on the applied transmembrane pressure, influent water matrix, and total hydraulic resistance of the membrane and any fouling layers that form during operation [18,20,41].

To sustain stable flux and minimize fouling, both systems use cross-flow filtration, where feedwater moves tangentially across the membrane surface. As mentioned in Section 2.2.1, this allows rejected solutes to me taken away from the membrane, reducing cake layer formation [14,18,28]. The selected operating pressures of two and 4 bars represent typical nanofiltration conditions, which are high enough to drive permeate flow but below the limits that could damage membrane and not too high that would increase energy consumption and cost [18,33,41].

Two membrane experimental setups were designed to maintain constant pressure, cross-flow velocity, and membrane surface area to maintain stable and comparable operating conditions between the two membranes. This controlled configuration enables a direct

comparison of flux behavior, rejection efficiency, and fouling tendencies under similar hydraulic conditions, while still accounting for the differences in material geometry, size, and composition between the ceramic and polymeric membrane modules.

In addition to the membrane treatment experimental setups, concerns regarding the pore size and alkalinity of the brewery wastewater during the water quality assessment, led to the exploration of precipitation and sand filtration pretreatment methods.

3.3.1 Experimental Setup 1 – Ceramic Membrane

The ceramic membrane experimental setup is designed have constant nanofiltration conditions to quantify flux, removal efficiency and fouling during brewery wastewater treatment, while also serving as the control and represent traditional tubular membrane nanofiltration [20,41]. This system is designed to maximize the durable properties of the ceramic membrane and minimize the membrane's fouling propensity while also creating similar treatment conditions as that of the polymeric experimental setup to make the results comparable.

The first setup is designed for the Inopor ceramic membrane. This setup is fully controlled be the pressure of the system, resulting in a cross-flow velocity dependent on the pressure.

The ceramic membrane setup consists of a Getriebebau Nord Gmbh & Co SK 180E-550-340-B pump coupled with a Cantoni SLH 80A-4 motor. The system is connected with the PUN-H-8X1,25 tubing (outer diameter 8 mm, inner diameter 5.7 mm), which can withstand a pressure of 10 bar, but it is recommended to maintain a pressure at 6 bar or below to prevent leaks in the connection joints. The configuration allows either recirculation of the concentrate or discharge of the concentrate. The pump and valve configuration ensures stable transmembrane pressures of 2 and 4 bars and corresponding cross-flow velocities of 0.65 and 1.1 m/s, which fall within the recommended nanofiltration operating ranges within a lab scale and minimize concentration polarization [18,33].

Based on the recommended system pressure limit of 6 bar, pressures of 2 bar and 4 bar were determined to assess the impact of different pressures and remain within system pressure boundaries. The larger inner diameter of the ceramic membrane led to less concern about clogging with direct treatment. Resulting in the determination of the treatment order being: 2 bar, 4, bar, 4 bar SF, 4 bar SF, 2 bar, and 4 bar for the ceramic membrane. During each test, the TMP and cross-flow velocity were held constnat by fixing the motor setting and needle valve position, trying to maintain minimal variation throughout operation [140].

System pressure is controlled using the dial on the motor and a 304-G1/4 needle valve. Feed and concentrate pressures are monitored with two ESI Technologies GS4200-USB pressure

sensors located before and after the membrane module. The pressure values are automatically recorded every ten seconds while the system is running. The feed flows through the system counterclockwise. The selected cross-flow velocities were chosen based on typical nanofiltration operating conditions that provide sufficient hydrodynamic shear to reduce cake layer formation and maintain stable flux over time [18,20,28].

Permeate exits the module into the beaker placed on a Kern EWJ balance. Initially, permeate mass was recorded every 10 seconds, but due to noisy data results, the interval was adjusted to 30 seconds. All automated data from the balance and sensors are logged directly onto a desktop computer. Between tests, the ceramic membrane system and membrane were chemically and hydraulically cleaned to restore baseline permeability [130,137].

The setup includes five valves that are explained in Table 3.3 below.

Table 3.3 Ceramic Membrane Experimental Setup Valves

Valve Number	Location	Purpose
Valve 1 and 2	Either side of the pump	Remain open through all experiments
Valve 3	Located on the permeate line	Controls whether permeate is produced
Valve 4	After the first pressure sensor before the membrane module	Used to drain the system after experiments
Valve 5 (needle valve)	On the concentrate line after the pressure sensor	Controls the pressure during experiments, and drains the system after use with valve 4

Description of valve locations and functions within the ceramic membrane experimental setup.

A schematic of the ceramic membrane lab setup is shown in Figure 3.1, and

Appendix Figure D.1 shows the actual lab setup.

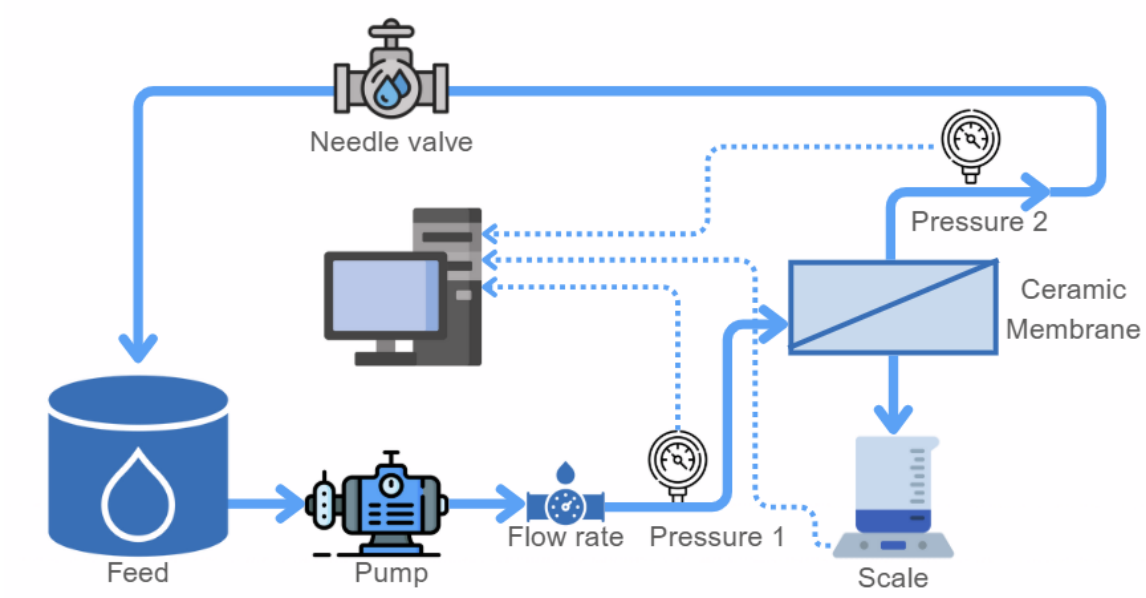

Figure 3.1 Ceramic Membrane Experimental Setup

Schematic diagram of the ceramic membrane experimental setup, showing the main components of feed circulation, pressure control, and permeate collection.

3.3.2 Experimental Setup 2 – Polymeric Membrane

The polymeric experiments were conducted using the Mexplorer unit from NX Filtration and Jotem Water Solutions. The Mexplorer is a portable membrane treatment system equipped with a Fluid-o-Tech PO211 rotary vane pump. The setup includes a rotameter for feed flow, three pressure gauges (1 – 10 bar), a high-pressure relief valve, and three needle valves for controlling feed pressure, permeate pressure, and concentrate [141]. This system enables controlled nanofiltration testing of the polymeric membrane under constant transmembrane pressures and cross-flow velocities comparable to the ceramic setup helping ensure a comparable assessment of flux, fouling and solute rejection [20,138].

Similar to the ceramic membrane the recommended maximum system pressure is 6 bar. Based on the maximum system pressure the system pressures of 2 and 4 bar were followed for the polymeric tests as well to allow for comparison between the two membranes. The Mexplorer pump maintains stable TMPs of 2 and 4 with a corresponding cross-flow velocity of 0.36 m/s, consistent with the manufacturers recommended hydrodynamic behavior for the membrane [138,141]. However, based on the 7 mm inner diameters of the membrane fibers potentially causing clogging, the experiments with sand filtered samples were conducted first before direct filtration. The order for treatment for the polymeric membrane was 2 bar SF, 4 bar SF, 2 bar SF, 4 bar SF, 4 bar, and 4 bar. Using sand filtered influents

minimizes particulate fouling and fiber plugging, which are typical issues in hollow fiber geometries operating at low shear rates [14,18].

The piping and fittings are PVC PN 10/16 – John Guest, along with 8 mm Festo PUN-H-8X1,25 tubing in different colors to distinguish streams: red (permeate), blue (concentrate), green (feed), and black (overpressure). Permeate production is measured using the same Kern EWJ balance as in the ceramic setup. Transmembrane pressure is determined manually from the feed and concentrate pressure gauges and recorded every minute. During each experimental run, TMP and cross-flow velocity are kept constant by fixing the inverter setting and concentrate valve position, to maintain constant target pressures [140].

During operation, only the concentrate needle valve is used for pressure regulation. Permeate pressure remains at 0 bar as it is atmospheric pressure. Flow rate is controlled by the Electroil inverter remote control, which was set at position 1 for all experiments except for forward flushing. During forward flushing, the dial was set to position 4, and the pressure was reduced in accordance with the unit's maintenance guidelines. The selected cross-flow conditions are sufficient to provide tangential shear that reduces cake layer formation awhile avoiding excessive stress to the membrane [18,28]. After each run the polymeric membrane and membrane setup were cleaned using the manufacturer's recommended cleaning procedure seen in Appendix Table D.1, to prevent mechanical damage while restoring initial permeability [40,141].

The schematic of the polymeric setup below, Figure 3.2, depicts the lab set up, and Appendix Figure D.2 shows the actual lab setup.

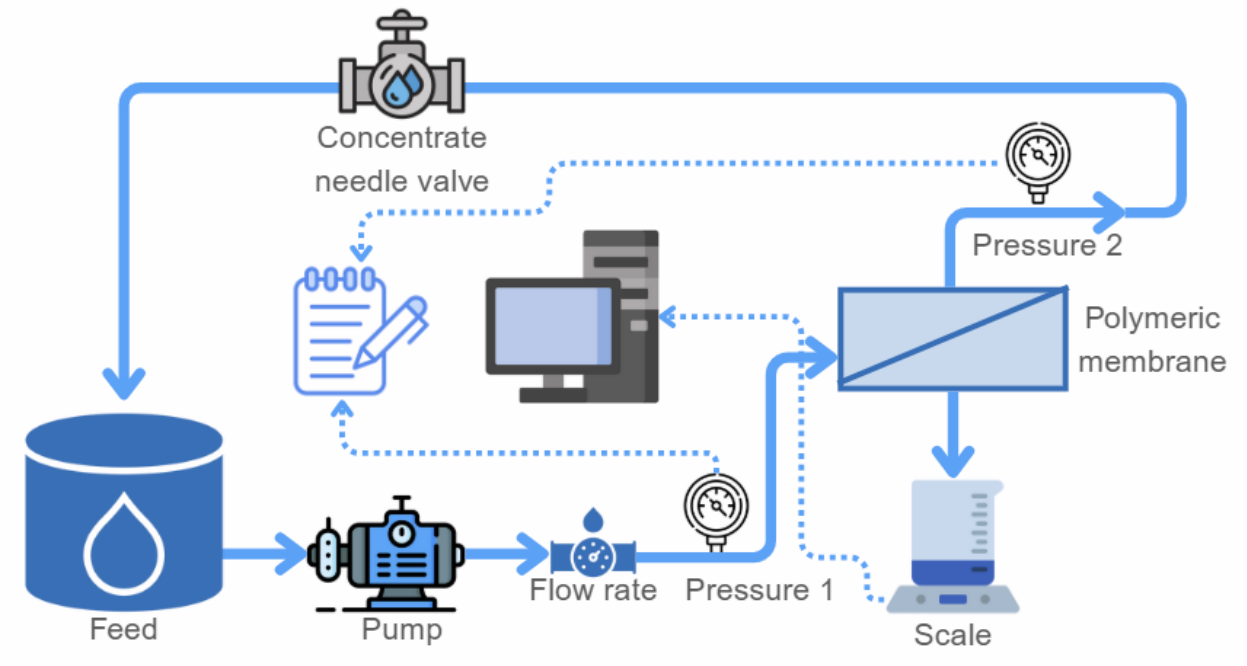

Figure 3.2 Polymeric Membrane Experimental Setup

Schematic diagram of the polymeric membrane experimental setup showing the main components for feed recirculation, transmembrane pressure control, and permeate collection. The schematic does not show the additional needle valves and pressure gauge as these components were not utilized during the treatment process.

3.3.3 Experimental Setup 3 – Additional Pretreatment Setups

In order to prolong the robustness of the membranes tested two additional experimental setups were designed for brewery wastewater pretreatment.

3.3.3.1 Slow Sand Filtration

Based on the particle content within the wastewater samples, sand filtration was identified as the best and most feasible pretreatment method for particle removal. The filter dimensions were designed based on the previously mentioned literature review. To adapt the design for laboratory use, the sand to gravel proportions were maintained but scaled down. The constructed sand filter consisted of a vertical column with a sieve at the base, containing approximately 20 cm of gravel at the bottom and 80 cm of quartz sand above [71]. The quartz sand used had granules ranging from 0.15 to 0.35 mm [18]. Prior to usage of the gravel and sand in the column, both the gravel and sand were thoroughly washed until the rinse water ran clear.

3.3.3.2 Precipitation

The objective of the precipitation experiments was to reduce the alkalinity of the brewery wastewater before membrane treatment. Two experimental phases were carried out, each using a different chemical additive. In the first phase powdered Calcium Carbonate ($CaCO_3$) was added and during the second phase phosphoric acid (H_3PO_4) was dosed. During both phases the pH was lowered to reach the optimal pH for precipitation using 0.1 M and 1 M NaOH. ($H_3PO_4^{3-}$

Experiments were conducted using 150 mL of Sample 3 wastewater, placed in glass beakers on magnetic stir plates. After dosing the respective chemicals and NaOH, the samples were stirred continuously for 30 minutes. Following this reaction time, the supernatant's alkalinity was analyzed, and the total suspended solids (TSS) of the whole sample were measured using the previously described methods.

Each experimental phase involved testing a range of dosages to identify the most effective conditions. Table 3.4 summarizes the dosages applied during Phase 1. Samples are labeled according to the phase number followed by the sample sequence within that phase.

Table 3.4 Phase 1 Precipitation Dosages

Sample name	Dosage of 1M NaOH (mL)	Dosage of CaCO3 (g)
Precipitation 1.1	3	0.1
Precipitation 1.2	3	0.1
Precipitation 1.3	1	None
Precipitation 1.4	1.25	None
Precipitation 1.5	1	0.057
Precipitation 1.6	3	None

Dosages of 1 M NaOH and $CaCO_3$ used during Phase 1 precipitation experiments.

Phase 2 of the precipitation tests was carried out using an 85% phosphoric acid stock solution with a molarity of 14.6. A preliminary model was first used to estimate the ion imbalance in the sample, which calculated that adding 31 µL of H_3PO_4 would balance the ions in the water matrix. To check if this dosage was actually most effective, both smaller and larger amounts were also tested. For each trial, 150 mL of Sample 3 was treated with

the chosen amount of H_3PO_4, and the resulting pH was measured. This phase of precipitation added 0.1 M NaOH as opposed to the 1 M previously used. The tested dosages are summarized in Table 3.5 below.

Table 3.5 Phase 2 Precipitation Dosages

Sample name	Volume of H_3PO_4 dosed (µL)	Volume of 0.1 M NaOH dosed (µL)
Precipitation 2.1 (calculated)	31	600
Precipitation 2.2	100	800
Precipitation 2.3	500	N/A (pH was out of range)
Precipitation 2.4	15	600
Precipitation 2.5	25	600
Precipitation 2.6	1	100
Precipitation 2.7	5	200

Dosages of H_3PO_4 and 0.1 M NaOH used during Phase 2 precipitation experiments.

3.4 Membrane Experimentation

The membrane testing was split into three phases:

1. Hydraulic integrity assessment
2. Membrane permeability evaluation
3. Treatment of brewery wastewater

3.4.1 Hydraulic Integrity Testing

The first step was to assess the hydraulic integrity of existing membrane setups in the Water Lab. All tested systems showed some degree of leakage. One constant pressure system required the least amount of leakage repairs was selected for the ceramic membrane setup. The repairs were conducted prior to the membrane permeability evaluation.

3.4.2 Membrane Permeability Evaluation

Permeability testing was then performed using Milli-Q water at pressure 1-7 bar for the ceramic membrane setup and pressures 1-6 bar for the polymeric membrane. Each pressure step was repeated twice to determine the permeability of the membranes. The evaluation included running Milli-Q water through the system for one hour for the ceramic membrane and 30 minutes for the polymeric membrane, while recording permeate volume and transmembrane pressure.

The permeability evaluation was conducted four times with four different ceramic membranes, as the coating process and material can lead to variability in pore size. The first membrane used for permeability testing was also used to assess ion removal efficiency. Once two membranes with comparable permeability profiles were identified, the evaluation continued to the next phase.

3.4.3 Treatment of Brewery Wastewater

The final phase was the application of the membranes to treat the brewery wastewater. Samples 4 and 5 were used for the ceramic membrane and Sample 6 was used for the polymeric membrane.

3.4.3.1 Ceramic Membrane

For all ceramic treatment steps, the permeate weight produced was recorded every 30 seconds, and pressure was logged every 10 seconds throughout the experiments. The following steps were all conducted in duplicate totaling eight times throughout the ceramic treatment process.

3.4.3.1.1 Nanofiltration of Brewery Wastewater

Experiments of nanofiltration of brewery wastewater were conducted using both settled and sand-filtered samples. The ceramic membrane was tested with the settled sample at 2 and 4 bars, and the sand-filtered sample at 4 bar. Two liters of Sample 4 and 5 were recirculated during testing. Direct filtration was run for four hours to generate sufficient permeate for water quality analysis. Before beginning filtration, two 5 mL feed water samples were collected for IC testing. During the experiment, the pressure was maintained at the pre-determined level, and samples of the recirculated feed/concentrate were taken at 30 minutes, 1 hour, 2 hours, 3 hours, and at the end of the 4-hour period.

3.4.3.1.2 Forward Flush

After direct filtration, 2 L of Milli-Q water was flushed through the system to remove residual brewery wastewater and particles. An additional 2 L of Mill-Q water was recirculated for one-hour at 2 bar to eliminate any membrane or system buildup.

3.4.3.1.3 Chemical Cleaning

Following the forward flush, the membrane underwent chemical cleaning using 2 L of 0.1 M citric acid for one hour at 2 bar. Citric acid was chosen for its anti-scaling properties and absence of sodium. Previous lab tests done using sodium hydroxide as a cleaning agent with the ceramic membrane showed that sodium was not removed from the membrane, and the concentration increased due to accumulation from the cleaning process. Necessitating the need for a sodium-free cleaning agent.

The citric acid concentration of 1.92 w/w% was chosen based on literature, considering potential scaling propensity of the wastewater and not using a cleaning reagent with sodium [130,132,142]. This concentration is at the higher end of the typical citric acid cleaning protocol, but it was warranted for the experimental conditions.

3.4.3.1.4 Recovered Permeability

After the chemical cleaning was completed, the membrane was flushed with 2 L of Milli-Q water and then permeability was retested with an additional 2 L of Milli-Q. The purpose of the permeability being retested after the direct filtration and cleaning process was complete was to determine if the cleaning stages restored the membrane back to its original permeability or if irreversible fouling had occurred.

3.4.3.1.5 Fouling Analysis

After completing all direct filtration and cleaning steps for the ceramic membrane, fouling was evaluated in duplicate to determine how long it would take for flux to decline. For this test, 2 L of Sample 6 was recirculated through the ceramic membrane at 2 bar for 24 hours. Following the 24-hour-cycle, the same forward flush, chemical cleaning, and permeability process described earlier were repeated. During the fouling analysis, permeate weight was recorded every minute as opposed to thirty seconds, but the pressure was recorded at the same frequency as previous experiments. At the end of the fouling test, an IC analysis was conducted on both the permeate and the concentrate to determine final concentrations and removal efficiencies.

3.4.3.2 Polymeric Membrane

Treatment with the polymeric membrane followed similar procedures to the ceramic membrane, with adjustments due to its larger size. The experimental setup did not include an automated way for pressure to be recorded, so feed and concentrate pressure was recorded manually from the pressure gauges every minute. To maintain comparable conditions, treatment time was reduced, and cross-flow velocity was lowered to limit permeate production and reduce the rate of concentration in the feed. The recirculated

volume was also increased to 5 L, rather than the 2 L for the ceramic membrane, to further match feed concentration rates.

During direct filtration, feed water was recirculated for one hour, followed by 30-minute forward flush, chemical cleaning, and permeability tests all with 5 L influent. Samples for IC analysis during direct filtration were taken at 15, 30, 45, and 60 minutes. Citric acid was used for the chemical cleaning reagent with a 0.5 w/w%, following the manufacturer's recommendation [134].

Throughout direct filtration with the polymeric membrane the volume of permeate produced exceeded the weight limit on the scale being used, so the collection vessel was replaced with an empty one after the final weight recording before the 600 g limit was reached. Initial tests were planned to only be conducted with sand-filtered samples at 2 and 4 bar, and if the membrane produces positive results additional testing of unfiltered Sample 6 would also be tested at 4 bar.

The fouling analysis with the polymeric membrane was conducted for four hours, which is much shorter than the 24- hour ceramic test. However, nearly all 5 L of feed water was converted to permeate in this time frame. Pressure was stable during this analysis and was recorded every 15 minutes, while the permeate weight was recorded every 30 seconds. At the end of the fouling test, IC analysis was also performed on the final permeate and concentrate.

3.5 Analytical Methods

- **Particle Size Distribution (PSD)**

Particle size distribution was measured to assess whether the maximum and minimum particle sizes in the wastewater could clog membrane pores or feed tubing. Measurements were conducted with a Microtrac Bluewave particle size analyzer. The results were used to determine which pretreatment methods were tested in the second experimental phase. If the maximum particle size exceeded the hollow fiber tube diameter, clogging and reduced permeate production would be expected. Conversely, if particle sizes were sufficiently small, direct nanofiltration without a pretreatment step would be possible.

- **Ion Chromatography (IC)**

Ion chromatography (IC) with the Metrohm Schiedam IC was used to quantify the concentrations of key ions in the samples. Details on the equipment and analytical methods are provided in Appendix XXX. The primary ions of concern were sodium, sulfate, nitrate, nitrite, and ammonium, which historically fluctuate around regulatory limits in the Biomakerij effluent. IC results were combined with membrane removal efficiencies to

assess the feasibility of different water reuse applications. Nanofiltration does not remove mono-valent ions, so additional treatment might be needed to meet water reuse limits.

Each sample was analyzed in duplicate for both settled and unsettled samples. Dilutions of 0%, 25%, 50%, and 75% were prepared, and in cases where initial ion concentrations exceeded the measurement limit, the diluted values were used to back calculate the undiluted concentrations. All results are reported in mg/L. The minimum detection limit is 1 mg/L and the maximum detection limit is 100 mg/L, results reported exceeding these limits are less accurate than within this range.

- **Total Organic Carbon (TOC)**

The total organic carbon (TOC) was measured to determine the viability of the water for reuse similar to the IC measurements. Measurements were performed in duplicate with 0% and 50% dilutions, and all initial sample concentration fell within the machine's measurement range. Samples were filtered using a 45µm filter and 30 mL of filtrate was transferred into a glass tube and acidified with 1.6 mL of 1 M HCl. The samples were then sealed with an aluminum sheet and a cap and then analyzed in the TOC apparatus.

- **Total Suspended Solids (TSS)**

Total suspended solids (TSS) were measured in addition to the PSD analysis to provide additional insight into the particle load in the water samples. The total solids concentration also supported the comparison between settled and unsettled water samples and helped inform whether pre-filtration would be required to reduce solids and minimize pore clogging during membrane treatment.

TSS was measured using 0.7 µm glass microfiber filters in a vacuum filtration system. A 250 mL sample was filtered in each test. Due to irregularities, particularly in the unsettled samples, all measurements were performed in triplicate. Both the sample and weigh boat were pre-weighed, oven-dried for 24 hours, and re-weighed prior to filtration. After filtration, the retained solids and weigh boats were oven-dried at 150°C for 24 hours, cooled in a desiccator for 30 minutes, and then weighed again. Final results are reported in mg TSS per liter of sample.

- ***E. coli* Counts**

E. coli measurements were a critical parameter, as they directly determine compliance with water reuse standards for different irrigation classes. Since *E. coli* had not previously been measured in the Biomakerij wastewater, baseline levels were unknown before this study.

Samples were acidified with 0.1 M HCl to adjust the pH between 6 and 7 based on the measurement sheet manual, and the volume of HCl added was recorded for dilution corrections. The analysis used agar-based *E. coli* test sheets where 1 mL of the acidified sample was pipetted into the center of the sheet, evenly distributed, and allowed to rest for five minutes before incubation. Samples were incubated for 24 hours at 37°C, and then the colonies of *E. coli* were counted and multiplied by 100 to calculate coliform forming units (CFU) per 100 mL. Due to the delay in the delivery of the test sheets, Samples 1, 2, and 4 were analyzed on the same day they were collected. For samples with high *E. coli* concentrations dilutions of 1:10 and 1:100 were also measured to provide more accurate coliform counts.

- **Alkalinity**

Biomakerij wastewater typically has a high pH and a history of scaling issues, making alkalinity a relevant for both treatment performance and membrane stability. High alkalinity can also cause deterioration of one of the membranes tested, highlighting the importance of this parameter.

Alkalinity was measured with a 702 SM Titrino by Metronohm, using a titration endpoint pH of 4.3 based on carbonate speciation. The titrant used for the titrations was 0.1 M HCl, prepared by adding 8.33 mL of 85% HCl to 1 L of Milli-Q water. The results from the experimental procedure were then used in Equation 9 to calculate the final alkalinity. Results are presented in milliequivalents per liter (meq/L) and later determined how much of the alkalinity was from hardness and bicarbonate.

After all water quality measurements were completed form the first three samples, the data was compared to relevant regulatory standards. These results were then used in system Modelling to predict the concentrations of each parameter after membrane treatment. This Modelling informed whether post-treatment quality would comply with legal limits and whether pretreatment steps would be required.

$$Alk\left(\frac{mg\ CaCO_3}{L}\right) = \frac{A * N * 50{,}000}{mL\ Sample} \tag{9}$$

- A= volume of acid used to titrate the sample
- N = normality of the acid

- **pH and Electrical Conductivity (EC)**

The pH of the brewery wastewater was measured as a fundamental indicator of its overall chemical stability. Since the Biomakerij wastewater is typically alkaline due to the brewing process and cleaning agents used, monitoring pH is important for evaluating

both treatment efficiency, and monitoring permeate quality. Within membrane treatment, extreme pH values can influence membrane surface charge, permeability, and fouling tendency [20,41].

pH was measured using an inoLab IDS Multi 9420. Calibration was performed daily before each the first measurement was taken, using buffer solutions of 4, 7, and 10 to ensure measurement accuracy. All measurements were conducted at room temperature immediately after sample collection to minimize CO_2 exchanges.

Electrical conductivity (EC) was measured using the same inoLab system to assess the total dissolved ionic content of the wastewater. Measurements were taken at 20°C after calibration with KCl solutions. The unit for the EC measurements is µS/cm. EC was used to evaluate the overall salinity and ionic strength of samples, parameters that directly influence precipitation behavior and scaling potential during membrane treatment. EC was not measured for all samples, as ion concentrations determined by IC were sufficient for Modelling reuse and suitability. The only samples where EC was measured was Sample 1 to have a baseline EC and Sample 3 to calculate the amount of phosphoric acid to dose for precipitation reactions.

3.6 System Calculations and Modelling

3.6.1 Membrane System Calculations

In addition to the Modelling listed above the equations below were used to calculate the flux and behavior of each of the membrane systems.

Membrane surface area (SAm):

This is the available surface area of the membrane and has a large influence on the amount of permeate produced.

For the ceramic membrane:

$$SA_m = \pi * l_m * d_i \quad (1)$$

- l_m is the length of the membrane
- $d_i$is the inner diameter of the membrane

For the polymeric membrane a membrane surface area, this equation cannot be used due to the many hollow fiber tubes of slightly varying sizes. The surface area of 650 cm^2 was used as an article published in collaboration with NX Filtration using the same membrane used this surface area [135].

Filtrate flow rate (Q):

$$[\mathrm{L/h}]\ Q = \frac{\Delta g}{\Delta s} \tag{2}$$

- Δg (g) is the weight of permeate produced during the time interval
- Δs (h) is the time of each of the sampling intervals

Flux (J)

$$[L/m * h]\ J = \frac{Q}{SA_m} \tag{3}$$

Transmembrane Pressure (TMP)

$$P_{TMP} = \frac{P_f + P_c}{2} - P_P \tag{4}$$

- P_{TMP} is the transmembrane pressure [bar]
- P_f is the feed pressure [bar]
- P_c is the concentrate pressure [bar]
- P_P is the permeate pressure [bar]. This value is 0 bar because it is atmospheric.

Permeability (Kw)

$$K_w = \frac{J}{P_{TMP}} \tag{5}$$

Reynolds number

$$Re = \frac{\rho * Q * D_{in}}{\mu * A} \tag{6}$$

Standard deviation (σ)

$$\sigma = \sqrt{\frac{\sum_{i=1}^{N}(x_i - \mu)^2}{N}} \tag{7}$$

- σ= standard deviation
- x_i= data point included
- μ= population mean

- N = number of data points

Cross- flow velocity (CFV)

$$[m/s]CFV = \frac{Q}{SA_m} \quad (8)$$

3.6.2 System Modelling

Two models were constructed for this experiment, the first predicted the expected removal efficiencies of different parameters based on literature and manufacturer recommendations, and the second model which used the measured removal efficiencies to predict the final water quality parameter concentrations dependent on different recoveries and recirculation parameters.

The first model developed for this study builds on the previous membrane treatment model created for the pilot project at the Biomakerij. It incorporates the expected removal efficiencies of various parameters to estimate their concentrations in both the permeate and concentrate streams. Simulations were conducted for average, best-case, and worst-case water quality scenarios based on results from the initial experimental phase. The model was applied to both membranes being researched, the ceramic and polymeric membranes. Removal efficiencies for the ceramic membrane were derived from experimental data, whereas the polymeric membrane efficiencies were based on a combination of prior experimental results and the manufacturer's published specifications.

The initial rate of concentration was predicted based on the published removal efficiencies values previously discussed in the literature review. Following treatment more accurate Modelling could be used to calculate the fraction of feedwater recovered. The ceramic membrane ranged depending on system pressure with a rate of recovery from 0.05-0.06% while the polymeric membrane ranged from 2-5% recovery. Based on these recovery rates, with one module being used the ceramic membrane will produce about 18.6 L/day and the polymeric membrane will produce 1,400-1,900 L/day if there is no recirculation and the full capacity is treated. If a partial percentage of the total capacity of 50% or 75% is treated without recirculation, then the ceramic daily permeate production will be 9 – 14 L/day and the polymeric membrane will be 700 – 1,400 L/day.

The second model can be seen in Appendix E that utilizes two different differential equations for Modelling concentrations after dead-end filtration at various recovery efficiencies and final concentrations with implementation of multiple recirculation rates. This model can be used in an in-depth cost assessment to predict concentrations based on the different recoveries and recirculation rates to provide more insight on system operating costs and parameters.

4 Results and Discussion

4.1 Water Quality of Collected Samples

This section presents the results of each of the water quality measurements for all six samples collected from the Biomakerij's daily capacity of 143 m^3/day at different points in time. The results of the water quality analysis will be explained in terms of chemical, physical, and biological characteristics. This section also identifies the water quality fluctuations over time as each of the samples were collected to identify the wastewater trends to better design a treatment system. Then the potential impact of the identified trends on the membrane treatment system will be assessed. Throughout all of the samples the pH remained relatively constant with an average of 8.3 ± 0.15. The samples collected appeared to acidify over time between the date of collection and use for the brewery treatment experiments, decreasing in pH by an average of 0.5 ± 0.1. The samples collected had headspace for oxygen exposure which likely allowed for continued biological activity, CO_2 dissolution, and further nitrification possibly causing this decrease in pH [18,143,144]. The EC was not measured for all samples, because the IC concentrations were sufficient for reuse, however the Sample 1 EC was 2.82 µS/cm and the Sample 3 EC was 3.27 µS/cm, both samples with a higher cation concentration than anion.

4.1.1 Chemical Water Quality Characteristics

The chemical water quality analysis focused on ion and chemical parameter concentrations, conducted by measuring ion chromatography, TOC, and alkalinity. These were selected based on the legal limits released by the RIVM and the effluent wastewater quality history at the Biomakerij [108]. Table 4.1 presents the average, maximum, and minimum concentrations of the key parameters across all 6 samples collected. Appendix Table **A.1** contains a table with every ion concentration for each sample. The table also includes the legal reuse limits for the key parameters that have legal reuse limits. The shading of the cells signify whether a concentration is below the legal limit (green) or if the concentration exceeds the permissible reuse limit (red). The monovalent ions above the legal limit are of particular concern, as they have lower removal efficiencies from nanofiltration [18,145].

The variations in chemical concentrations across the samples are attributed to differences in the types of beers brewed and ongoing adjustments to chemical softeners and cleaning agents. The averages of nitrite and nitrate concentrations are skewed higher by Sample 6, which also had a significantly lower sulfate concentration. The reduction in sulfate concentration was the result of switching the iron dosage from iron sulfate to iron chloride (Table 3.1). This change in dosing compound effectively decreases the sulfate concentration below the reuse limit, while simultaneously mitigating the dangerous buildup of hydrogen

sulfide in the MNR greenhouse [115]. The sodium concentrations are within the middle to high range expected of brewery affluents as seen in Table 2.3 [41,92,95].

Table 4.1 Chemical Water Quality Results from all Samples Collected

Ion	Unit	Average Conc. Samples 1-6	Maximum Concentration	Minimum Concentration	Legal Limit
Fluoride*	[mg/L]	1	4 (6)	<0.1 (2,3,4,5)	1.5
Sodium*	[mg/L]	592	784 (2)	458 (6)	120
Ammonium*	[mg/L]	9	29 (2)	<0.1 (4,5)	1.5
Chloride*	[mg/L]	48	87 (3)	27 (5)	100
Nitrite	[mg/L]	2	4 (6)	<0.1 (2,3)	N/A
Bromide	[mg/L]	5	5 (1,3,4,5,6)	4 (2)	N/A
Nitrate*	[mg/L]	1	4 (6)	1 (1,2,3,4,5)	10
Potassium	[mg/L]	43	57 (4,5)	25 (1)	N/A
Magnesium	[mg/L]	37	61 (4,5)	19 (1)	N/A
Calcium	[mg/L]	104	135 (6)	64 (1)	N/A
Sulfate*	[mg/L]	153	238 (2)	10 (6)	100
Phosphate*	[mg/L]	1	5 (6)	<0.1 (1,4,5)	1
pH	[-]	8.3	8.1 (1,6)	8.5 (5)	
TOC	[mg/L]	37	49 (3)	30 (2)	
Alkalinity	[meq/L]	63	81 (5)	25 (6)	
% Alkalinity from hardness	[% meq/L]	15%	33% (6)	7% (1)	

* The ions with asterisks are particularly important for reuses as they are the ions with legal reuse limits [105,108].

The shading of the cells indicate if the average, maximum, or minimum concentrations are above or below the legal limit, green shading represents below the legal limit and red shading represents above the legal limit. The values in the parenthesis besides the values in the maximum and minimum columns are the sample number the concentration is from.

The TOC concentration remained relatively stable in comparison to other parameters measured, varying by 18 mg/L between the Sample 3 maximum and Sample 2 minimum. Figure 4.1 shows Sample 3 with the highest concentration of 48.5 mg/L due to the system overflow. Both membranes have a high expected removal efficiency of TOC, so after NF treatment the permeate concentration is expected to be below the legal reuse limit [41,91,95,105,108]. However, the recirculation of the concentrate will increase the influent TOC concentration resulting in a greater likelihood of a removal efficiency lower than anticipated [41].

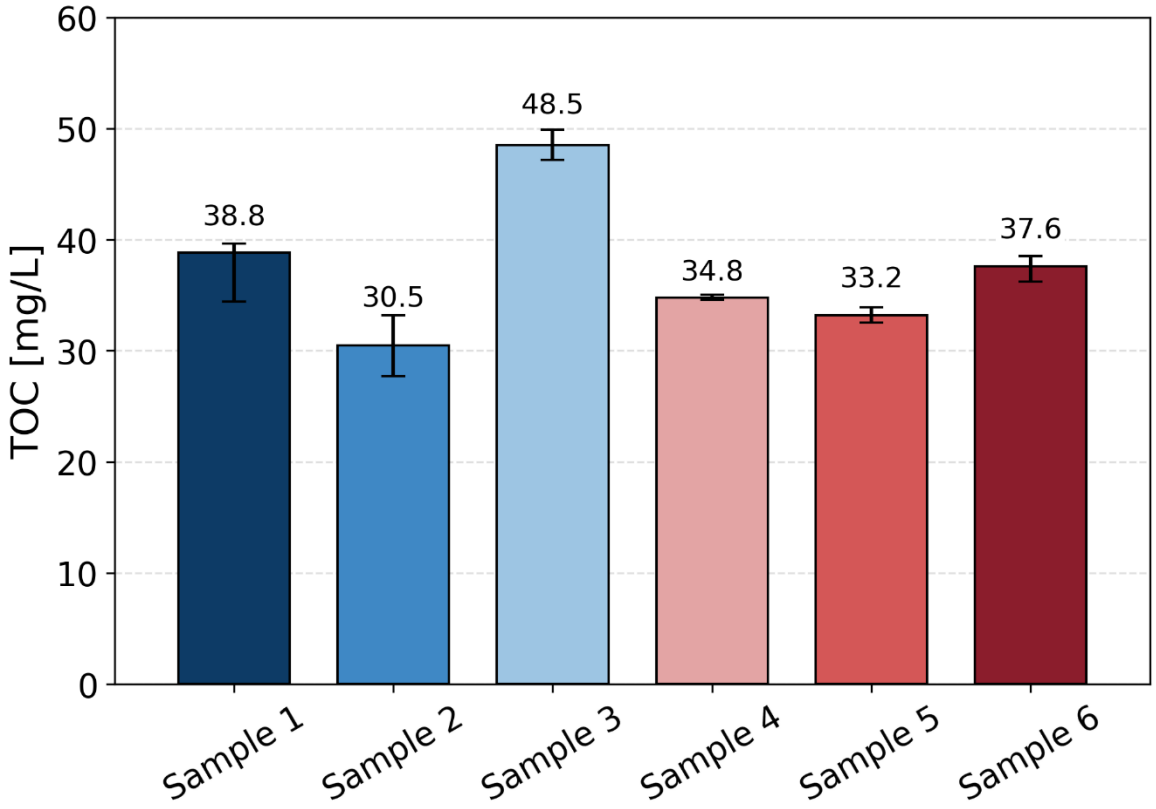

Figure 4.1 TOC [mg/L] Concentrations of all Samples Collected

TOC concentrations of all brewery wastewater samples collected, showing variability between sampling events. The highest concentration during the overflow period is from Sample 3 due to overflow.

In Table 4.1, the average alkalinity of all the samples is 63 ± 18 meq/L. This wide range seen in Figure 4.2 further emphasizes the concentration fluctuations over time due to the brewery variability. The figure also includes the alkalinity concentrations alongside regional tap water to emphasize the high concentration of Samples 1-5. The elevated alkalinity could be from minerals in the pre-treated ground water or from cleaning and softening chemicals used in the brewery [78,120].

Sample 6 has the minimum alkalinity of 25.4 meq/L, 55 meq/L less than the maximum concentration of 80.4 meq/L of Sample 5. The lower alkalinity of Sample 6 is likely due to a chemical detection sensor placed in the brewery prior to sample collection, significantly reducing the total chemicals used. The sensor was installed prior to the collection of Samples 4 and 5, the large equalization tank volumes delayed its effects. Additionally, the pipe scaling and complete pipe blockage observed right before Samples 4 and 5, produced mineral precipitates that were scraped off during maintenance. The resulting fine powder of scalent material may have partially redissolved into the brewery wastewater, contributing to the subtle increase in alkalinity levels [73]. High alkalinity levels in nanofiltration influent are a concern for polymeric performance and can cause irreversible fouling [41].

Table 4.1 also shows that approximately 8% of the total alkalinity in the brewery wastewater is from the total hardness in the sample, serving as an indication that most of the alkalinity originates from carbonate and bicarbonate species [18,120]. The hardness was calculated from the IC measured magnesium and calcium concentrations, while iron, strontium, and manganese concentrations were not included because of their negligible concentrations.

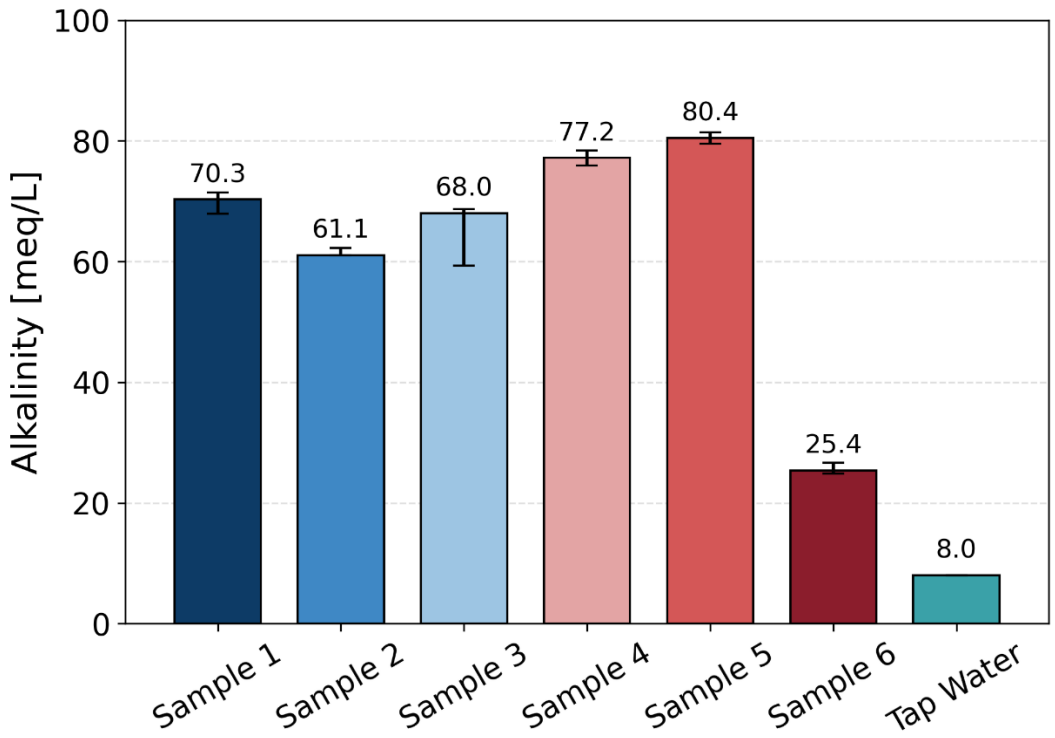

Figure 4.2 Alkalinity [meq/L] of all Samples Collected

The figure shows the alkalinity over the time which samples are collected relative to the tap water in the region to indicate the hardness either from the groundwater source or added in the brewery. The decrease in concentration between Sample 6 and the other samples is a result of the decreased use of chemicals in the brewery.

4.1.2 Physical Water Quality Characteristics

The physical characteristics of the brewery wastewater samples specifically pertain to the particles that pose a risk of plugging the polymeric membrane fiber's inner diameter. The samples' propensity for plugging the membrane's fibers was assessed through the PSD and TSS of the samples. In addition to posing a concern for plugging the membrane fibers, higher particle load typically results in more rapid fouling [28,31,51]. The particle size distribution (PSD) shows the particle sizes, and the total suspended solids (TSS) quantifies particle concentration. By measuring both TSS and PSD, the immediate and long-term risks to membrane performance can be assessed. The physical particles within each of the samples can be seen in Appendix Figure A.1 through Appendix Figure A.6.

Figure 4.3 depicts the PSD for both the settled and unsettled samples. The dashed red line represents inner diameter of a fiber in the polymeric membrane. Particles exceeding this threshold of 700 µm risk plugging the fibers at the inlet of the membrane which can result in larger trans-membrane pressure, and a decrease in flux [14,18,141]. In addition to plugging

a few fiber inlet, particles accumulate on the inlets accelerating cake layer formation and blocking more fibers, further contributing to hydraulic resistance and performance decline [28,47,51,53]. The particle size is less of a concern for the ceramic membrane due to its much larger inner diameter of 7,000 µm.

Sample 3 clearly exhibits a maximum particle size 300 µm larger than the other unsettled samples and is the only sample exceeding the 700 µm threshold. This was a further reflection of the impact a system overflow has on the brewery wastewater quality. During a system overflow the effluent bypasses the drum filter maintaining the large particles that are typically removed by the 10 µm drum filter. Resulting in Sample 6 being the worst-case scenario for particle sizes and potentially causing a rapid decline in polymeric membrane flux due to fouling.

To ensure polymeric membrane robustness under variable conditions, pretreatment is necessary to remove particles above the inner diameter threshold and reduce total suspended solids concentrations [18,71,72,146]. Reducing particles larger than the fiber inner diameter prevents the pore blocking mechanism, while lowering the overall solids concentration by slowing cake layer formation, both helping to maintain a stable membrane flux [28,53,71,72,146]. Alternatively, during periods of overflow the polymeric membrane treatment could be halted until the influent brewery wastewater stabilized.

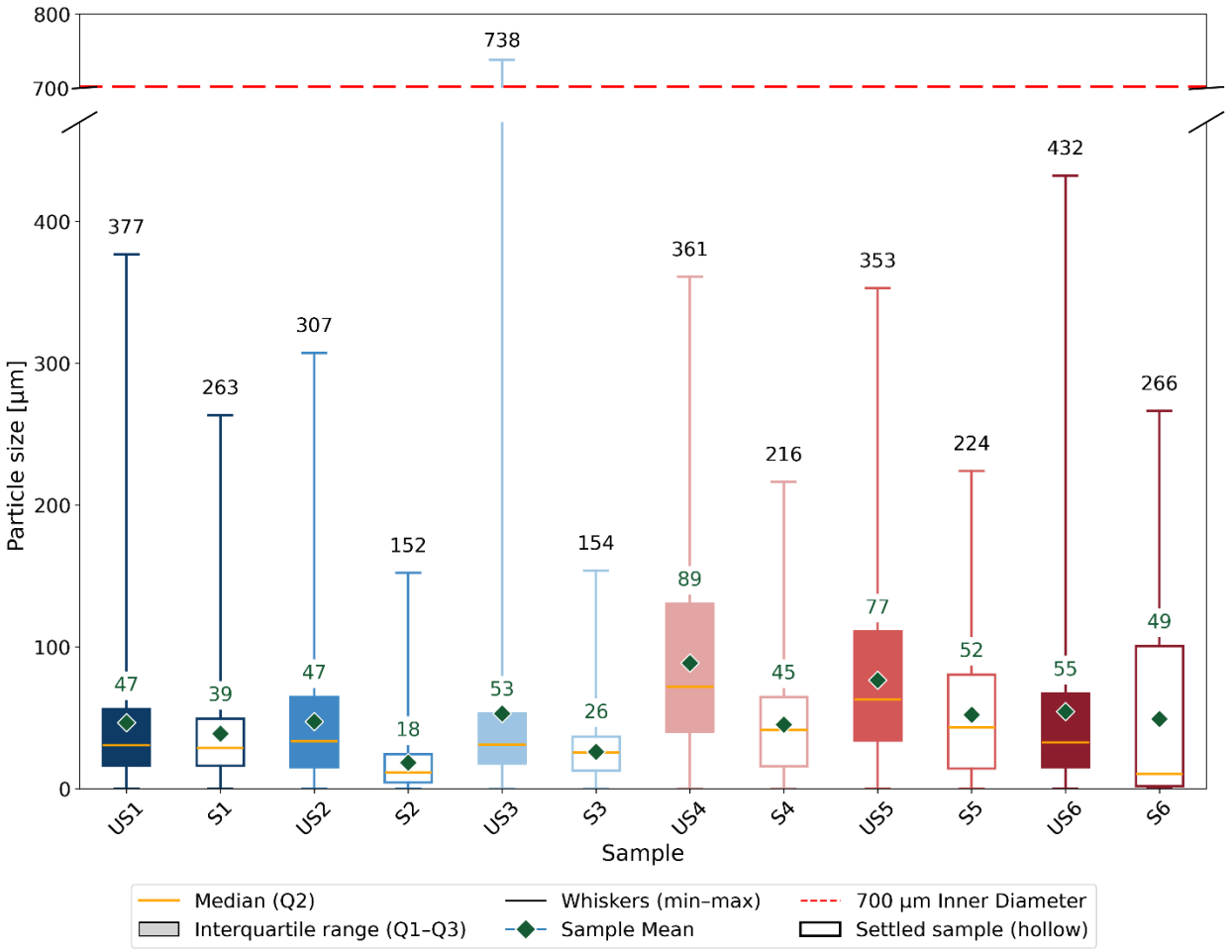

Figure 4.3 Particle Size Distribution [µm] of all Samples Settled and Unsettled

The box plot above shows the size distribution of particles in each of the settled and unsettled samples. The shaded boxes show the unsettled samples and the hollow boxes are the settled samples. The 0.7 mm cutoff is the inner diameter of the fibers in the hollow fiber membrane.

While PSD, or maximum particle size, governs the risk of fiber-inlet plugging, TSS provides a measure of overall fouling potential and cake layer formation [28,53].

The volume of suspended solids in the influent brewery wastewater directly influences long-term membrane performance, because higher concentrations accelerate cake layer formation, increase transmembrane pressure, and increase the cleaning frequency needed [28,47,51,53]. Figure 4.4 shows TSS concentrations for each sample. Sample 3 has the largest volume of solids, with an unsettled TSS of 133.3 mg/L and a settled TSS of 68.0 mg/L, reflecting the impact of overflow periods on TSS concentrations, making it the worst-case scenario. Conversely, Sample 2 had the lowest TSS concentrations with 9.3 mg/L for unsettled and 4.0 mg/L for the settled sample. Due to these lower concentrations Sample 2 is the most favorable influent condition for physical water quality, and thus the best-case-

scenario for membrane operation due to less particulate loading and reduced fouling potential [18,47,51,53]. The approximately 14-fold difference between the unsettled TSS concentrations of Sample 3 and Sample 2 demonstrates the substantial impact operational conditions of the brewery and MNR system can have on solids loading entering the membrane system.

After a settling period of a week, Sample 3 still had the largest concentration of solids of the settled samples with a concentration of 68 mg/L, more than double the 29.9 mg/L concentration of settled Sample 6, the next largest settled concentration. A sludge volume index (SVI) test was conducted for Sample 1, however, the solids layer on the bottom was too thin to provide conclusive results, the results can be seen in **Error! Reference source not found.**. Due to the inconclusive results of Sample's SVI testing, sample volume needed for SVI testing was not accounted for when collecting Sample 3, so there was insufficient volume to conduct further SVI testing. These observations further highlight the need for a pretreatment method to reduce suspended solids concentration prior to membrane filtration to prevent rapid fouling, cake layer formation, and maintain flux stability under variable brewery operating conditions, especially for the polymeric membrane [18,47,51–53]. Based on these conclusions from TSS and PSD the pretreatment method of sand filtration was explored, and the results can be seen in Section 4.3.2.

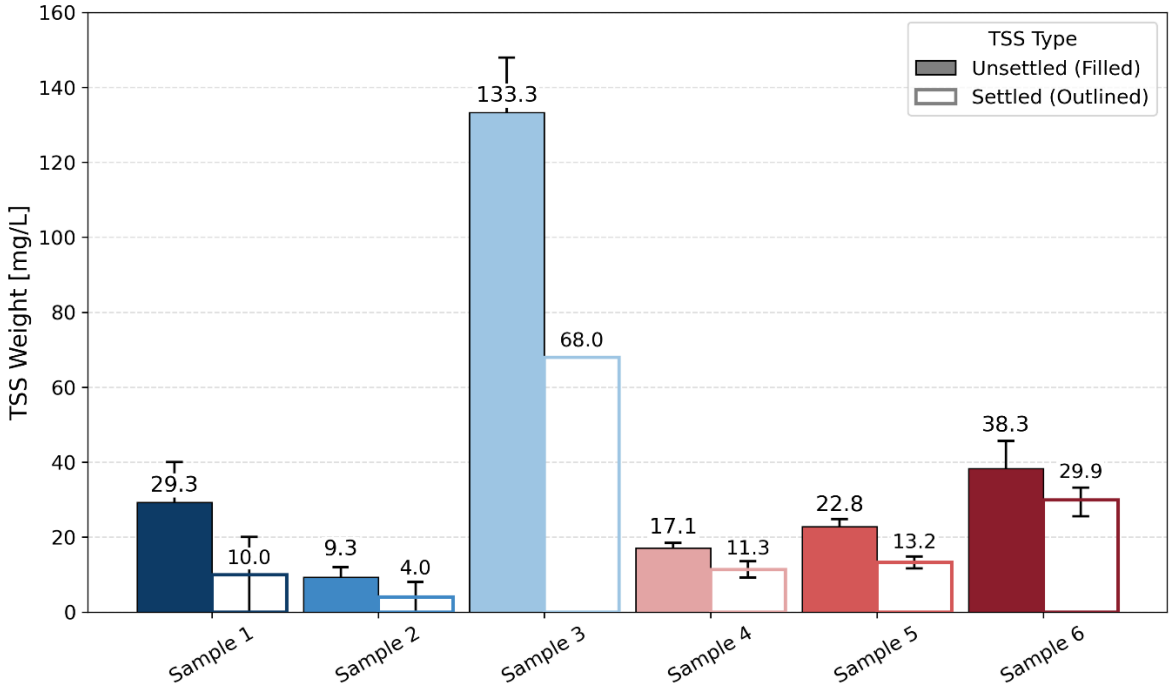

Figure 4.4 TSS [mg/L] Concentration of all Samples

The TSS concentrations of all samples both unsettled (filled) and settled (outlined).

4.1.3 Biological Water Quality Characteristics

The biological quality of the brewery wastewater from the Biomakerij had not been measured prior to this thesis. Due to brewery wastewater often containing *E. coli* (a fecal matter indicator), measurements were conducted to determine its appropriate reuse classification [5,80,81]. As mentioned in Section 3.5, these measurements were conducted in an educational lab, and verification of these results in an accredited lab is recommended prior to implementing reuse.

Across the initial five samples, *E. coli* concentrations were relatively consistent, with the exception of unsettled Sample 3, due to the system overflow, allowing more *E. coli* to bypass the MNR system and drum filter. As shown in Figure 4.5 plot A on the left, the *E. coli* concentration of unsettled Sample 3 was 7920 CFU/100 mL, compared to the next highest, Sample 5 with a concentration of 2160 CFU/100 mL and the lowest concentration from Sample 2 with a concentration of 120 CFU/100 mL. As for the settled samples, Sample 3 still has the highest concentration of 960 CFU/100 mL, the second largest also being settled Samples 4 and 5 with a concentration of 480 CFU/100 mL, and the lowest settled sample concentration is still Sample 2 with a concentration of 300 CFU/100 mL. The lower concentrations in the settled samples for all but Sample 2, show that most often settling lowers bacterial concentration, but still does not reach Class A reuse regulations [105,106].

Similar to the trend between settled samples having lower bacterial concentrations than the unsettled samples, the trend in *E. coli* concentrations exactly matches the trend in TSS concentrations. Thus, with more particles in the sample there is greater bacterial concentrations [53].

In the same Figure 4.5, in plot B on the right shows the *E. coli* concentrations for Sample 6, which exhibited significantly higher concentrations of 64,800 CFU/100 mL for the unsettled sample and 59,400 CFU/100 mL for the settled sample. This is nearly 10 times larger concentration than the highest concentration of the first five samples, which is a result of the domestic and industrial MNR tanks being combined. The concentrations of Sample 6 exceed the reuse legal limits by several orders of magnitude. To achieve Class A (Figure 2.7) reuse standards, Sample 6 requires a log-4 removal [105,106].

These findings show two key implications, the first being overflow events and influent variability influence the fecal matter present in the brewery wastewater [110,111]. The second is that only allowing the sample to settle prior to reuse without a tertiary treatment is insufficient for agricultural reuse [85,107]. Based on typical nanofiltration *E. coli* removal efficiencies, nanofiltration should be able to remove sufficient concentrations to qualify for reuse classifications [102,103,107].

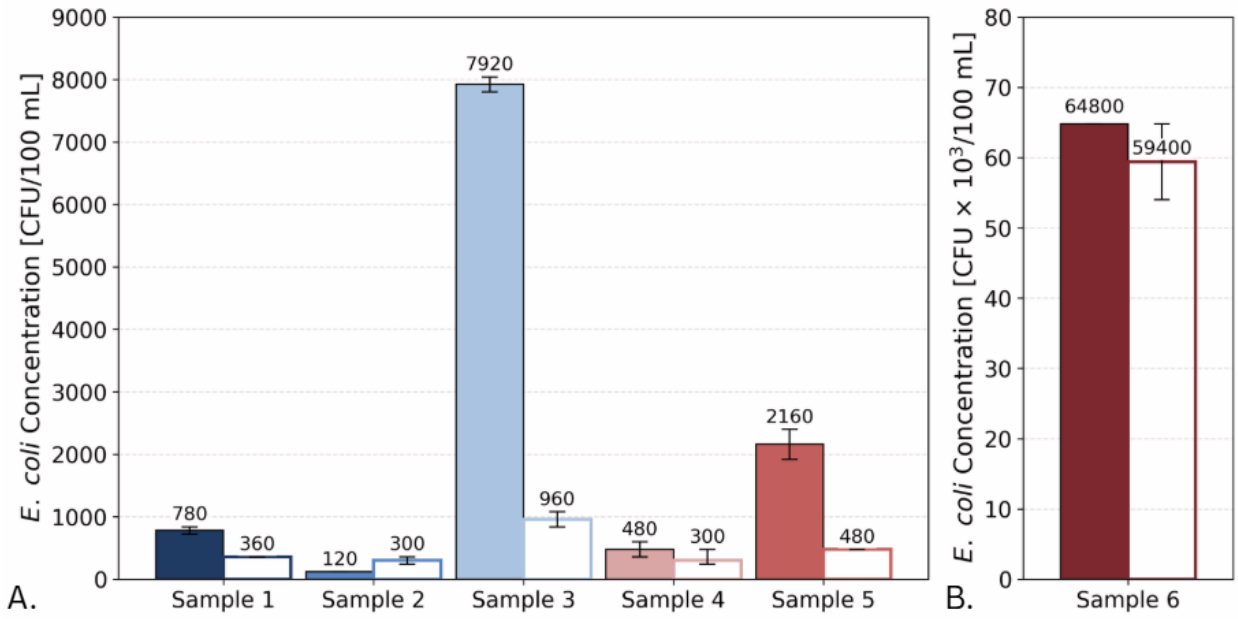

Figure 4.5 *E. coli* [CFU/100 mL] Concentration of all Samples Settled and Unsettled

Plot A on the left is the E. coli concentrations for Samples 1-5, and Plot B on the right shows the E.coli concentrations for Sample 6 with the y-axis in the thousands. The shaded bars are the unsettled samples, while the unshaded bars are the settled samples. The values above the bars are the averages, and the whiskers show the maximum and minimum concentrations.

Figure 4.6 outlines the biological reuse class regulations previously identified in Section 2.5 and classifies which of the samples meet the legal regulations. Unsettled Samples 1, 3, 5, and 6 along with settled Sample 6, do not qualify for any reuse classes and require a log 2 to log 4 removal to achieve Class A regulations. Unsettled Sample 2 and settled Samples 1-5 qualify for Class C and D reuse, still needing a log 1.1-2 reduction to reach Class A quality.

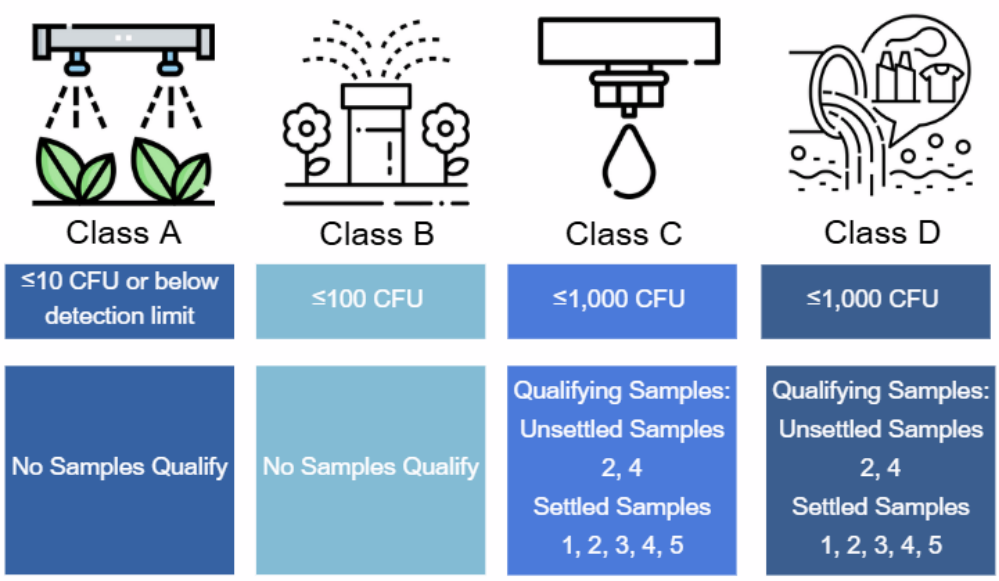

Figure 4.6 Initial Sample Reuse Qualifications

Unsettled Sample 2 and settled Samples 1-5 qualify for Class C and D reuse, while unsettled Samples 1, 3, 5, and 6 and settled Sample 6 do not qualify for any reuse. None of the samples qualify for Class A and B reuse.

4.2 Membrane Experimentation Results

Having established the influent characteristics, the following section evaluates how these conditions influenced membrane performance.

4.2.1 Ceramic Membrane

4.2.1.1 Ceramic Membrane Permeability Results

Permeability testing was first conducted to determine the baseline performance of the ceramic membrane prior to beginning brewery wastewater treatment. Based on the results of the permeability tests, an influent volume of 2 L was selected to ensure sufficient permeate volume for water quality analysis.

Four separate Inopor 0.9 nm ceramic membranes were evaluated during permeability testing. The first was used for preliminary permeability testing and ion removal efficiency calculations. Membranes two and three were intended to be used for brewery treatment, but produced little to no permeate, showing a much lower permeabilities around 1-2 LMH*bar^{-1} compared to the 7-8 LMH*bar^{-1} permeability measured of the first membrane. This performance discrepancy from membranes two and three highlights the potential pore size variability in ceramic nanofiltration membranes, reflecting that ceramic NF membrane technology and its pore size consistency is not fully standardized yet [90]. A similar study

using the same NF ceramic membranes found that nominal NF pore size in ceramic membranes can differ from the true pore size structure as a result of manufacturing tolerances and sintering processes [90].

Membrane four exhibited permeability comparable to membrane one and was therefore selected for all brewery wastewater treatment tests. The average permeability after initial permeability baseline testing was found to be 7.5 ± 0.4 LMH. bar^{-1}, consistent with values reported for commercial ceramic NF membranes [94,136].

Permeability data recorded during the brewery treatment tests is shown in Figure 4.7. During brewery wastewater treatment, permeability varied across operating conditions, with minimum permeabilities ranging from 1.84 to 2.86 LMH*bar^{-1}. However, all maximum permeabilities were quite similar ranging from 3.45 to 3.63 LMH*bar^{-1}. The shaded lines in the figure represent the raw data, while the solid lines are the rolling averages. The constant peak fluctuations in the raw shaded data are a result of the ceramic membrane low permeability and short time intervals of the scale collecting the permeate. The trends between the different operating conditions are quite similar, beginning between 1.8 - 2.8 LMH*bar^{-1} and increasing by about 0.6 - 1.3 LMH*bar^{-1} throughout testing. One main difference in permeability trend is three hours and fifteen minutes into the 4 bar direct-filtration tests, there is a decline in permeability from 3 to 2.5 LMH*bar^{-1}. This is consistent with the higher propensity of fouling discussed with larger particle loads at higher TMP [14,18].

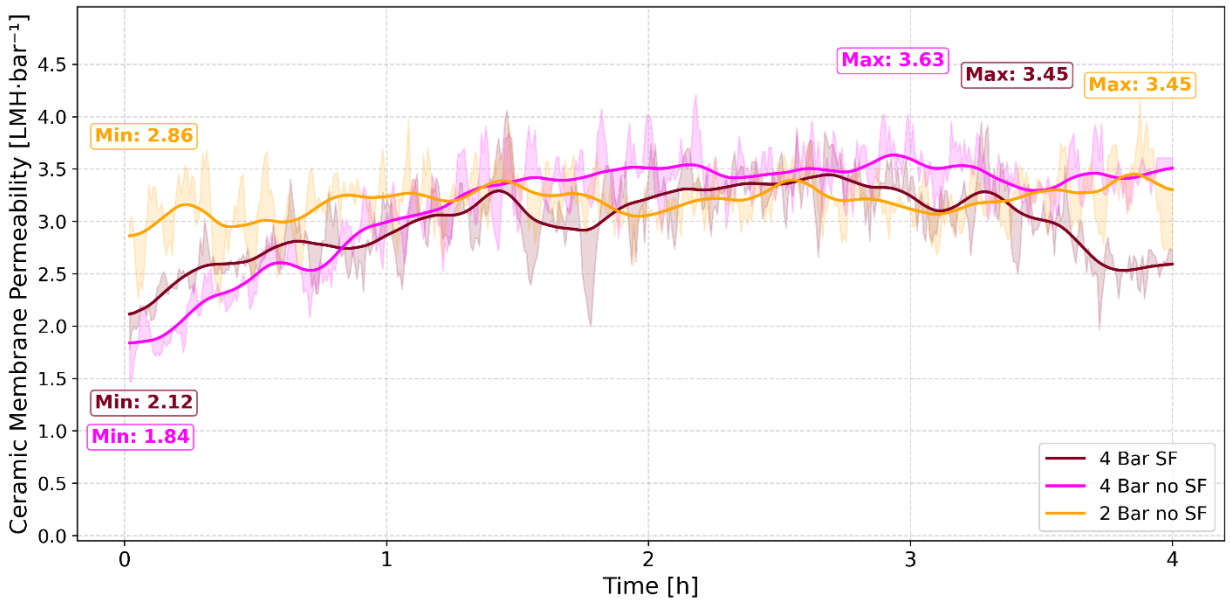

Figure 4.7 Permeability [LMH*bar^{-1}] of Ceramic Membrane During Brewery Wastewater Treatment

The solid lines represent the rolling averages of the permeability during testing, and the shaded background values represent the raw data. The raw data fluctuations are a result of low permeability relative to the frequency of permeate production being recorded.

4.2.1.2 Ceramic Membrane Flux Results

After the preliminary permeability testing, the four-hour brewery tests were conducted using Samples 4 and 5. Followed by a one-hour forward flush (Flush), one-hour citric acid (CA) chemical cleaning, and one-hour flush with milli-Q water (Perm) to determine the permeability after treatment and cleaning.

The ceramic membrane had an average permeate total recovery of 3.3% at 2 bar and 5.8% at 4 bar during the four hour treatment of brewery wastewater. As shown in Figure 4.8, normalized flux increased gradually, from 0.8 – 1.1 J/J_0 to 1.25 - 1.5 J/J_0, during the first two hours of treatment for all conditions, indicative of system stabilization during the initial conditioning phase of the membrane [14,53]. The flux trends for 4 bar direct treatment and sand filtered samples were comparable, both increasing by about 0.6-0.8 J/J_0. However, there is an observed decline of 0.3 J/J^0 the last 45 minutes, of the 4 bar no SF operating, that neither of the other operating conditions experienced. This is likely associated organic or particulate fouling with the cake layer formation mechanism, reflecting the influence of higher TMP and suspended solid volumes on fouling behavior consistent with the results seen in the permeability measurements [14,18,47,53]. The sand filtered 2 bar tests

increased even more gradually with a 0.4 J/J^0 increase in normalized flux over the four hour treatment duration, half of the 0.8 J/J^0 increase experienced by the 4 bar no SF testing.

The overall trends of each operating condition's normalized flux remained nearly identical to their permeability trends, indicating the pressures selected for testing did not have a significant influence on the resulting permeability [94,136]. Similar to Figure 4.7, the permeability plot, the shaded lines around the cumulative averages represent the raw scale measurements, which are noisy due to the low permeate production and short time intervals of the laboratory scale (precision ± 0.03g, accuracy 01g). Despite measurement noise, clear performance trends were observed across all operating conditions.

Figure 4.9 includes the same line plot with normalized flux during the treatment of brewery wastewater seen in Figure 4.8, alongside the average, maximum and minimum flux during the cleaning following the brewery treatment. The permeability from all operating conditions, ranging from 1.05 to 1.20 J/J^0 on average, with the 4 bar no SF treatment having the highest post-treatment permeability recovered and 2 bar no SF the lowest. The post-treatment flux of the permeability tests are nearly identical to the averages measured during the first hour of treatment which ranged from 1.1 to 1.2 J/J^0, suggesting that the membrane recovered to its original permeability [51,52]. The variability in the post-treatment flux as opposed to a general decreased is indicative of reversible fouling opposed to irreversible fouling [52,53].

Overall, the results indicated that ceramic nanofiltration maintained stable and reproducible performance under varying operating conditions. The similarity between normalized flux trends across all tests and the consistent flux recovery during the permeability tests demonstrate that the fouling was largely reversible and effectively mitigated with the cleaning protocol [51,90,94]. The minimal difference in normalized permeability between pressures, with a 0.15 J/J^0 difference, suggest that TMP had a limited effect on short-term fouling development within the 2-4 bar range, which aligns with the low fouling propensity for ceramic NF membranes [94,136]. These findings confirm that the ceramic membrane is robust for variable brewery wastewater conditions, achieving reliable hydraulic stability with manageable fouling behavior, though testing a broader range of pressures is recommended to confirm long term operational resilience [40,41,52,53].

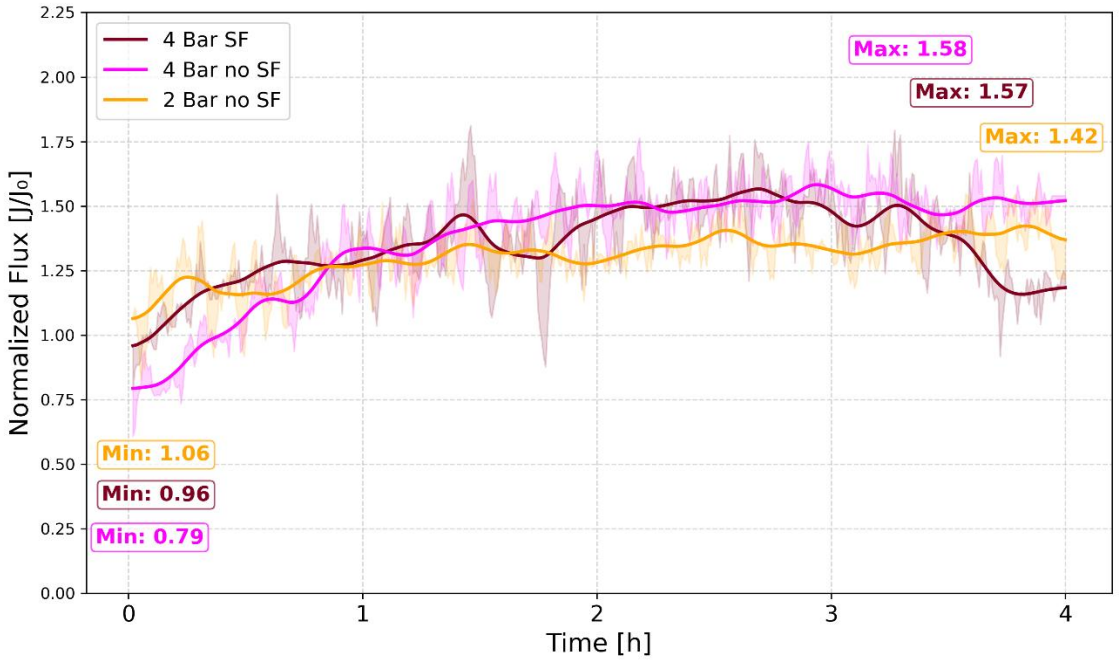

Figure 4.8 Ceramic Membrane Normalized Flux [J/J_0] During Brewery Wastewater Treatment

The figure has the rolling averages of the normalized flux during the brewery treatment in the solid lines with the raw data shown as the shaded lines. The maximum and minimum values of each operating condition are labeled on the plot.

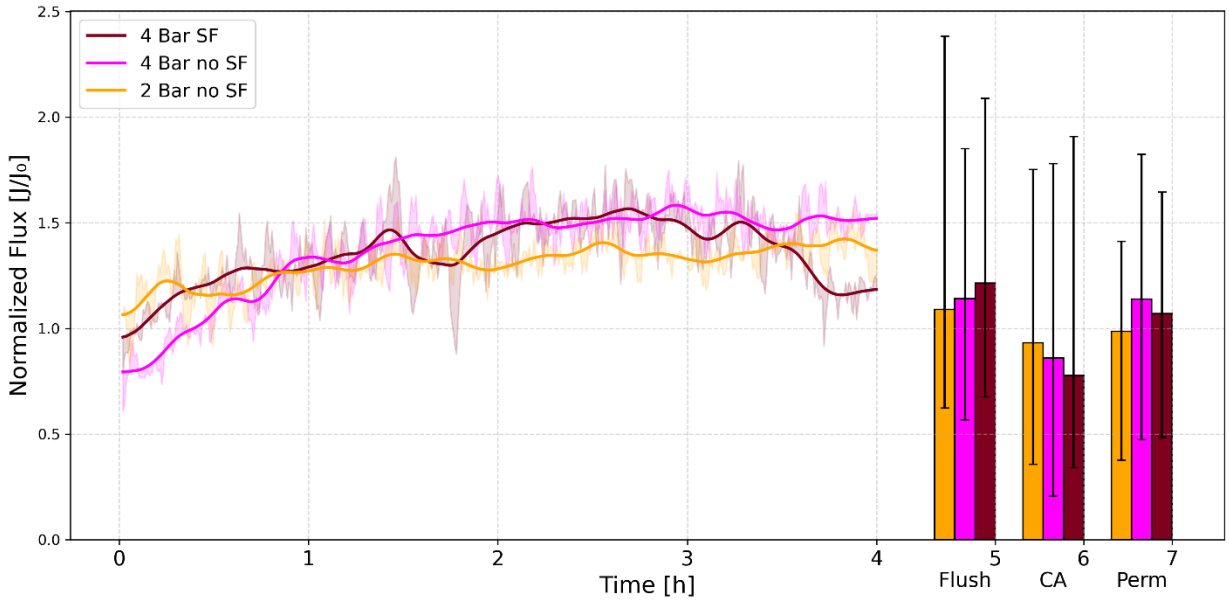

Figure 4.9 Normalized Flux of Ceramic Membrane Brewery Wastewater Treatment Including the Post-Treatment Cleaning

This figure shows the same line graph as Figure 4.8 on the left, relative to the average normalized flux measured during the post treatment cleaning in the bar graph on the right. The labels of the bar graph are "Flush" for forward flush, "CA" for citric acid chemical cleaning, and "Perm" for permeability testing. The values on the x-axis show at what hour into the testing the measurements were completed.

4.2.1.3 Ceramic Membrane Fouling Test Flux Results

After limited fouling was observed during the four hour brewery wastewater treatment, two 24-hour fouling tests were conducted at 2 bar using 2 L of unfiltered Sample 6 to have a better understanding of the fouling behavior. Figure 4.10 shows the permeate flux throughout the experiment for the two tests. In both experiments, the flux initially increased during the first 3-5 hours, with maximum fluxes at 7.78 LMH and 7.40 LMH for Tests 1 and 2 respectively. The initial flux increase was also observed in the shorter brewery treatment tests, reflect pressure stabilization, commonly observed in pressure-driven membranes [14,45].

After peak flux was reached, both tests exhibited a gradual decline over the remainder of the test, consistent with fouling, likely cake layer formation [14,18,53]. The flux decreased to 3.71 LMH in Test 1 and 4.63 LMH in Test 2, when the fouling tests were complete. This 40-50% decline from peak flux is within the range commonly found for nanofiltration of influents with high organic loads [31,41,47]. A visual inspection of the membrane inlets and outlets was done following the fouling tests, not a full bisection, as show in Figure 4.12, which showed minimal impact from treatment, which was expected for ceramic nanofiltration of brewery wastewater [39,40,94].

The cleaning performance of the fouling tests can be seen in Figure 4.11. During the forward flush, flux recovered to 7.75 LMH after Test 1 and 7.48 LMH after Test 2, showing a 96-98% return to the first experiments peak flux. However, the permeability following Test 1 was 6.75 LMH while after Test 2 it was 5.80 LMH, roughly a 1 LMH decline between Test 1 and 2, suggesting a small amount of irreversible fouling likely occurred [53]. This partial loss of recoverable permeability can be seen in ceramic membrane treatment performance of brewery wastewater, where chemical cleaning cannot completely remove the effects of irreversible fouling [14,40,47,94]. Although, this irreversible fouling could be mitigated, the strength of the ceramic membrane material allows for a cleaning agent with a higher chemical concentration to be used without damaging the membrane, possibly minimizing the irreversible fouling [39,94,130].

Based on the flux trends experiencing a gradual overall flux decline, rather than any abrupt flux declines, indicate that the fouling mechanisms likely occurring are particulate fouling cake layer formation, rather than biofouling or scaling, aligning with typical fouling behavior

observed in ceramic membranes [39,41]. The overall flux stability, high flux recovery, and minimal irreversible fouling support the ceramic membrane material's robustness [40,94].

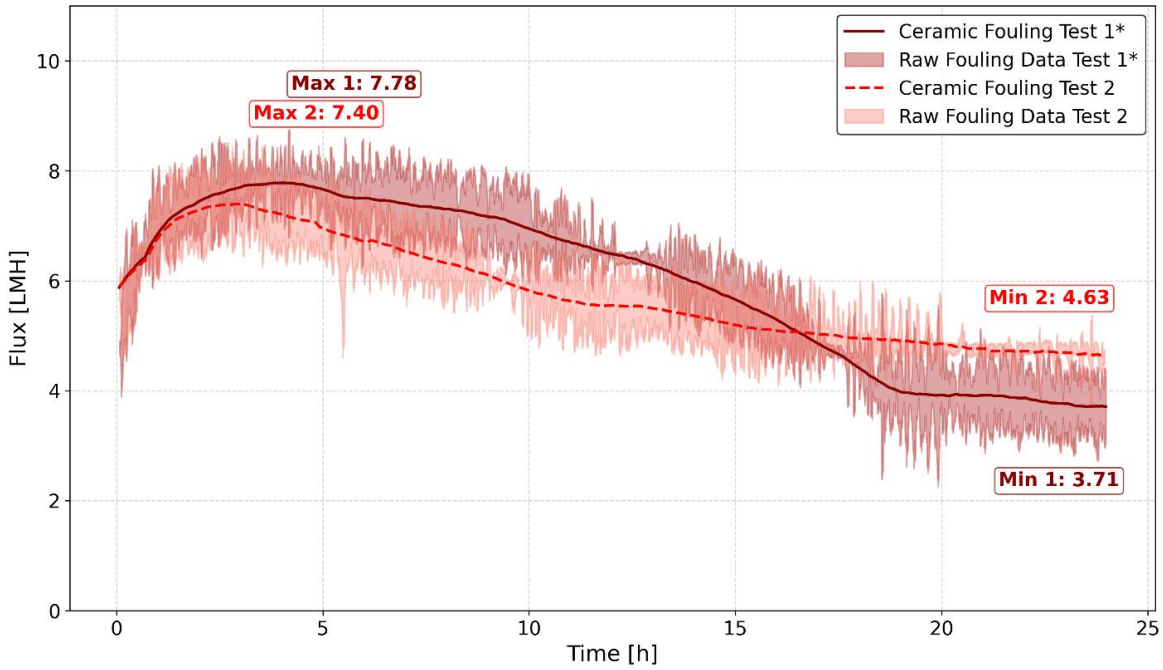

Figure 4.10 Flux [LMH] from Ceramic Membrane Fouling Tests

The solid and dashed lines are the rolling averages of the flux during the ceramic membrane fouling tests

** Following Fouling Test 1, forward flush, chemical cleaning, and permeability measurements were run for 30 minutes each prior to Fouling Test 2.*

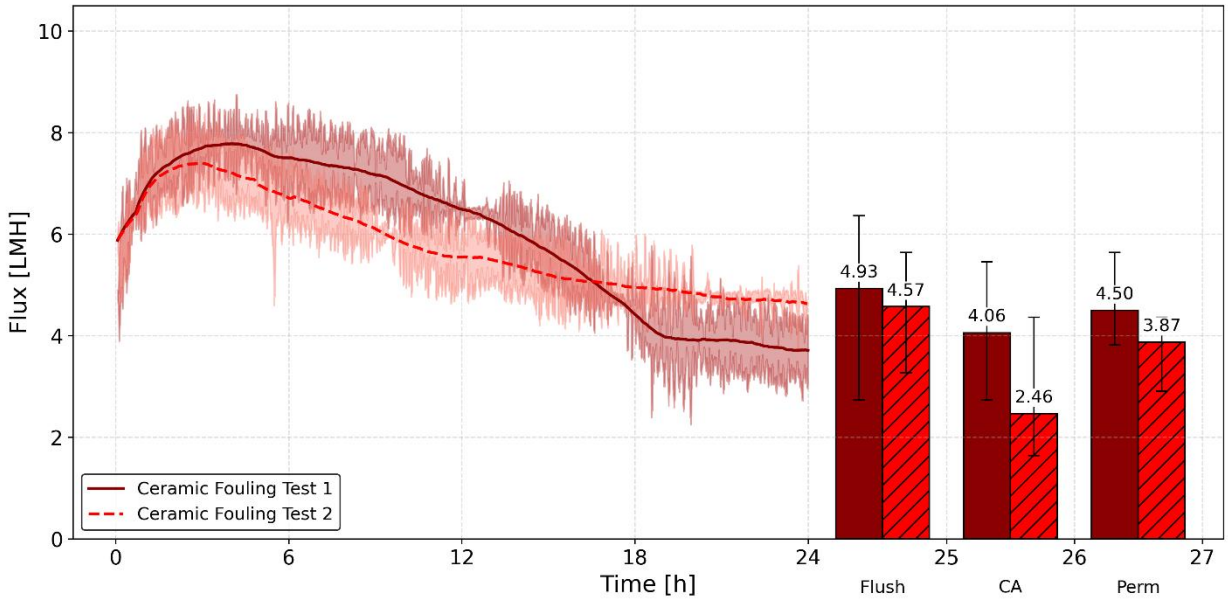

Figure 4.11 Flux [LMH] from Ceramic Membrane Fouling Tests Including Post-Treatment Cleaning

This figure shows the same plot as Figure 4.10, but with the average flux in the post treatment cleaning procedures. "Flush" is the forward flush, "CA" is the citric acid chemical cleaning, and "Perm" is the pos-treatment permeability.

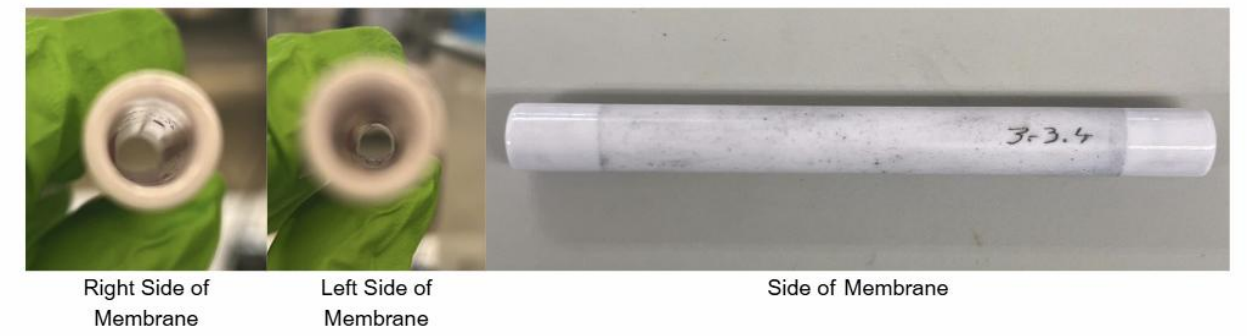

Figure 4.12 Ceramic Membrane After Brewery Wastewater Treatment

The images show the ceramic membrane after all brewery tests and fouling treatment tests, little to no particle accumulation or impact can be seen.

4.2.1.4 Ceramic Membrane Permeate Water Quality

This section evaluates the chemical and biological quality of the ceramic membrane permeate to determine its suitability to be reused as irrigation. The previously discussed

physical water quality concerns regarding particle size (Section 4.1.2), were completely removed by the polymeric membrane resulting in visually clear permeate with no visible solids seen in Appendix Figure B.1. The following results focus on the dissolved parameters and biological indicators, that are the remaining water quality constraints for reuse.

4.2.1.4.1 Ceramic Membrane Chemical Permeate Quality Results

The ceramic nanofiltration membrane's impact on permeate chemistry is presented in Table 4.2. The average concentrate pH across all operating conditions was 8.1 ± 0.1, while the average permeate pH was 8.3 ± 0.1. This pH shift could be attributed to Donnan exclusion behavior, where charge interactions influence proton distribution across the membrane, coupled with residual biological activity and further nitrification [41,45,147].

Table 4.2 Ion Removal Efficiencies of Ceramic Membrane Nanofiltration

Ionic Valence	Ion	% NF Retention 2 bar	% NF Retention 4 bar	% NF Retention 4 bar SF	Legal Limit
Monovalent	Fluoride	7% **	7%**	*	1.5
	Sodium	*	*	33%**	120
	Ammonium	73% ± 13%	*	*	1.5
	Chloride	11% ± 4%	10% ± 4%***	13% **	100
	Nitrite	62% ± 16%	61% ± 17%	68% **	N/A
	Bromide	14% ± 5%	14% ± 5%	17% **	N/A
	Nitrate	13% ± 5%	13% ± 5%	17% **	10
	Potassium	20% ± 6%	19% ± 6%	24% **	N/A
Divalent	Magnesium	24% ± 9%	23% ± 9%	30% **	N/A
	Calcium	59% **	17% ± 0.1%**	15% **	N/A
	Sulfate	26%**	26% **	*	100
Trivalent	Phosphate	21% ± 6%	22% ± 6%	24% **	1
Additional Parameters	TOC	15% **	57% **	47% **	
	TN	26%**	31% **	33%**	

*All measurements were out of range for this ion

** All data from this test is based on duplicates from one test due to inconclusive results from the second test with these conditions
*** The permeate concentration was just around the legal limit

Ion removal efficiencies of the ceramic NF membrane under different operating pressures and feed conditions, showing average removal efficiency ± standard deviation, compared to the corresponding reuse limits [105]. The green shading represents being below the limit and the red shading means the concentration is above the limit. No shading represents no legal limit.

Ion Removal Efficiency

Samples 4 and 5 were used as the influent brewery wastewater for the ceramic membrane treatment. Table 4.2 summarizes ion removal efficiencies and indicates whether permeate concentration meets legal reuse thresholds. The 4 bar sand filtered operational condition showed the highest overall ion removal efficiencies, where increasing TMP can slightly increase the removal efficiency of ions [14,40,45].

The 2 bar direct filtration condition experienced similar patterns in removal efficiencies, but slightly lower for some monovalent anions, with the exception of nitrite and ammonium. This behavior is consistent with steric hindrance typically being the dominant exclusion mechanism in nanofiltration, where hydrated radius and MWCO determines transport through the membrane. As a result, most multivalent species, should have a higher removal efficiency than monovalent ions [31,40,45] However, the exceptions of ammonium and nitrite indicating that multiple mechanisms are likely influencing the removal efficiencies [47,53].

Overall, the removal efficiencies align with expected performance of the ceramic membrane when treating brewery wastewater, showing stable chemical parameter removal efficiencies across operating conditions. The mixed trend, with high ammonium and nitrite removal efficiencies, and low chloride and sulfate removal efficiencies indicated multiple exclusion mechanisms are occurring with no sign of a dominant mechanism based on these results, but it is likely that electrostatic repulsion may play a role but are not the dominant exclusion mechanism due to the similar removal efficiencies between sulfate and magnesium [39–41,94,148].

Nitrite

Nitrite removal efficiency was the highest observed of all analyzed ions with conclusive results from all operating conditions, ranging from 61% - 68%, with the maximum removal observed from the 4 bar sand filtered sample. The measured removal efficiencies align with the expected removal of nanofiltration discussed in the literature review [99,100]. The nitrite ion is a monovalent ion with a relatively small hydrated radius, so typically lower removal

would be expected in terms of the steric hindrance exclusion mechanism. However, the consistent high removal efficiencies across the various operating conditions indicate that other exclusion mechanisms are likely causing this removal efficiency [39,40,99,148].

Sodium

Sodium concentrations of Samples 4 and 5 were typical for brewery wastewater (Table 2.3) [41,85,86]. Sodium removal efficiency of nanofiltration is typically low as seen in (Table 2.5), due to minimal monovalent anion rejection, but preliminary ion testing with the first ceramic membrane found a 10-15% range in removal efficiency, which was lower than the 33% removal efficiency measured during the 4 bar SF treatment [41,92,95]. This is very dependent on the influent water matrix [90,149]. The high influent concentrations coupled with the low removal efficiency resulted in a permeate with a sodium concentration above the IC detection limit. Based on this it is safe to assume that the permeate sodium concentration was still significantly above the 120 mg/L reuse regulation limit from the inconclusive operational conditions. As previously stated in Section 2.4.1, some crops are tolerant of high salt levels, but salt accumulation poses a risk for soil deterioration [41,86]. To prevent this risk an additional sodium removal step could be implemented as post-treatment, such as ion exchange, or the addition of fungus in the soil[86,150].

Chloride

Chloride, another monovalent anion with a low expected and measured removal efficiency ranging from 10-13%, producing a permeate below the legal reuse limit of 100 mg/L for all operation conditions [41,92,95]. This low rejection is expected for monovalent ions due to their smaller hydrated radius and weaker electrostatic interactions compared to multivalent ions, consistent with expected NF exclusion mechanism behavior in other NF brewery wastewater treatment [31,40,41,45,151]. Slightly higher rejection was observed at 4 bar direct filtration, which may reflect increased concentration polarization effects occurring at a higher TMP [14,45]. Although chloride levels do not exceed the legal reuse limits, continued monitoring is advised due the variability of chemicals used in the brewery and the dosage of iron chloride in the MNR system.

Sulfate

Sulfate removal efficiency was 26% for 2 and 4 bar direct filtration, while 4 bar SF had inconclusive results, which is half of the expected removal efficiency for NF of 62% ± 17% [92,95]. However, this lower removal efficiency is consistent with ceramic NF studies that found ceramic membranes to have lower surface charge density and different pore structures, which can influence sulfate removal, compared to polymeric membranes that were included in the expected average removal efficiency [39,90,136]. The permeates of all

operating conditions did not meet the required reuse threshold, disqualifying the permeate for reuse. However, the samples used as the influent for the ceramic membrane brewery tests were during the period when iron sulfate was being dosed in the MNR system, had Sample 6 been the influent when iron chloride was dosed instead the permeate concentrations would qualify for reuse [40]. This ion should be continuously monitored if reuse is implemented to confirm the permeate remains below the limit.

Nitrate

The nitrate concentration of the influent Sample 4 and 5 was slightly above the legal reuse limit, and slightly higher than the initial sample concentrations, indicating some possible nitrification between sample collection and usage for brewery treatment [18,111]. The nitrate removal efficiency ranged from 13 - 17%, lower than the expected efficiency of 63% ± 13% [92,99,101]. The permeates produced from all operating conditions are above the legal reuse limit, however with further MNR system and NF operational condition optimization, the permeate concentration could meet regulations [40,149].

Alkalinity

The volume of permeate produced during the ceramic membrane experiments was limited, requiring the need to prioritize which analysis would be the most beneficial. Once Sample 6 showed that the chemical detection sensor installed at the brewery successfully reduced the alkalinity, the concentrations were not as critical for reuse. Consequently, ion concentrations and *E. coli* measurements were prioritized as they were more likely to prevent reuse. However, sufficient permeate was produced during the ceramic membrane fouling tests to measure the alkalinity, resulting in an alkalinity removal efficiency of 61% ± 1%. The high alkalinity removal efficiency from the fouling test combined with the alkalinity concentrations of the influent after the chemical sensor system was installed, should result in the ceramic nanofiltration membrane sufficiently lowering the permeate concentration [18,40].

4.2.1.4.2 Ceramic Membrane Biological Permeate Quality Results

As previously discussed in Section 2.5, *E. coli* was used as a biological indicator of fecal contamination in the brewery wastewater. Settled Samples 4 and 5 were used as the brewery wastewater influent for the ceramic membrane treatment, which as seen in Section 4.1.3, qualified for Class C and D reuse. While the unsettled Sample 5 did not qualify for any reuse classifications signifying the importance that settling not only removes particle load but also meet some reuse regulations without additional treatment.

In the membrane experimentation section, the bacterial removal is expressed in log removal value (LRV) rather than CFU/mL as seen in previous sections to best assess membrane

performance. The LRV values for the brewery wastewater treatment tests were calculated using the higher influent concentration between Samples 4 and 5, representing a conservative, worst-case feed condition. The fouling test LRV was calculated using Sample 6, which contains one degree of magnitude higher *E. coli* concentration.

Across all operational conditions tested, the permeate showed no detectable coliform growth, resulting in identical LRV values of 2.7 as seen in Figure 4.13. The average of the fouling tests exhibited a higher LRV of 3.8 due to the higher feed concentration, which had a single coliform forming unit on both measurement from test 1 and no coliform forming units from the Test 2 measurements. With these measured removal efficiencies, the elevated levels during periods of overflow will likely produce a permeate qualifying for Class A reuse, which is a more likely worst case-scenario influent concentration once the industrial and domestic MNR tanks are separated again. This shows the ceramic nanofiltration membrane achieved high disinfection removal efficiencies, even with the elevated bacterial influent during the fouling tests for longer periods of time.

All permeate produced from each of the operating conditions in the initial brewery treatment experiments qualify for Class A agricultural reuse with concentrations below or equal to 10 CFU/100 mL. For the fouling tests, the permeate from Fouling Test 1 qualified for Class B reuse, whereas Test 2 met Class A criteria, which could be due to variations in the biological fouling behavior occurring during treatment. These results show that ceramic nanofiltration maintains high biological removal efficiency while higher concentrations are in the influent and is capable of reaching Class A qualification even for prolonged treatment time.

These findings show the robustness of the ceramic membrane for brewery wastewater reuse and reinforce the importance of managing influent variability and preventing overflow events and separating the industrial and domestic wastewater. While the membrane achieved Class A reuse for all brewery treatment tests with Samples 4 and 5, using the reclaimed water for Class B agriculture would guarantee that the concentrations comply with reuse regulations.

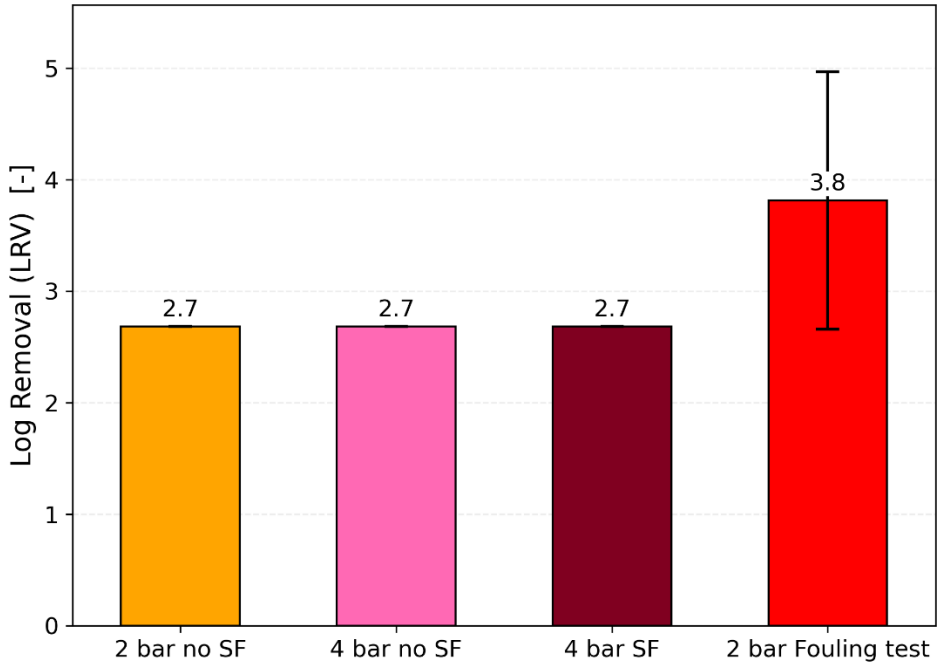

Figure 4.13 Ceramic Membrane *E. coli* LRV [-] including Fouling Test

The figure shows the E. coli LRV of the ceramic membrane across all operating conditions with Samples 4 and 5 as influent for the first three tests and Sample 6 as the influent for the fouling tests.

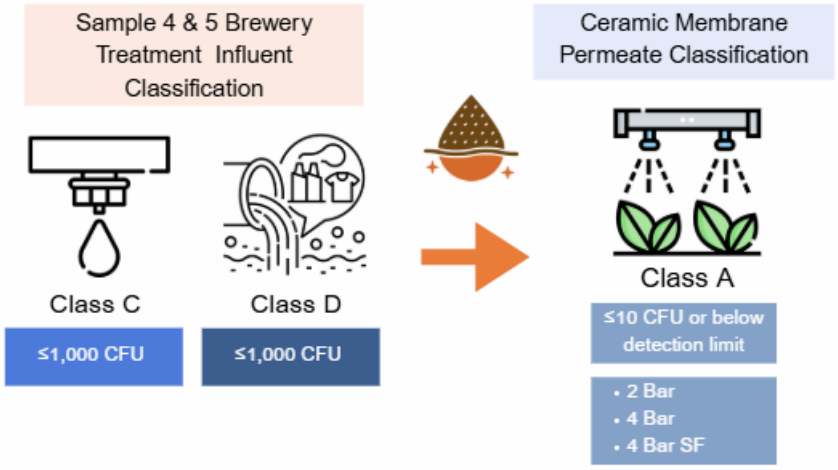

Figure 4.14 Ceramic NF Membrane Permeate Biological Reuse Class
The influent Samples qualified for reuse Class C and D, however after ceramic nanofiltration all initial brewery tests qualified for Class A reuse.

Overall, the ceramic membrane exhibited high mechanical and chemical stability, maintaining consistent performance across repeated filtration tests [40,94,136]. While flux

decline was observed during the prolonged fouling tests, the membrane's structural resilience and tolerance to chemical cleaning demonstrate its suitability for long-term operation under variable feed conditions [52,94]. The observed removal trends indicate that multiple separation mechanisms may have contributed to the overall performance, including steric hindrance, interactions influenced by the membrane's surface hydrophilicity, and electrostatic interactions [40,90,149]. Although the relative influence of each exclusion mechanism cannot be quantified, the results provide insight into how material properties affect solute retention and fouling behavior [53,90]. These findings contribute to addressing sub-question 2 by characterizing the behavior of the ceramic membrane under the tested experimental conditions.

4.2.2 Polymeric Membrane

4.2.2.1 Polymeric Membrane Permeability Results

Prior to testing the membrane permeability, the NX start-up procedure was followed. The membrane was first soaked in Milli-Q water for 24 hours, then flushed with demineralized water for four hours without recirculation to remove residual glycerin and sodium bisulfite used for preservation [134]. After the start-up procedure, the initial permeability testing was conducted to determine the baseline performance prior to treatment across pressures 1-6 bar. Ion removal tests were not conducted for the polymeric membrane as there is sufficient literature on its removal efficiencies, so only one polymeric membrane was used.

The initial permeability of the polymeric membrane was determined to be 10.0 ± 0.3 $LMH*bar^{-1}$, this value is a reference for the brewery treatment experiments. The permeate volume produced during this evaluation was significantly higher, producing one to two degrees of magnitude more permeate, than that from the ceramic membrane, due to its nearly 30 times larger surface area. Considering this and the practical constraints of sample transport, an experimental influent of 5 L was selected to ensure sufficient volume for all analysis, while trying to match the ceramic membrane experimental conditions.

The permeability throughout the brewery treatment tests can be seen in Figure 4.15. During treatment all operational conditions experienced a gradual increase in permeability of 2 – 3 $LMH*bar^{-1}$ during the treatment. The only operational condition that achieved the baseline permeability was 4 bar direct treatment. The lowest permeability of all operation conditions was the sand-filtered tests at 2 bar, which had a permeability of 5.32 - 7.13 $LMH*bar^{-1}$, likely a result of the lower TMP [18,31]. The 4 bar sand filtered experiments showed the overall highest permeability throughout the whole testing period, ranging from 7.44 to 8.74 $LMH*bar^{-1}$, slightly below the baseline permeability of 10.0 ± 0.3 $LMH*bar^{-1}$.

However, the 4 bar direct filtration tests had the higher peak permeability of 10.25 $LMH*bar^{-1}$ at 45 minutes. This is likely due to blockage of pores from rapid cake layer formation due to the higher solids volume followed by shear induced sloughing [18,41,54,55,58,61,72,152]. Both of the sand filtered operating conditions display much smoother permeability trends compared to the direct filtration sample, showing that the pre-treatment of sand filtration successfully helped stabilize the permeability during treatment.

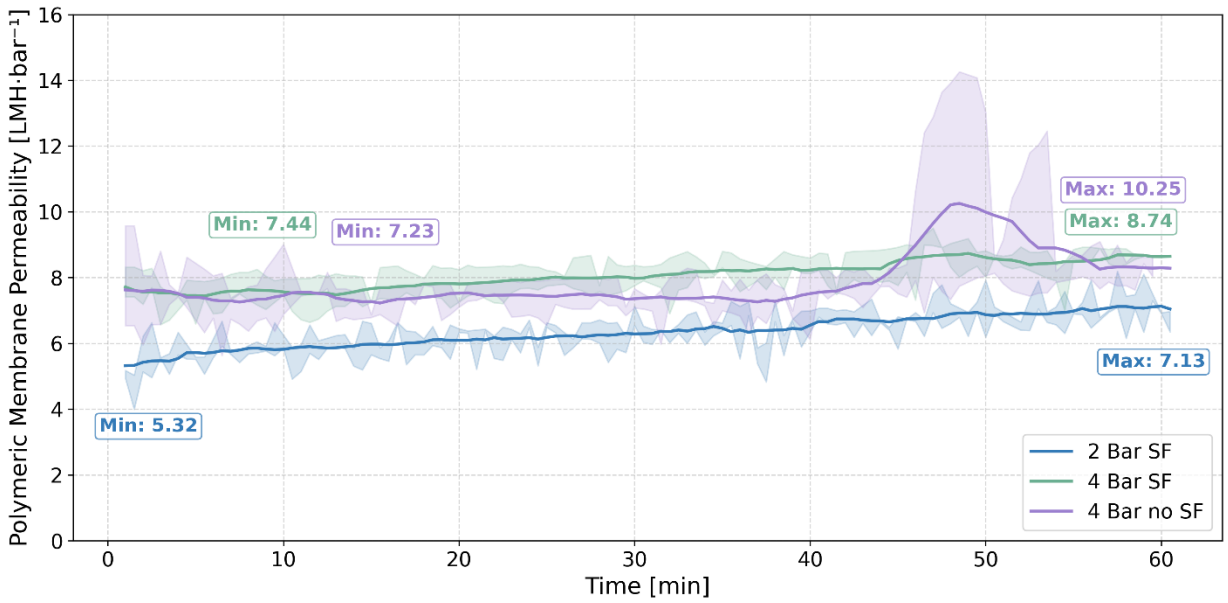

Figure 4.15 Permeability [LMH*bar^{-1}] of Polymeric Membrane During Brewery Wastewater Treatment

The figure shows the normalized permeability of time for three different operation conditions. The solid line is the rolling average during treatment while the shaded values are the raw data.

4.2.2.2 Polymeric Membrane Flux Results

Following the polymeric membrane baseline permeability evaluation, the brewery treatment experiments were conducted with 5 L of Sample 6 as the influent under varying operating conditions to assess flux behavior and removal efficiency. The experiments were run for an hour, which is shorter than the four hour ceramic membrane test, to maintain comparable influent concentrations by accounting for the higher rate of permeate production.

Due to concerns discussed in Section 4.1.2 regarding the potential for fiber plugging based on the particle size analysis, the initial influents used for polymeric membrane treatments were sand filtered at 2 bar and 4 bar, followed by direct filtration at 4 bar and the fouling test at 2 bar.

Permeate recovery on average was 17.6% at 2 bar was and 42.6% at 4 bar during the one hour brewery treatment tests. The normalized flux throughout the experiments at all operating conditions is shown in Figure 4.16. The darker solid lines represent the rolling averages of the duplicate tests, and the shaded regions in the background display the raw data. All tests began with a similar normalized flux around 1 J/J^0. Sand filtered conditions exhibited a gradually increasing and stable flux, reaching a peak of 1.17 J/J^0 at 4 bar and 1.26 J/J^0 at 2 bar. While 4 bar direct filtration exhibited a distinct fluctuations, decreasing to 0.90

J/J^0 after 15 minutes, followed be a gradual increase reaching 1 J/J^0 at 43 minutes, where a sharp spike to 1.26 J/J^0 occurs at 47 minutes with a sharp decline to 1.05 J/J^0 until 56 minutes, where the flux remains stable until the end of the test. This transient fouling cycle suggests sequential pore narrowing, surface cake accumulation, and shear-induced detachment [54,55,57–59].

The reduced flux variability of the sand filtered influents indicate improved hydraulic stability, likely due to less fouling, showing the influence sand filtration has at minimizing particulate caused fouling and biofouling [41,62,67,71]. Furthermore, between the sand filtered influents the 2 bar operational condition experienced the largest flux increase of ~0.30 J/J^0, at the lowest pressure making it the most energy-efficient and stable configuration and of the three brewery treatment operational conditions tested [18,41].

Figure 4.17 presents the same line graph as Figure 4.16 alongside the average normalized flux from the post-treatment cleaning stages. The average fluxes from the forward flush, chemical cleaning, and permeability tests remained stable, and returning to an average permeability of 9.5 ± 0.1 $LMH*bar^{-1}$ for all operating conditions including the fouling tests, nearly the original 10.1 $LMH*bar^{-1}$ baseline permeability. The consistency of the permeability recovering indicates that most likely no irreversible fouling occurred. However, visible particles on the polymeric membrane fiber's inlets after the fouling tests seen in Figure 4.18, indicate the presence of foulant accumulation at the inlet not removed by the post-treatment cleaning process consistent with initial cake layer formation that could lead to fiber plugging [18,53,147].

The polymeric membrane brewery wastewater treatment with the sand filtered influents display stable flux performance and nearly 100% permeability recovery. Direct filtration at 4 bar, successfully produced a permeate, but the transient fouling trends may intensify under longer operating conditions, reinforcing the support of sand filtration as a pretreatment to protect the hollow fiber inlets and limit cake layer development [18,53,71].

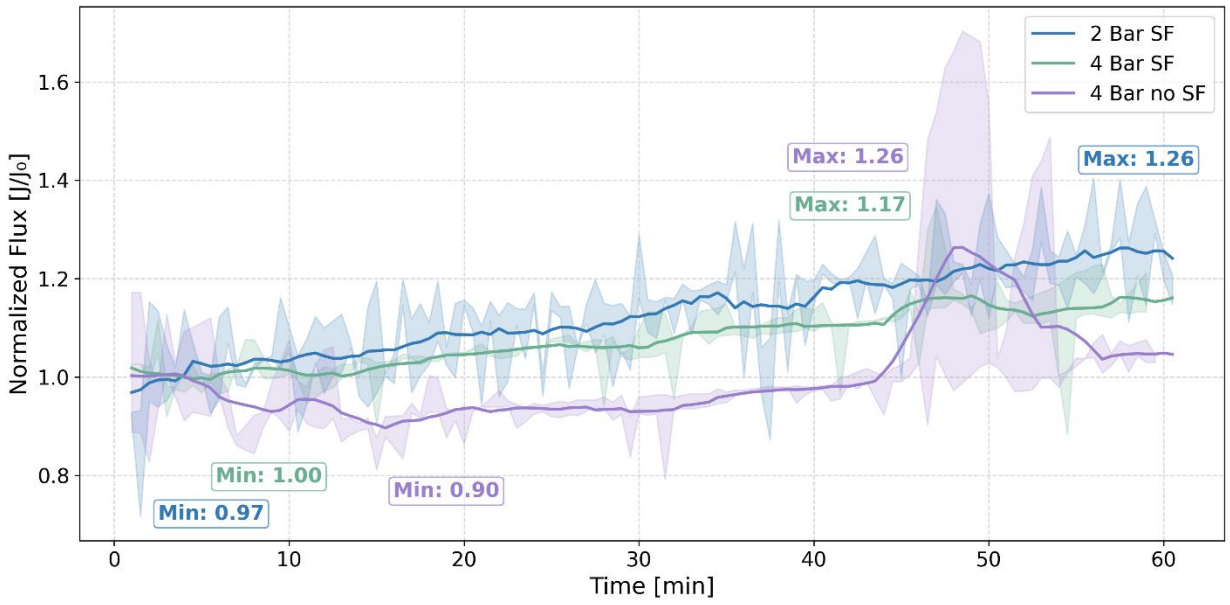

Figure 4.16 Normalized Flux [J/J^0] of the Polymeric Membrane Experiments

The figure shows the normalized flux of the polymeric membrane during brewery treatment across the three operating conditions. The solid lines are the rolling averages, while the shaded values are the raw data. The maximums and minim values are also labeled for each operating condition.

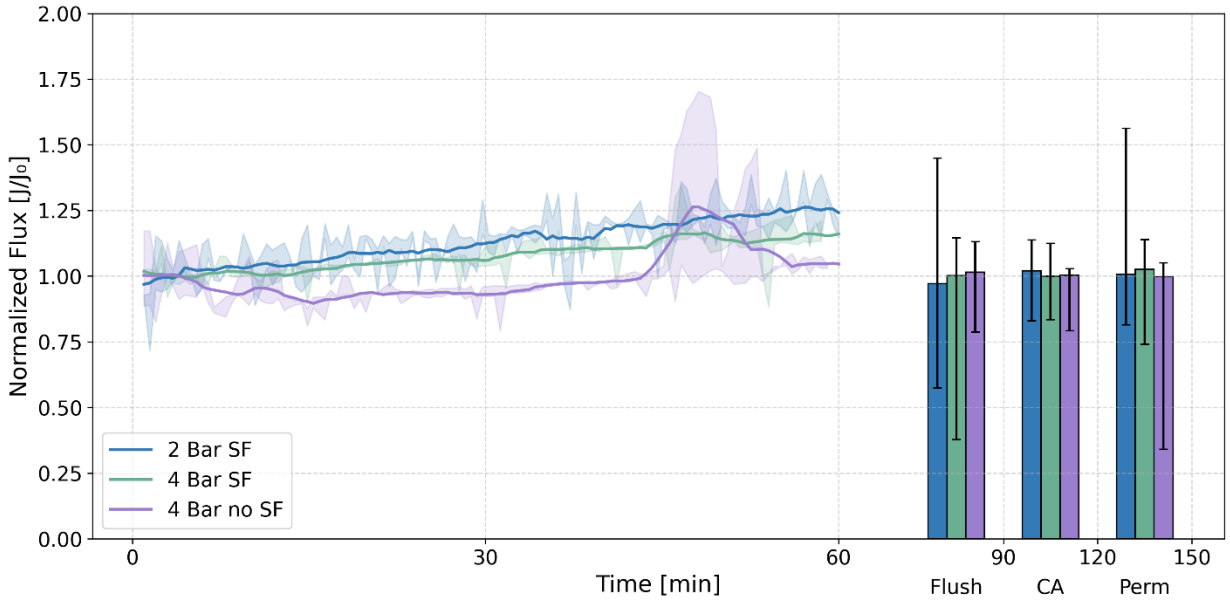

Figure 4.17 Normalized Flux [J/J^0] of Experiments and Cleaning for the Polymeric Membrane

The figure above shows the same normalized flux graph of the polymeric membrane during brewery treatment alongside the post treatment cleaning in the bar graph on the right. The labels of the bar graph are "Flush" for forward flush, "CA" for citric acid chemical cleaning, and "Perm" for permeability testing. The values on the x-axis show at what time into the testing the measurements and testing were completed.

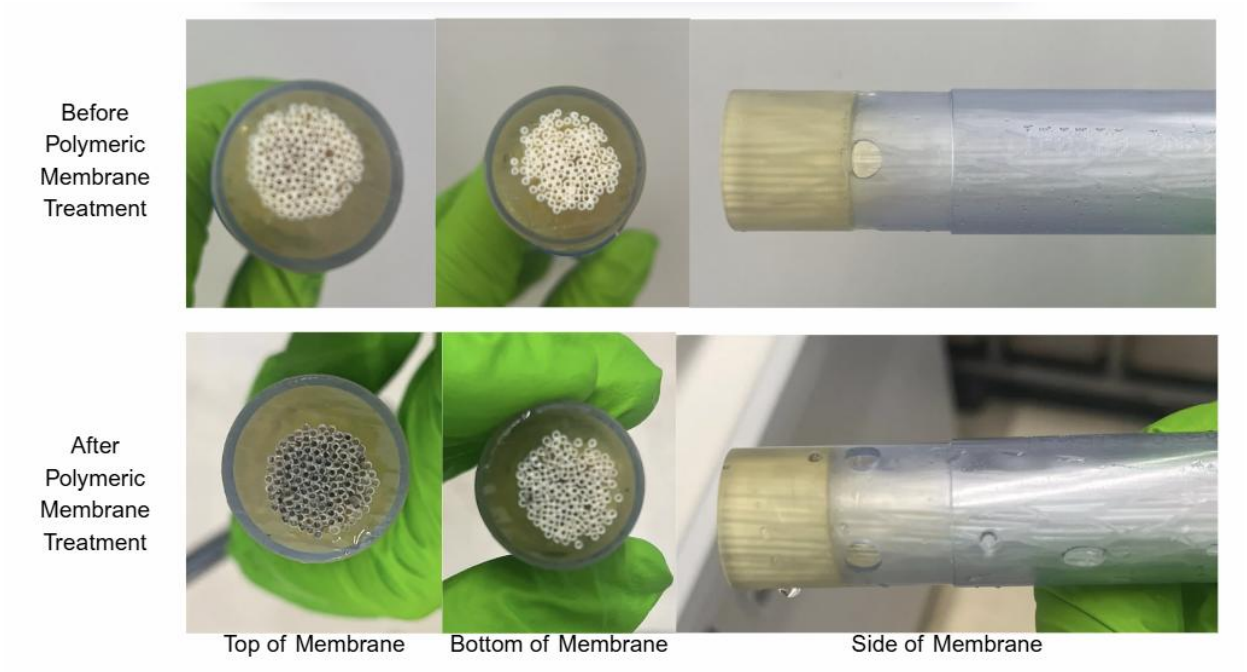

Figure 4.18 Polymeric Membrane Post-Treatment

The images show the polymeric membrane before and after all brewery tests and fouling treatment tests. In the bottom images, discoloration and particle accumulation at the fiber inlet can be seen compared to the membrane before treatment.

4.2.2.3 Polymeric Membrane Fouling Test Flux Results

Two polymeric membrane fouling tests were conducted using 5 L of Sample 6, recirculated for four hours at 2 bar. Polymeric Fouling Test 2 ran slightly longer than four hours as fouling signs were not yet apparent after four hours. Nearly complete conversion of influent to permeate was achieved during these fouling tests, achieving 93.1% recovery in Test 1 (275 mL influent remaining) and 96.3% recovery in Test 2 (115 mL influent remaining), the remaining influent during fouling Test 1 can be seen in Appendix Figure B.3. Figure 4.19 shows the average absolute flux profiles of the fouling tests since only one pressure condition was evaluated, with the solid line representing Test 1 and dashed line representing Test 2.

Both tests exhibited irregular fluctuations in flux likely due to particulate fouling cake layer formation followed by shear induced detachment. Short-term biofilm growth followed by

shear-induced sloughing or erosion may have also contributed to these fluctuations under the recirculating conditions [54,55,57,58]. Test 1 exhibited its second largest spike and first spike at approximately 45 minutes of 23.7 LMH, consistent with sudden detachment of accumulated biomass or cake material, mirroring the patterns observed in the 4 bar direct filtration brewery treatment [18,53]. Fouling Test 2 showed similar behavior in the first peak but reached lower flux values throughout the test, with the initial peak being a double peak at the same time as Test 1's first peak but only reaching 16.6 LMH the lowest flux value of all its peaks. The lower peak values exhibited in Fouling test 2 is possibly due to residual pore blocking or cake layer formation from Test 1 that were not removed during the post treatment cleaning [53,153]. The large oscillations in flux observed likely signify detachment of cake layer or biofilm consistent with shear force detachment based on the magnitude of the fluctuations opposed to particle size erosion [54,55,57–59]. The overall constant oscillations insinuate either steady-state particulate or biofouling, beneath the oscillations there is a gradual increase in flux trends, alluding to the fact that steady-state conditions have not been reached [57,140]. If steady-state conditions were attained the trend would be flat and with the decrease in flux equally the increases in the oscillations [140].

During Fouling Test 1 a 28.95 LMH maximum flux peak was reached after 175 minutes followed by a pronounced decline in flux until the end of treatment reaching 6.29 LMH at the end of treatment. During Fouling Test 2 similar behavior occurred slightly delayed reaching a 21.55 LMH maximum peak after 240 minutes followed by a sharp decline till the end of treatment reaching a minimum flux of 8.79 LMH. These sharp declines at the end of treatment are indicative of near-complete pore blockage and reduced permeate production [18,20,152]. This decline was likely intensified by the high solids concentration from the continuous recirculation of the same 5 L influent without the permeate volume dilution, resulting in an elevation of the polymeric membrane's fouling propensity. Additionally, towards the end of the fouling test treatments, the small remaining influent volume required tilting the vessel to allow the feed tube to reach the influent, which may have further exacerbated the sharp decline in flux. It is likely that had the influent volume been larger, particulate fouling and biofouling growth and regrowth would have continued likely reaching steady-state and not experience complete fouling within the four hour treatment [54,57,140,152].

Figure 4.20 shows the results of the post treatment cleaning procedure on the flux. The marginally lower flux averages between Test 1 and Test 2 of 0.02 LMH in forward flush, 1.12 LMH during chemical cleaning are contradicted by the 0.72 LMH higher flux recovery of Test 2 during the post-treatment permeability tests. The contradiction of the higher flux attained during the Test 2 permeability tests indicates that irreversible fouling may not be occurring [18,53]. However, the delayed failure of Test 2 compared to Test 1 may indicate changes to

the fouling surface chemistry or pore structure throughout treatment, consistent with irreversible fouling mechanisms for fouling membranes [53,154].

These fouling tests demonstrate that the polymeric membrane can sustain extended operation on brewery wastewater that has not been pretreated while intermittently recovering flux through shear force and particulate erosion. However, the oscillations in the flux trends and end of treatment loss of flux indicate a vulnerability to rapid fouling under concentrated and unfiltered feed conditions. Although the permeability nearly fully recovered, the delayed flux decline observed in Fouling Test 2 may indicate partial pore or fiber plugging, where localized obstruction reduced the flow area and temporarily delayed the onset of complete fouling, which could still be reversible with strong cleaning procedures [18,20,57]. These observations imply that while short-term operation is stable, continuous recirculation without dilution increases fouling propensity and may lead to more rapid deterioration of the polymeric membrane [18,53]. To maintain a more stable flux for longer term treatments, prefiltration of the influent, a lower recovery rate without full recirculation, and periodic cleaning, are recommended to improve system robustness and prevent reaching the critical fouling point [18,20,57]. With the implementation of these recommendations, it is likely critical fouling could be delayed and could display more stable long term flux behavior [54,57,72].

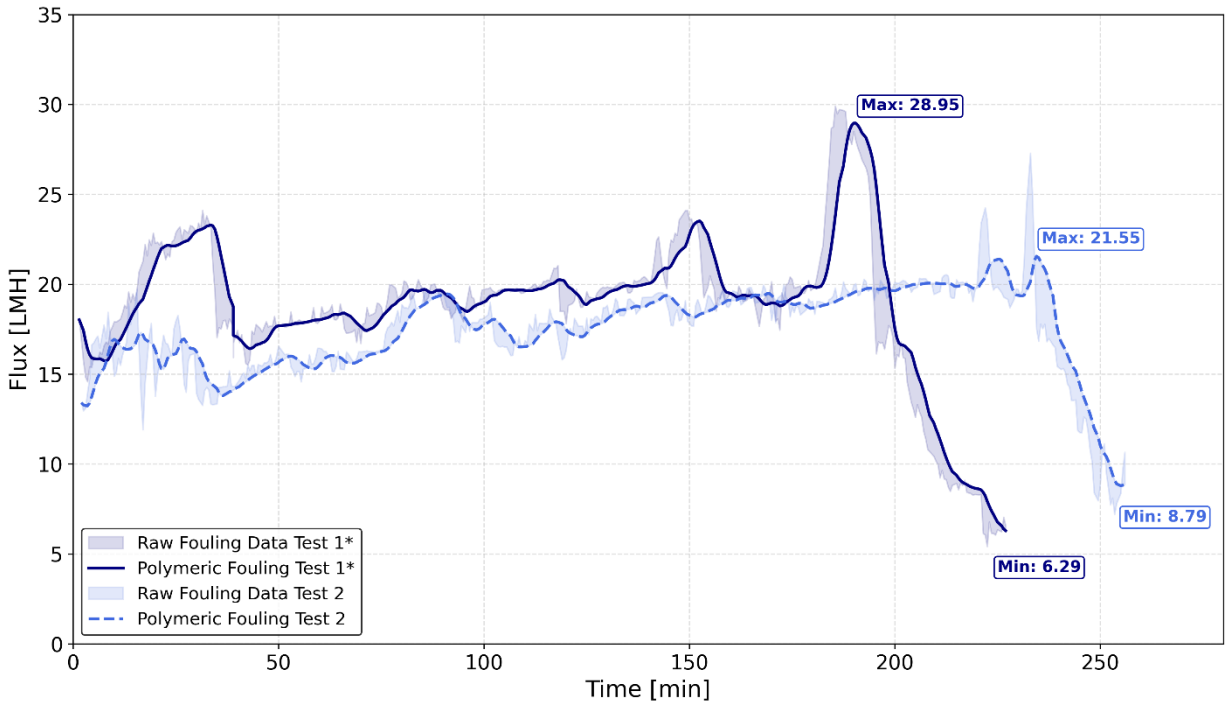

Figure 4.19 Flux [LMH] of Polymeric Fouling Tests

The figure shows the rolling average flux of the polymeric membrane during the fouling tests. Fouling Test 1 being is the solid line and Fouling Test 2 is the dashed line. The maximum and minimum values during the experiments are also labelled.

**Following Fouling Test 1, forward flush, chemical cleaning, and permeability measurements were run for 30 minutes each prior to Fouling Test 2.*

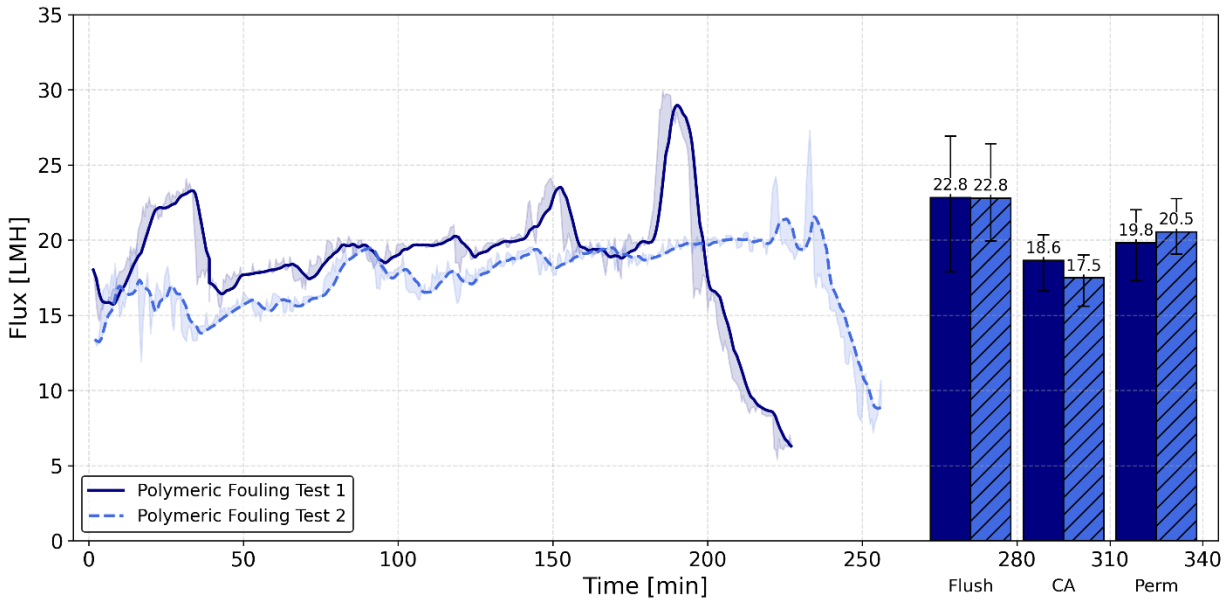

Figure 4.20 Flux (LMH) of Polymeric Membrane Fouling Tests Including Post-Treatment Cleaning

This figure shows the same plot as Figure 4.19, but with the average flux in the post treatment cleaning procedures. "Flush" is the forward flush, "CA" is the citric acid chemical cleaning, and "Perm" is the pos-treatment permeability.

4.2.2.4 Polymeric Membrane Permeate Water Quality

This section evaluates the chemical and biological quality of the permeate produced by the polymeric membrane to determine its suitability for irrigation reuse. The previously discussed physical water quality concerns regarding particle size (Section 4.1.2), were completely removed by the polymeric membrane and all permeates produced are clear and qualify for reuse, seen in

Appendix Figure B.2.

4.2.2.4.1 Polymeric Membrane Chemical Permeate Quality Results

Similar to the ceramic membrane results, the following section details the polymeric membrane permeate's chemical quality results in terms of membrane removal efficiency, to highlight the impact of the membrane on the permeate. The average pH of the polymeric membrane treatment concentrate was 7.8 ± 0.1, and the average permeate pH was 7.9 ± 0.2. This behavior of the permeate pH being higher than the concentrate pH is possibly an indication of further nitrification and biological behavior within the influent [18,41].

Table 4.3 Ion Removal Efficiencies of Polymeric Membrane Nanofiltration

Ionic Valence	Ion	% NF Retention SF 2 bar	% NF Retention SF 4 bar **	% NF Retention 4 bar	Legal Limit
Monovalent	Fluoride	54% ± 10%	66% **	39%± 1%	1.5
	Sodium	10% ± 4%	14%	16% ± 1%	120
	Ammonium	10% ± 5%	14%	15% ± 1%	1.5
	Chloride	4% ± 0%	2% **	3%**	100
	Nitrite	*	7%**	*	N/A
	Bromide	2% ± 1%	0.5% ± 1%	3% **	N/A
	Nitrate	5% ± 2%	*	6% **	10
	Potassium	11% ± 5%	16%	17% ± 1%	N/A
Divalent	Magnesium	30% ± 8%	41%	32% ± 1%	N/A
	Calcium	27% ± 11%	38%	56% ± 3%	N/A
	Sulfate	88% ± 3%	92% **	94% ± 0%	100
Trivalent	Phosphate	59% ± 9% ***	66% ***	34% ± 31%***	1
Additional Parameters	TOC	76% ± 3%	83% ± 3%	83% ± 1%	N/A
	TN	29% ± 0%	40% ± 1%	39% ± 0%	N/A
	Alkalinity	37% ± 4%	29% ± 1%	36% ± 1%	N/A
	% Alkalinity from hardness	29% ± 2%	22% ± 0%	17% ± 0%	N/A

*All measurements were out of detection limit or were inconclusive

** All data from this test is based on one experiment's duplicates due to inconclusive results from the second test

*** The permeate concentration was out of range so a concentration of 0.99 mg/L is assumed

Ion removal efficiencies of the ceramic NF membrane under different operating pressures and feed conditions, showing average removal efficiency ± standard deviation, compared to the corresponding reuse limits [105]. The green shading represents being below the limit and the red shading means the concentration is above the limit. No shading represents no legal limit.

Sample 6 was used as the influent for the polymeric membrane brewery wastewater treatments. This sample had lower alkalinity and sulfate concentrations relative to the other collected samples. The experimental condition with the highest overall ion removal efficiency was the test at 4 bar with the sand filtered sample. During testing, ion concentrations in both the influent and permeate were measured to calculate the removal efficiencies. Table 4.3 summarizes the polymeric membrane removal efficiencies of chemical water quality parameters. Key chemical parameter removal efficiencies will be analyzed below.

Sulfate

Sulfate proved to have the greatest removal efficiency during the polymeric membrane treatments, ranging from 88 - 94% removal with the lowest from 2 bar SF and the highest from 4 bar direct filtration. The measured sulfate rejection was much higher than the expected removal efficiency of 62% ± 17% [92,95]. Although the influent was already below the legal limit, this high removal efficiency would be advantageous if $FeSO_4$ were reintroduced as the dosed iron compound for phosphate removal, mitigating the risk of H_2S formation [114,115]. The high sulfate rejection indicates strong divalent ion selectivity and suggests the polymeric membrane can still produce a permeate meeting the legal limits if the dosing compound in the MNR system were changed again. [15,18]

Chloride

Chloride removal was low, ranging from 2-4%, consistent with previous NX Filtration results of this membrane, but lower than the 45% ± 32% removal of all nanofiltration membranes [41,92,95]. This low removal efficiency is due to chloride's molecular weight being below the polymeric membrane's MWCO, its nanofiltration removal depends on electrostatic Donnan exclusion, hydrophilic interactions and dielectric exclusion mechanisms, which are greatly influenced by the water matrix [148]. Despite the low measured removal efficiency, the feed concentration of 10 mg/L, the permeate concentration is below the 100 mg/L legal limit qualifying it for reuse [106].

Sodium

The reduced chemical usage in the brewery resulted in Samply 6 having a lower sodium concentrations compared to the other samples, but the 462 mg/L concentration is still more than three times the legal reuse limit of 120 mg/L [106]. Sodium removal ranged from 10-16%, with the sand filtered 4 bar tests having the highest removal efficiency, approximately triple the manufacturer's expected 5% removal efficiency (Table 2.5), but still lower than the 39% ± 24% average removal of all nanofiltration membranes [41,92,95]. However, even with

this slightly lower influent concentration and higher than manufacturer measured removal efficiency, the permeate concentrations remain well above the reuse threshold. While system optimization may slightly improve sodium removal, concentrations would likely remain above the legal limit [155,156]. Ion exchange could be considered as a post-treatment option to meet reuse regulations [150]. The current measured permeate concentrations are 395.5 ± 9.6 on average between all operational conditions, being the main chemical parameter preventing agricultural reuse.

Ammonium

Ammonium concentrations in Sample 6 were second the highest of all analyzed samples at 19.0 ± 0.1mg/L, typically indicating the likelihood of an overflow even soon after, as seen in Sample 2 when the overflow occurred in Sample 3. Removal ranged from 10-15%, with the highest removal efficiency during 4 bar sand filtered conditions, exactly as predicted by NX Filtration, but below the 28% ± 28% average of a variety of nanofiltration membranes [41,92,95]. The average permeate concentration of all operating conditions was 18.5 ± 0.5 mg/L and remained 13 times the legal reuse limits, however, during different periods in the MNR system, such as Sample 4 or 5, with lower ammonium concentrations, these removal efficiencies would likely produce a permeate compliant of the legal limits [141,148]. If the MNR system is working as predicted the nitrification process converting the ammonium to nitrite and nitrite being converted to nitrate in the MNR tank should greatly decrease the ammonium concentration.

Nitrate and Nitrite

Nitrate experienced low removal efficiencies ranging from 5-6%, with the 4 bar sand filter test results being inconclusive. Low rejection is consistent with literature showing the lowest rejection of oxidized nitrogen species is typically nitrate [147,148]. Although the nitrate removal efficiency was low the permeate concentration remained below the legal limit of 10 mg/L due to the low influent concentration. The nitrite removal efficiencies were largely inconclusive, with the exception of a 7% removal efficiency during the 4 bar sand filtered influent. The low removal efficiencies or out of detection range for both of these compounds are consistent with previous studies reporting higher rejection of ammonium compared to oxidized nitrogen species [99,121,148]. The high total nitrogen removal relative to the inorganic nitrogen concentrations indicates a high concentration of organically bound nitrogen in the influent. The low nitrate and nitrite removal efficiencies emphasizes the importance of having biological stability and MNR performance to prevent oxidized nitrogen species from being in the membrane treatment influent to allow for reuse.

TOC

TOC removal efficiency of 76-83% was within the range of 70-85% for the expected removal efficiency for nanofiltration [15,18]. Effective organic removal supports microbial stability and reduces biofouling potential [25].

Alkalinity

The lower influent alkalinity, due to the reduced chemical usage in the brewery, contained a larger portion of alkalinity due to hardness compared to the other collected samples. The membrane further reduced the alkalinity of the permeate by removing 27-56% calcium and 30-41% of magnesium that cause hardness, lowering the scaling potential in the permeate. Reduced hardness improves permeate scaling stability, supporting irrigation use, but concentrate recycling can still cause localized scaling [124,128].

Short duration polymeric nanofiltration of Sample 6 brewery wastewater demonstrate that the membrane consistently delivers permeates compliant with physical clarity, with strong rejection of multivalent ions, specifically cations, and TOC, which align with the findings of other studies [41,141]. While sodium and ammonium concentrations remained above the legal limits, with some system optimizations and reduce chemical usage it is possible the permeate with meet effluent limits [93]. For usage without meeting sodium levels salinity resistant crops could be used or possible polishing methods such as ion exchange could be implemented [86]. Overall, the polymeric membrane demonstrates promising reuse potential under controlled influent conditions and appropriate pretreatment.

4.2.2.4.2 Polymeric Membrane Biological Permeate Quality Results

Biological water quality was evaluated using log removal values (LRV) of *E. coli* in the permeate relative to the influent. All polymeric membrane experiments were conducted using Sample 6 as the influent. As discussed in Section 4.1.3, this sample had exceptionally high *E. coli* concentrations, two to three orders of magnitude larger than the other samples, due to the inclusion of domestic wastewater in the MNR system's brewery wastewater tanks. Consequently, the initial unsettled, settled, and sand filtered samples did not qualify for any reuse classifications.

Figure 4.21 shows the average LRVs for each treatment condition, including the fouling tests. The directly treated settled sample had a lower influent concentration than the sand filtered influents. The highest *E. coli* removal was 4.8 from direct filtration at 4 bar, where no coliform growth was observed on any measurements. The 4 bar sand filtered sample had an LRV of 4.3 with one coliform of the four measurements, while the 2 bar sand filtered permeate had an LRV of 3.2 with four coliforms detected across all tests. The fouling tests had the lowest LRV of 2.5 and measured eight coliforms across the four measurements, likely driven by concentration effects associated with continuous recirculation of a fixed feed volume

[54,57,140]. Concentrating solids and microbial load by recirculating the feed can increase membrane compaction and rigidity, reducing biological rejection performance, an effect similarly observed in high-solids nanofiltration [157,158].

Based on these results, permeate produced from the 4 bar direct treatment and 4 bar sand filtered brewery treatment tests qualify for Class A agricultural water reuse standards, while the 2 bar sand filtered and fouling test permeate qualify for Class B reuse, seen in *Figure 4.14*.

These results demonstrate that under the worst case scenario biological influent concentrations, polymeric nanofiltration consistently achieves Class A reuse in short term treatment at 4 bar, while 2 bar meets Class B. The lower LRV during the fouling tests highlights that biological performance is sensitive to loading and hydraulic parameters, reinforcing the importance of periodic influent stabilization, or dead- end filtration phases, to minimize microbial concentration cycling under full scale operation [47,54]. Once domestic wastewater is separated from industrial wastewater tanks, influent *E. coli* concentrations will be substantially lower, suggesting that Class A reuse could be achieved by all the tested operating conditions based on measured removal efficiencies [87].

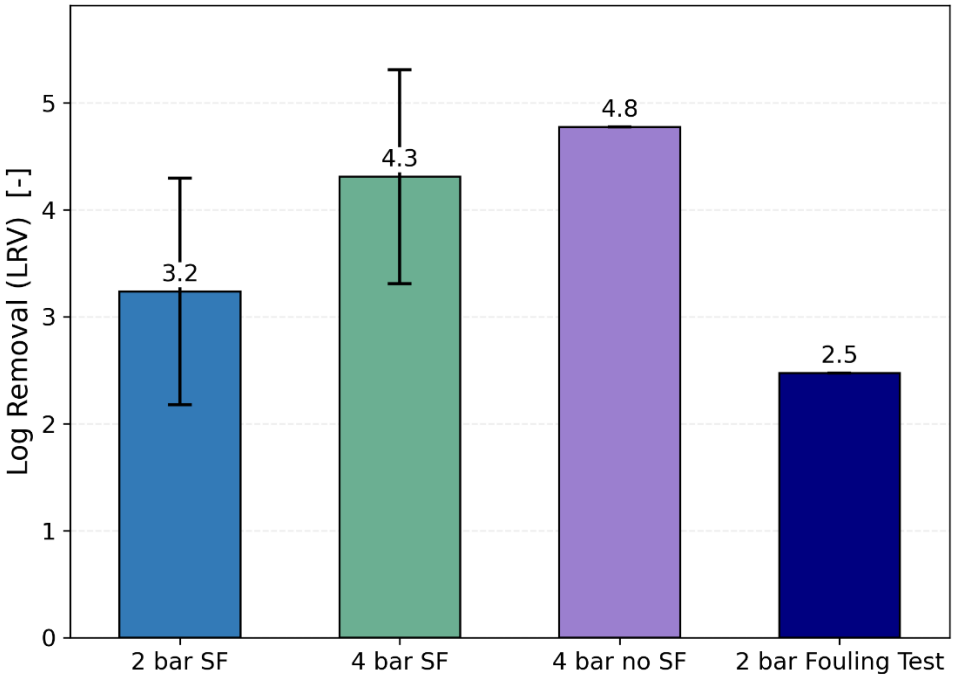

Figure 4.21 Polymeric Membrane *E. coli* LRV [-] Including Fouling Test

The figure above shows the LRV of E. coli during the different operating conditions of polymeric membrane brewery wastewater treatments and fouling tests.

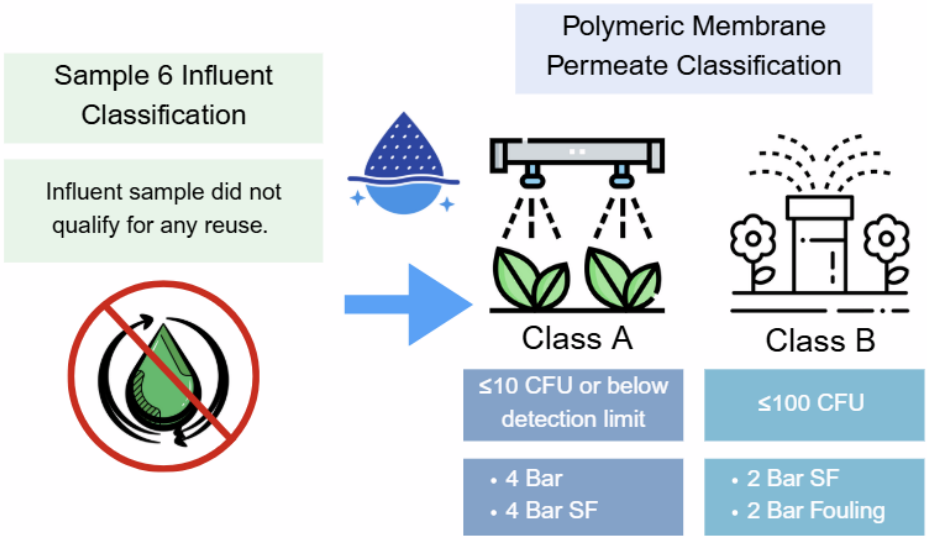

Figure 4.22 Polymeric Permeate Biological Reuse Class

The influent used for all polymeric membrane treatment was Sample 6, which initially did not qualify for any reuse classifications. After polymeric nanofiltration the 4 bar direct and sand filtered permeates qualified for Class A reuse. Conversely, the 2 bar SF brewery treatment test and 2 bar direct filtration fouling test permeates qualified for Class B reuse.

Overall, the polymeric membrane demonstrated stable flux behavior and moderate removal efficiencies under the tested conditions. Minor variations in performance between operating conditions were likely due to differences in TMP, pretreatment, and fouling development [47,53]. Evidence from the removal patterns suggest that several if not all nanofiltration exclusion mechanisms likely acted in combination, steric hindrance, electrostatic interaction, dielectric interactions and hydrophilic interactions [29–31]3. Further surface characterization would be required to distinguish their individual contributions, but these results support that both physical and chemical interactions likely influenced observed removal efficiencies [36]. This analysis supports sub-question 2 by clarifying the mechanisms potentially responsible for the polymeric membrane's performance.

These findings establish key operating parameters and removal characteristics of the polymeric membrane system, which are evaluated in the subsequent comparative section and cost analysis.

4.2.3 Comparison of Membrane Results

The initial permeability results showed the polymeric membrane to have a higher initial permeability. The following section well compare the treatment performance of both membranes, with reference to the permeability behavior, flux trends, and the resulting chemical and biological permeate quality to evaluate their comparative reuse potential.

4.2.3.1 Comparison of Permeability

Figure 4.23 shows the permeability profiles of both membranes during the brewery wastewater fouling tests. The polymeric membrane maintained significantly higher permeability, with 14.12 and 10.26 LMH*bar^{-1} maximums for Test 1 and Test 2, respectively, and minimums of 3.07 and 4.19 LMH*bar^{-1} at the final testing measurements. This signifies a 59-78% loss of permeability from peak to final permeability. Comparatively the ceramic membrane exhibited lower permeability, with maximums of 3.65 and 3.25 LMH*bar^{-1}, which are approximately the same as the minimum values of the polymeric membrane, and minimum values of 1.71 and 2.22 LMH*bar^{-1} for Test 1 and Test 2. This is a 23-32% loss from peak permeability of the ceramic membrane.

The average permeabilities of the polymeric membrane for Test 1 and 2 were 9.0 ± 2.2 and 8.28 ± 1.4 LMH*bar^{-1}, signifying a 10-17% reduction from the clean-water baseline permeability of 10.0 ± 0.3 LMH*bar^{-1}. In contrast, the average permeabilities of the ceramic membrane for Test 1 and Test 2 were 2.8 ± 0.8 and 2.6 ± 0.4 LMH*bar^{-1}, corresponding to a 35-37% decline from its baseline permeability of 7.5 ± 0.4 LMH*bar^{-1}. The higher baseline permeability of the polymeric membrane is likely due to the ~29 times larger effective surface area and a pore size twice that of the ceramic membrane, both of which enhance permeability, but also increase its susceptibility to fouling [37,138].

It is important to note, the influent used in all fouling tests was Sample 6 and was not pretreated with sand filtration, exposing the membranes to the full particulate, organic and biological load of settled Sample 6, which contained exceptionally high *E. coli* concentrations. The elevated microbial load likely accelerated biofilm accumulation on the membrane surface, intensifying fouling and causing the permeability oscillations observed in the polymeric membrane [54,55,58]. Continuous recirculation of this biologically active feed further promoted regrowth after sloughing events, exacerbating the repeated fouling and recovery cycles seen the polymeric permeability trends in Figure 4.23 [54,55,57,58].

Distinct differences in fouling behavior were observed between the two membranes. The polymeric membrane had pronounced permeability oscillations with transient recoveries, characteristic of particulate fouling or biofilm growth followed by shear-induced sloughing and particle erosion [54,55,57,58]. The fouling propensity can be seen in the sharp oscillations and temporary recoveries of the polymeric membrane. Which is typical of hollow fiber geometries, where the narrow lumens restrict flow, promote localized foulant accumulation, and generate periodic detachment events that temporarily restore permeability [54,55,57,58].

Conversely, the ceramic membrane had a more gradual and stable permeability decline of about 1.5 LMH*bar^{-1}, 23-32% difference between maximum and minimum permeability

likely caused by fouling dominated by cake layer formation and adsorption rather than pore blocking [39,40,135,136]. This aligns with the reversible fouling mechanisms discussed in Section 2.2.2.1, where accumulated foulants can be removed through hydraulic cleaning, reducing the chance of irreversible pore blockage or chemisorption [18,53].

Ultimately, these results confirm that while the polymeric membrane achieves higher baseline and operational permeability, its performance with direct filtration of brewery wastewater is more variable and sensitive to short-term fouling events [41,138]. The ceramic membrane demonstrates greater hydraulic stability and consistent resistance to fouling under continuous operation but has a much lower permeability at a higher cross-flow velocity [41,142]. In terms of best suited operational parameters, this indicates that the polymeric membrane is better suited for systems where high flux and lower energy consumption are prioritized, whereas the ceramic membrane offers flux stability for longer operations of variable influent without pretreatment [138,142].

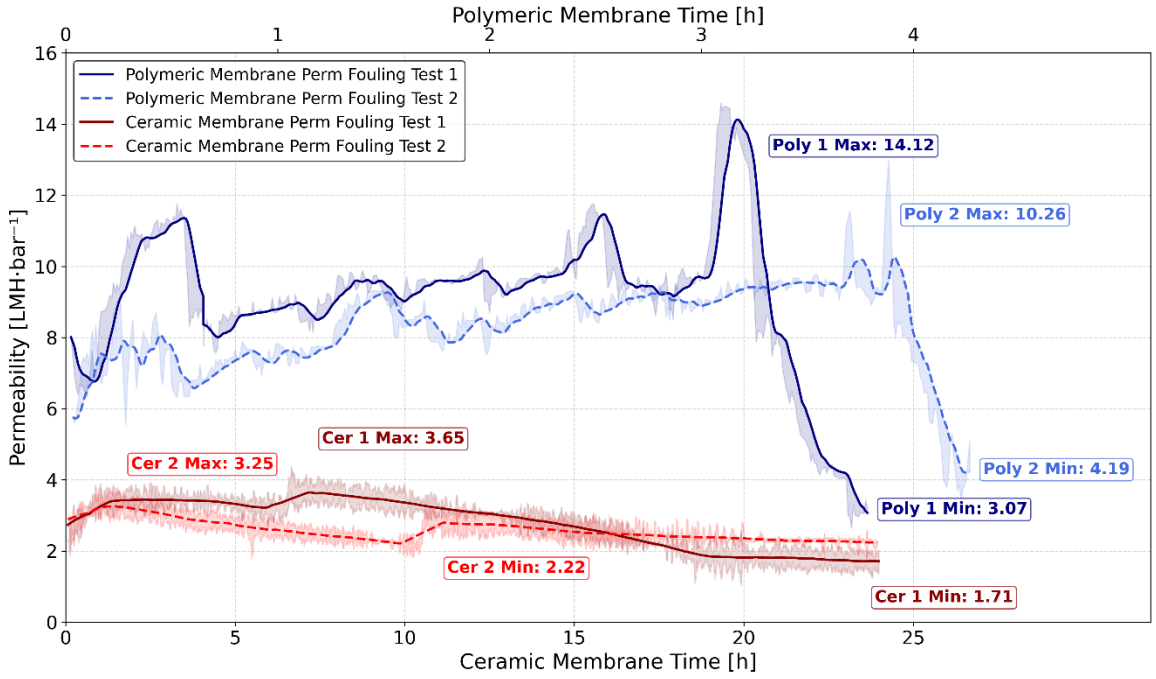

Figure 4.23 Permeability [LMH*bar^{-1}] of Both Membrane During Fouling Tests

The figure combines Figure 4.7 and Figure 4.15 to best compare the results of the permeability for both membranes during the fouling tests. The blue lines are the polymeric membrane, and the red lines are the ceramic membrane fouling tests.

4.2.3.2 Comparison of Flux

The overall flux of the two membranes differed significantly due to the polymeric membrane's surface area being nearly 30 times larger than that of the ceramic membrane (Table 3.2). As absolute flux is normalized by membrane surface area direct comparison between the two membranes possible [18,20]. A comparison of the membranes' respective fluxes will be conducted relative to the fouling tests, as both membranes used Sample 6 as the influent brewery wastewater. Figure 4.24 presents the absolute flux in LMH of both membranes during the fouling tests, with the same plot characteristics as each membrane's respective plots in Sections 4.2.1.3 and 4.2.2.3 with the solid and dashed lines showing the cumulative averages and shaded as the raw data.

The polymeric membrane exhibited a considerably higher flux reaching maximums of 28.95 and 21.55 LMH for Tests 1 and 2 despite operating at a lower cross-flow velocity (Table 3.2), and minimums of 6.29 and 8.79 LMH at the end of testing. Conversely, the maximum flux values of the ceramic membrane were 7.78 and 7.40 LMH and the minimums were 3.71 and 4.63 LMH for Fouling Tests 1 and 2. The higher flux of the polymeric membrane is attributed to its membrane geometry but also increases its susceptibility to fouling due to the smaller hollow fiber inner diameters [54,55,57,138]. This is evident in the oscillations and intermittent recovery in the polymeric membrane's flux profile, consistent with sequential particulate fouling and detachment or biofilm growth, sloughing, and reattachment cycles characteristic of dynamic particulate fouling and biofouling behavior [54,55,58]. These fluctuations align with the permeability variations observed earlier, reaffirming that particulate fouling cake formation and reattachment or biofilm detachment and regrowth were likely the dominant fouling mechanisms during the polymeric membrane fouling tests of brewery wastewater [18,54,55,57].

On the other hand, the ceramic membrane demonstrated a smother and gradual decline in flux, suggesting the dominant fouling mechanism was most likely surface cake layer formation without observable signs of detachment [40,135]. The relatively stable decline and smaller range of 3-4 LMH between peak and final flux suggest that the hydrodynamic conditions in the tubular geometry limited excessive particle accumulation, maintaining a near-steady-state fouling layer [37,40,135]. The difference in flux profile behaviors of each membrane is likely attributable to membrane geometry and material properties [37,39,40,136,138]. The hollow fiber polymeric membrane has narrow lumens that enable localized fouling and shear-induced detachment [37,54,55,58]. Alternatively, the tubular ceramic membrane has a higher tolerance for suspended solids and more uniform flow distribution [43,136,159].

Figure 4.25 compares the average fluxes measured during the post-treatment cleaning steps of the fouling tests for both membranes. The polymeric membrane exhibited higher fluxes across all cleaning steps, with less than 10% difference between Tests 1 and 2, indicating stable and reproducible cleaning performance. In contrast, the ceramic membrane showed lower overall fluxes and a slightly greater difference between the two tests, suggesting partial irreversible fouling or more compacted deposits that limited full recovery. These results confirm that fouling in the polymeric membrane remained largely reversible with the exception of the delayed critical fouling in Test 2, and the ceramic membrane possibly experienced a small amount of irreversible fouling, possibly due to inorganic scaling or dense cake formation [18,53].

Despite this, the ceramic membrane's greater mechanical and chemical robustness allows for the use of more aggressive chemical cleaning, than the ones used during the experiment, without material degradation, enabling longer operational lifespans and stable long term performance [130,136,159].

Overall, the polymeric membrane produced a higher more variable flux, achieving nearly complete permeate recovery, 93-96%, of 5 L influent in four hours, with likely with a lower energy consumption per unit volume, but showing strong susceptibility to fouling [15,18,129,136,138]. The ceramic membrane reached an average permeate recovery of 15.2-15.8% of the 2 L influent over 24 hours and likely has a greater energy consumption, however, it exhibits a much higher resistance to fouling, and has more long-term stability, and lower cleaning frequency needed [14,18,43]. These findings align with literature observations that polymeric membranes excel in short-durations with high permeate production, while ceramic membranes provide superior reliability, fouling tolerance, and longevity in continuous or variable influent conditions [41,135,159].

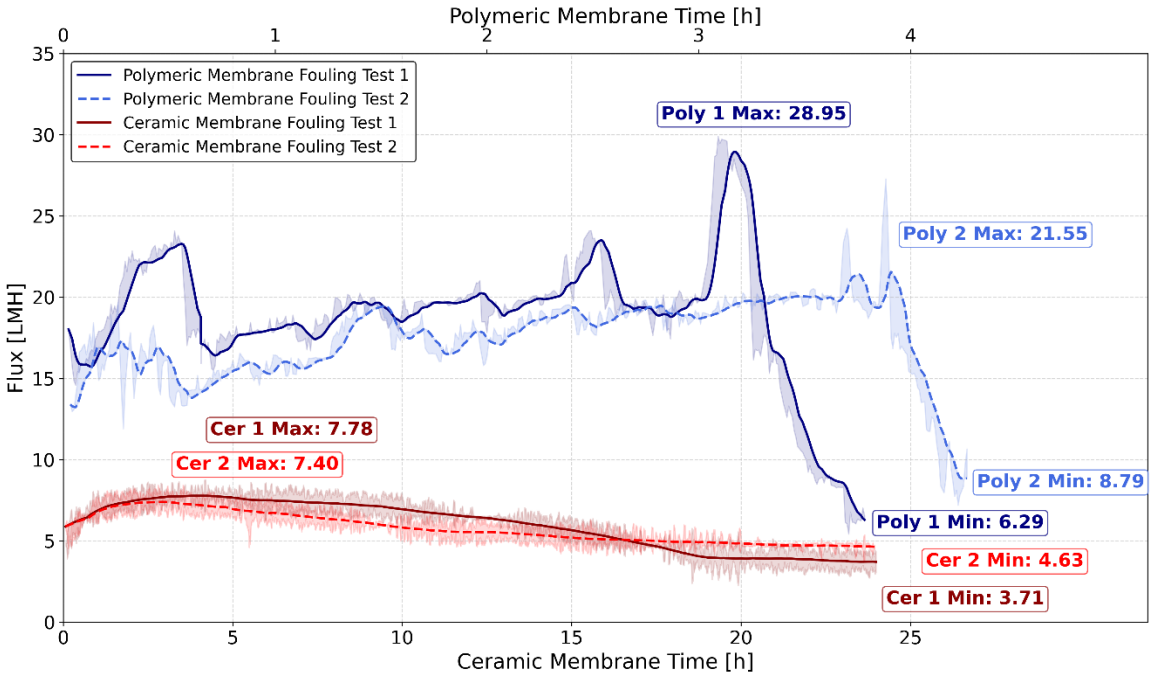

Figure 4.24 Flux [LMH] of Both Membranes During Fouling Tests

The figure combines the trends from Figure 4.10 and Figure 4.19 of the flux of both membranes during the fouling tests. The polymeric absolute flux is shown in blue, while the ceramic absolute flux is shown in red.

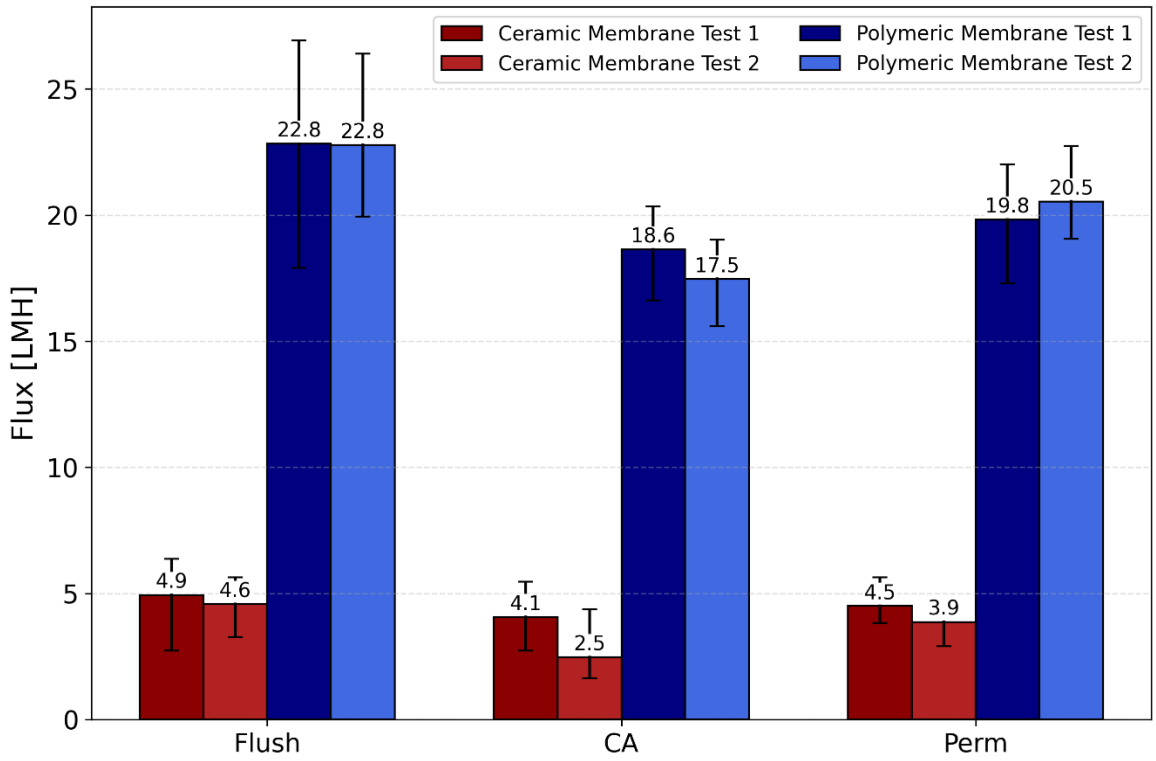

Figure 4.25 Average Flux [LMH] of Post-Treatment Cleaning Procedures after Fouling Tests

The figure shows average fluxes of the post treatment cleaning procedures following the fouling tests from both membranes. The polymeric absolute flux is shown in blue, while the ceramic absolute flux is shown in red.

4.2.3.3 Comparison of Permeate Chemical Water Quality

The comparison of chemical permeate quality will be discussed in terms of removal efficiencies during the brewery treatment tests to attempt to normalize the different water quality of the treated samples. However, this will not be a completely equal comparison as previously discussed in Section 2.2.2.2 the influent water matrix greatly impacts the removal efficiencies of a membrane [61]. The application of the polymeric and ceramic membrane were on different samples for the brewery treatment test, thus with different influent brewery wastewater matrices and impacts. The main chemical water quality differences are the sulfate, ammonium, phosphate, and alkalinity concentrations.

Sample 6 was used as the influent for the polymeric membrane brewery wastewater treatments and was collected after the phosphate removal coagulant was changed from $FeSO_4$ to $FeCl_2$, resulting in lower influent sulfate concentrations compared to the Samples 4 and 5 used in the ceramic membrane treatments seen in Section 4.1.1. This change in

dosage also seems to not be as efficiently removing the phosphate concentration compared to Samples' 1-5 phosphate concentration, so Sample 6's phosphate concentration is higher comparatively. These changes in nutrient levels impact the overall efficiency of the MNR system resulting in more nitrogen dosed, which exceeded the required concentration for the BOD:N:P ratio [111]. This likely caused the higher ammonium concentration in Sample 6 indictive of when an overflow is likely occurring soon. Additionally, Sample 6 was collected after the brewery reduced its chemical additives, causing a lower alkalinity relative to the samples treated by the ceramic membrane. Both membranes achieved their highest overall chemical water quality removal under the 4 bar sand filtered condition.

Fluoride:

Fluoride influent concentrations in samples 1-5 were very low ranging close to 0-1 mg/L, but Sample 6 had a concentration of 4 mg/L. The ceramic membrane had an average fluoride removal efficiency of 7% ± 0.4%, while the polymeric membrane had a removal efficiency of 47% ± 12%. The polymeric membrane removal efficiency was closer to the expected fluoride removal of 60% ± 38%, which is higher than most monovalent ions and aligns with typical fluoride nanofiltration removal efficiency [97,98,101,160]. Although monovalent, fluoride often shows higher NF removal efficiencies than other monovalent ions because its strong solubility and high charge density give it a larger effective hydrated radius, increasing the efficacy of steric hindrance and Donnan exclusion mechanisms [98,149,160]. However, the 40% difference between the two membrane's removals could be a result of the polymeric membrane's stronger negative surface charge, that increased electrostatic interactions [14,96,160]. Consequently, the observed fluoride removal efficiencies in both membranes led to all permeates complying with legal reuse limits.

Chloride:

As discussed in Section 4.2.2.4.1, chloride rejection in nanofiltration is typically low due to its monovalency and small molecular size relative to the membrane pore size [148]. The ceramic membrane achieved an average removal efficiency of 13% ± 5%, with the highest at 2 bar, supporting the relationship between lower transmembrane pressure and improved monovalent ion rejection [160]. In contrast, the polymeric membrane achieved a 3% ± 1% chloride removal. This difference could be attributed to the ceramic membrane's smaller pore size (Table 2.1). Both membrane removal efficiencies are below the expected removal efficiency of chloride from general NF filtration that have a removal efficiency of 45% ± 32%, which could be attributed to not all removal efficiencies included in the expected removal used wastewater as an influent [41,92,95]. Regardless of the different removal percentages the permeates from both membranes qualify for reuse applications. However, the low rejection of chloride also highlights a potential limitation of both membranes for long-term

irrigation use, as chloride accumulation in soil can lead to salinization of soil over repeated reuse cycles harming both the soil and crops grown [87–89]. This risk emphasizes the need for continuous concentration monitoring in the reclaimed brewery wastewater, especially if the iron dosing compound is changed back to iron chloride.

Nitrite:

Nitrite, another monovalent ion, depends heavily on surface charge and Donnan exclusion for removal [20,45,46,101]. All influent concentrations used for the brewery wastewater treatment were slightly above the 1.5 mg/L limit. The ceramic membrane experienced an average removal efficiency of 64% ± 18%. While the polymeric membrane's feed and permeate were mostly inconclusive, except for a 7% removal efficiency was observed and 4 bar SF. The ceramic membrane produced a removal efficiency close to the expected 68% ± 7% removal efficiency, while the lower removal of the polymeric membrane could be attributed to the inconclusive results [99,100]. Results for both ammonium and nitrite concentrations for both membranes had many inconclusive results, however, for the conclusive results both membranes follow the common NF removal efficiency trend with ammonium typically having a higher removal efficiency than nitrite [14,18,100]. It is unclear what occurred in the polymeric membrane nitrite concentration to cause mostly inconclusive results, especially since the Sample 6 initial concentration was 4 mg/L above the detection limit. However, changes in the nitrogen concentrations after collection shows some degradation or nitrification processes occurring after collection. This indicates that nitrite stability in stored brewery wastewater may be low, and on-site treatment conditions such as aeration or recirculation could significantly alter the available nitrogen species, thereby influencing removal efficiencies [25,44].

Bromide:

Bromide concentrations were consistent across all samples. The ceramic membrane had an average removal efficiency of 15% ± 4%, while the polymeric membrane showed slightly lower signs of removal 2.5% ± 1%. These low efficiencies align with bromide removal efficiencies from nanofiltration and are likely influenced by both membrane exclusion mechanisms coupled with interactions of the influent water matrices [161]. As bromide has no reuse limit, both membranes are acceptable [105,108]. Nevertheless, given bromide's potential role as a precursor for disinfection by-products, particularly bromate under oxidative post-treatment, its permeate concentrations should still be considered when designing full-scale reuse systems [161].

Nitrate:

Nitrate typically has the lowest nanofiltration removal efficiency among inorganic nitrogen species [99,100]. The ceramic membrane achieved an average removal of 14% ± 4%, while the polymeric membrane achieved only 5% ± 2%. Based on the conclusive ion results, the nitrogen compound measured with the lowest removal efficiency for both membranes was nitrate. Both membrane removal efficiencies are significantly below the expected removal efficiency of nitrate from general NF filtration that have a removal efficiency of 63% ± 13% [92,99,101]. This disparity between the measured removal efficiencies and the expected removal efficiencies could be attributed the influence of the influent water matrix on exclusion mechanisms, as not all of the removal efficiencies in the expected removal were measured from wastewater nanofiltration. These results directly support past studies which found nitrate the nitrogen compound least removed by nanofiltration due to its weaker hydrogen bonds when hydrated causing it to have a fluctuating radius size, making size exclusion more effective for the other compounds [18,99,105,148]. The higher performance of the ceramic membrane could be attributed to its greater size exclusion from its smaller pore size[18,148,156]. The low nitrate removals across both membranes also reaffirms that nanofiltration alone may not be sufficient for nitrogen control in brewery wastewater and would possibly require some additional biological or pretreatment polishing [20,108,121].

Phosphate:

The phosphate concentrations of Sample 4 and 5 used for the ceramic membrane was much lower than Sample 6 used with the polymeric membrane. The ceramic membrane achieved an average removal efficiency of 17% ± 4%, while the polymeric membrane reach an average removal of 53% ± 13%, surpassing the manufacturer removal efficiency by over 10% [95]. The ceramic membrane removal efficiency was less than half the expected efficiency for general NF membranes which is 42% ± 2%, while the polymeric membrane removal efficiency is approximately 10% higher [90,95]. The insoluble phosphate within brewery wastewater is likely removed from size exclusion and Donnan effect exclusion mechanisms due to the ions valency and hydrated radius [14,18,90,162]. The higher polymeric removal was likely a result of the higher influent concentration and stronger negative surface charge of the polymeric membrane [14,41,90]. The higher phosphate rejection of the polymeric membrane indicates effective phosphorus retention under the tested conditions, which could reduce the needed amount of phosphate removing precipitation compounds dosed in the MNR system [100].

Sulfate:

The influent sulfate concentration of the polymeric membrane was 130 mg/ L less than the influent use for ceramic membrane treatment, due to the change in the iron dosing compound. The ceramic membrane had an average removal efficiency of 26% ± 0%, while

the polymeric membrane reached an average removal efficiency of 92% ± 4%. The ceramic membrane removal efficiency is about 36% less than the expected removal efficiency for general NF filtration which is 62% ± 17%, while the polymeric membrane surpassed this efficiency by 30% [92,95]. This difference in removal efficiency is similar to that of phosphate, likely a reflection of the higher influent concentration and the stronger negative surface charge of the polymeric membrane [20,148,156]. The sulfate concentrations in the ceramic membrane permeate exceeded reuse thresholds, indicating that despite partial removal, additional polishing treatment or dilution would be needed with for these influent conditions [18]. However, based on the Sample 6 sulfate influent concentrations and the measured removal efficiencies, the ceramic membrane would likely produce a permeate with sulfate concentrations below the reuse limit with the Sample 6 influent conditions.

Sodium:

Influent sodium concentrations were consistently high, roughly 350 – 400 mg/L above the legal limit for reuse [105]. The ceramic membrane permeate exceed most detection limits, with the exception of 4 bar SF having a 33% removal efficiency, similar to the predicted removal efficiency of general NF membranes that have a removal efficiency of 39% ± 24% [41,92,95]. While the polymeric membrane achieved an average 13% ± 3% removal, which is about 10% higher than predicted by the manufacturers [95]. However, both permeate sodium concentrations remained well above the legal reuse limit of 120 mg/L [105,108]. Given the potentially harmful risks sodium poses to soil and crop properties previously discussed in Section 2.4.1, the reclaimed wastewater could be only used salt resistant crops such as cabbage or Swiss chard if further chemical reductions in the brewery are not made [87–89]. Alternatively, ion-exchange post-treatment could be implemented to reach the legal reuse limit [20]. This highlights sodium as the primary ion limiting the permeate for reuse from both membranes, due to its high influent concentration and low removal efficiency, and thus should be considered a critical control parameter for the tertiary treatment of brewery wastewater.

Ammonium:

The influent concentration of treated with the ceramic membrane was already below the detection limit, while the polymeric membrane treated an influent with a concentration nearly 13 times the legal reuse limit of 1.5 mg/L [105].The sudden peak in ammonium concentration seen in the polymeric membrane influent is typically seen at times preceding overflow events. Due to the low influent concentration of the ceramic membrane treatment, many of the treatment results were inconclusive, except for the 2 bar direct filtration operation condition which had a 73% ± 13% removal efficiency. The polymeric membrane had a 13% ± 4% average removal efficiency, producing a permeate that does not meet reuse

guidelines [105]. The conclusive ceramic membrane removal efficiency was 45% higher than the predicted NF removal efficiency of 28% ± 28%, while the polymeric removal efficiency was more than half the predicted efficiency [41,92,95]. Even with the large variation in removal efficiency between the two membranes, they both showed ammonium to be the nitrogen compound with the highest removal efficiency. The high measured removal efficiency of ammonium in the ceramic membrane aligns with literature attributing this behavior to Donnan exclusion because of the negative membrane surface charge and steric hindrance due to the size of ammonium's hydrated radius [25,44–46,99,148].

Potassium:

The potassium concentration in the influent treated by the ceramic membrane was 20 mg/L higher than that of the polymeric membrane influent and the resulting average removal efficiencies were 21% ± 5% and 15% ± 4% respectively. There is no legal potassium limits, and potassium can have benefits in moderation for irrigation [105,163,164].

Magnesium:

As a divalent ion, magnesium exhibited higher removal efficiency than potassium, with the average ceramic removal of 26% ± 8% and the polymeric removal was 33% ± 6%. Both values align with expected nanofiltration behavior, and magnesium concentrations pose no reuse concerns, and can be potentially beneficial like potassium [105,163,164].

Calcium:

The calcium removal efficiencies were 38% ± 20% for the ceramic membrane and 40% ± 17% for the polymeric membrane. While calcium also has no legal reuse limit, excessive influent concentrations and recirculation can cause an increased risk of scaling on the membrane surface [18,73,74].

TOC:

TOC is measured as its concentrations are directly correlated to BOD and COD concentrations which were elevated above the legal limit in the untreated influent brewery wastewater. TOC removal efficiency for the polymeric membrane was 81% ± 3%, notably higher than the 40% ± 18% removal efficiency of the ceramic membrane. This difference may be attributed to the more extensive biofouling on the polymeric fibers, as evidenced by the flux fluctuations observed in Figure 4.16 [31,55,57]. The higher TOC removal efficiency in the polymeric membrane also indicates more effective rejection of organic macromolecules, though this may result in accelerated organic fouling under extended operation [18,41].

Alkalinity:

Alkalinity of the permeate produced by the ceramic membrane was only measurable for the fouling tests, which showed a 62% ± 1% removal, while the removal efficiency of the polymeric membrane during all of the brewery tests was 35% ± 5%. Since both used the same Sample 6 influent for these experiments, the higher ceramic removal is likely due to its smaller pore size, higher hydrophilicity, and porosity [41,159]. Lower alkalinity in the polymeric permeate could also cause a slight increase pH variability during reuse, while the higher removal efficiency from the ceramic membrane may contribute to a more chemically stable permeate over longer treatment durations [18,40].

Consequently, in response to sub question three regarding the influence of chemical properties, it can be concluded that the polymeric membrane demonstrated greater efficiency in removing di- and trivalent ions and TOC, while the ceramic membrane was more effective in removing most monovalent ions. The polymeric membrane achieved removal efficiencies 48-64% higher than the ceramic membrane for sulfate, phosphate and TOC, indicating stronger steric hindrance and charge exclusion capacity for larger or multivalent parameters (Table 4.2 and Table 4.3). Conversely, the ceramic membrane exhibited 10-15% higher removal for smaller monovalent ions such as chloride, nitrite, and nitrate, likely consistent with its smaller pore size.

Although multiple exclusion mechanisms can occur simultaneously during nanofiltration, the observed difference between the two membranes suggest that steric hindrance and Donnan exclusion dominated during the brewery wastewater treatments. The ceramic membranes smaller pore size of 0.9 nm was expected to enhance steric hindrance. However, its lower removal of di- and tri- valent ions compared to the polymeric membrane indicates that electrostatic interactions likely played a larger role in determining removal efficiencies. The polymeric membrane's material properties may have resulted in the stronger repulsion of multivalent ions, leading to higher removal efficiencies despite its larger 2 nm pore size [41,136,148].

To more accurately compare chemical removal performance between the two membrane types, further testing using membranes with identical pore sizes is recommended to minimize the influence of steric effects [44]. Both membrane permeates do not qualify for reuse due to their sodium concentrations [105,108]. The ceramic membrane permeate produced had an average concentration of 111 ± 2 mg/L for sulfate and 13 ± 1 mg/L for nitrate surpass the respective reuse limits of 100 mg/L and 10 mg/L, disqualifying the water for reuse [105,108]. The 18 ± 1 mg/L average ammonium concentration in the polymeric membrane permeate, compared to the reuse limit of 1.5 mg/L, also prevents it for reuse [105,108].

4.2.3.4 Comparison of Permeate Biological Quality

The biological removal efficiencies will be compared using the results from the fouling tests, because the same influent was used that represents the worst-case scenario for influent *E. coli* concentrations. The ceramic membrane achieved a log 4 removal efficiency, while the polymeric membrane achieved a log 3 removal as shown in Figure 4.26. Consequently, the ceramic membrane permeate meets Class A reuse requirements, whereas the polymeric permeate qualifies for Class B reuse (Figure 4.27). The higher removal efficiency of the ceramic membrane is likely due to its smaller pore size, enhancing steric exclusion [165]. However, based on the MWCO of both membranes complete *E. coli* removal from both membranes was expected.

The presence of coliforms in the polymeric permeate may result from increased membrane rigidity due to high recirculation concentrations, altering the MWCO [157,158,166]. Without recirculation, Class A reuse could potentially be achieved for both membranes. Furthermore, the influent used was Sample 6, containing concentrations one to two orders of magnitude higher than the concentrations than all other collected samples. The Sample 6 concentration was 59,000 more CFU/100mL than Samples 4 and 5 used in the ceramic brewery treatment tests. These results from the fouling tests therefore represent the most conservative removal efficiencies of the membranes used, demonstrating the systems' performance under extreme loading conditions. Lower influent concentrations could also yield Class A qualifying permeate. Further measurements should be conducted in an accredited lab to confirm these results before the implementation of reuse.

For the biological answer to sub question three, the ceramic membrane demonstrated superior biological removal compared to the polymeric membrane, qualifying its permeate for Class A reuse, while the polymeric permeate qualifies for Class B. Both membranes therefore show potential for producing biologically safe permeates for agricultural reuse, with optimization of hydraulic and operational parameters reuse reliability could also be increased [40,41].

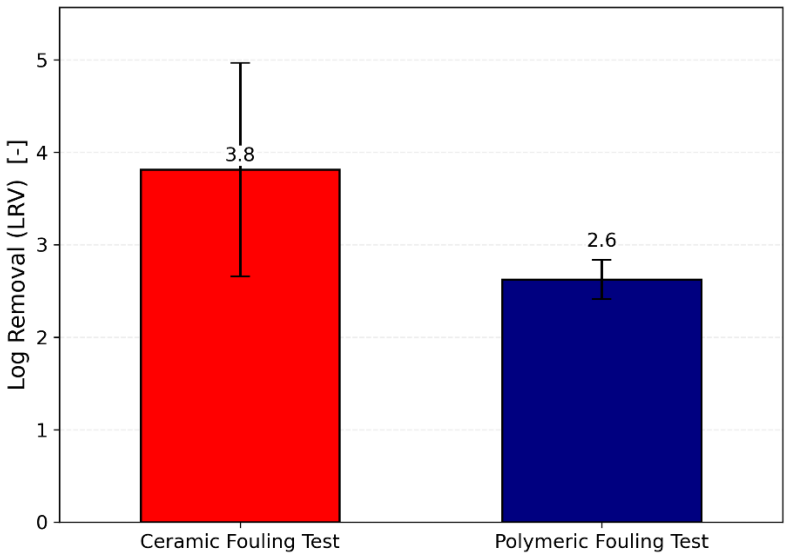

Figure 4.26 Comparison of Membrane LRV During Fouling Tests

The figure shows the LRV of the ceramic membrane (red) and polymeric membrane (blue) fouling tests.

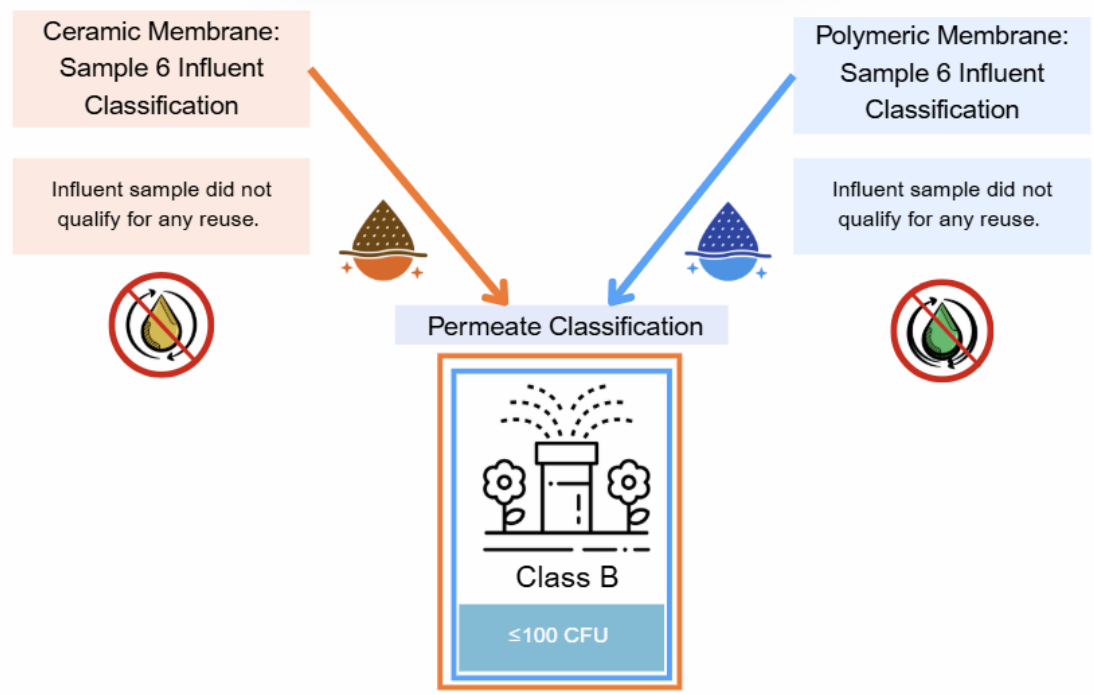

Figure 4.27 Membrane Permeate Reuse Classification From Fouling Tests Comparison

The graph shows that for both membrane fouling tests the influent Sample 6 did not meet any reuse categories, but both permeates after nanofiltration qualified for Class B reuse.

4.2.3.5 Cost Analysis for On-site Implementation

The cost of pressure-driven membranes generally increases as pore size decreases, reflecting higher removal efficiency and system complexity [167]. Nanofiltration is often selected as a lower cost solution for brewery wastewater reclamations due to its production of sufficient quality permeate for a lower cost than reverse osmosis [14,15,18–22]. Nanofiltration systems also have a broad range of costs based on material type and energy demand. Ceramic membranes typically have higher unit and energy costs than polymeric membranes but offer greater durability and longer service life [137,146].

This section presents a preliminary cost comparison between the two membrane types. The polymeric membrane module used was €2,500, which is considerably more expensive than the €193 ceramic membrane module as seen in Table 4.4. However, when the cost is normalized by membrane surface area, the polymeric membrane costs less than half per cm^2. The analysis assumes treatment of the Biomakerij's full daily capacity (143 m^3/day), continuous 24-hour operation, a pump efficiency of 0.8 [168], and an energy price of € 0.33 per kWh [169].

As shown in Table 4.4, the energy cost for both membranes of €2,471 yr^{-1} and €2,443 yr^{-1} for the ceramic and polymeric membrane respectively, are nearly identical when treating the same daily capacity, differing greatly from current studies [137,146]. The only notable difference arises from operating pressure, which directly and linearly influences energy consumption. The main differences in cost arise from flux and geometric design, with the polymeric membrane operating at 6 – 29 LMH, and the ceramic membrane operating at 4 – 8 LMH, resulting in a 93-96% recovery of the polymeric membrane compared to the 1.3% recover of the ceramic membrane over 4 hours with direct filtration of brewery wastewater at 2 bar. Consequently, the cost per cubic meter of permeate is one to two orders of magnitude lower for the polymeric membrane ranging from € 0.2-0.4 m^{-3} at 100% recovery, compared to €10-17 m^{-3} for the ceramic membrane. This large disparity is primarily due to the polymeric membrane's hollow fiber geometry, which provides a 630 cm^2 larger effective surface area compared to the ceramic membrane [18,41].

However, this cost assessment represents a simplified assessment and does not yet account for cleaning frequency, maintenance, transmembrane pressure variability, or replacement frequency which could significantly influence the long-term operating costs. The typical lifespan of ceramic membranes is 15 – 20 years, compared to 5-7 years for the polymeric membrane [170]. A completed levelized cost of water evaluation would require the inclusion of chemical cleaning and maintenance costs, replacement frequency, and performance degradation over time as well as recovery efficiency and cleaning downtime under real operating conditions [136,146].

Additionally, a mass-balance-based model in Appendix XXX was developed to estimate the effect of measured recovery efficiencies and recirculation of ion concentrations and water quality. By coupling membrane removal efficiencies with hydraulic operation, this model can be used to predict, energy demand, cleaning frequency, and concentrate management costs, thereby supporting a more comprehensive cost evaluation to determine which membrane is more optimal.

Table 4.4 Cost Comparison

	Ceramic Membrane		Polymeric Membrane	
Cost per membrane module (€)	193		2,500	
Avg. Permeability	7.5		10	
Cost per cm^2 of surface area (€)	8.8		3.9	
Pressure (bar)	2	4	2	4
Avg flux (Lm-2h-)	15	30	20	41
Daily Energy Consumption (kWh)	11	21	11	20
Annual Energy Cost (€)	1,262	2,471	1,263	2,443
Daily Permeate Production (L/day)	0.8	1.6	32	64
Cost per m^3 of permeate at 50% recovery (€/m^3)	14.4 – 20.3	10.1 – 11.6	0.4 – 0.5	0.3 – 0.3
Cost per m^3 of permeate at 75% recovery (€/m^3)	11.6 – 17.5	7.2 – 8.7	0.3 – 0.4	0.2 – 0.2
Cost per m^3 of permeate at 100% recovery (€/m^3)	10.1 – 16.0	5.8 – 7.3	0.3 – 0.3	0.2 – 0.2

Comparison of operational performance and cost parameters for the ceramic and polymeric NF membranes at 2 and 4 bars, including flux, energy consumption, and permeate cost estimations at varying recovery rates.

4.3 Pretreatment Experimental System Results

This section explains the results of the pretreatments explored in response to the water quality analysis in Section 4.1 .

4.3.1 Precipitation

Investigating precipitation as a method of pretreatment was decided upon after the alkalinity from Samples 1, 2, and 3 were measured. The high values ranging from 61.1-70.3 meq/L for Samples 1-3 coupled with a discussion with NX Filtration regarding the detrimental impact high alkalinity has on the membranes led to the need for lower alkalinity before treating the samples with the polymeric membrane. During each of these experiments' 0.6 mL of 0.1 M NaOH were dosed to reach an optimal pH after an initial test with dosing $CaCO_3$ was found to be unsuccessful. In hindsight the addition of the NaOH aided the reaction in occurring but also inhibited the full impacts of lowering the alkalinity. The precipitation experiments with $CaCO_3$ and NaOH proved to be successful at causing precipitation but increased the alkalinity of each of the samples.

As previously mentioned in the methodology and seen in Table 3.5. Various concentrations of H_3PO_4 were dosed into samples and allowed to react for 30 minutes while being stirred. The concentration dosed in Precipitation 2.1 was based on the IC ion concentrations for Sample 3 and the measured EC of 3.26 µS/cm being implemented into an ion balance model to determine how much was needed to neutralize the 129 mg/L $Ca2^+$ and 32 mg/L Mg^{2+} concentrations. The model found that the cation concentration was 28.6 meq/L while the anion concentration was 7.2 meq/L. Based on this it was expected that adding 296 mg/L of H_3PO_4 to 150 mL of Sample 3 would neutralize the anion imbalance within the water. An additional concern of dosing H_3PO_4 is causing the phosphate concentration to increase from the initial concentration of 1 mg/L above the legal limit of 1 mg/L [105,108]. However, if the H_3PO_4 was dosed at an early stage in the biofilter- aeration tank then the later iron dosage could be adjusted for this higher phosphate concentration, and the precipitant could fall to the bottom when the water settles. Precipitation 2.1, 2.2, 2.4 -2.7 were dosed with 0.6 mL of 0.1 M NaOH and Precipitation 2.3 was dosed with 1.0 mL of 1 M NaOH. Sample 3's original alkalinity was 65 meq/L.

Table 4.5 Phase 2 Precipitation Results

Experiment Number	H_3PO_4 Dosed [mg/L]	Final PO4 Concentration [mg/L]	Final Alkalinity [meq/L]
Precipitation 2.1	94	52	87
Precipitation 2.2	302	233	63
Precipitation 2.3	1508	Out of range	170
Precipitation 2.4	45	18	83
Precipitation 2.5	75	64	76
Precipitation 2.6	3	5	66
Precipitation 2.7	15	27	64

Results from Phase 2 precipitation experiments showing the relationship between the H_3PO_4 dosage, final phosphate concentration, and final alkalinity.

In Table 4.5 above Precipitation 2.1 is the calculated dosage of H_3PO_4 expected to neutralize the ion balance. However, from the results this dosage coupled with the NaOH dosage increased the alkalinity. The first round of these reactions were Precipitations 1-5, which after these results showed an increase in alkalinity of 1-105 meq/L, except for Precipitation 2.2 which had a decrease in alkalinity of 2 meq/L. The Precipitation 2.1, that was the expected neutralization concentration of H_3PO_4 needed, experienced an alkalinity increase of 23 meq/L. Based on these increases a second round was conducted with a smaller H_3PO_4 dosages. However, Precipitation 2.6 still had an increase in precipitation concentration of 1 meq/L relative to the influent, and Precipitation 2.7 only decreased alkalinity by 1 meq/L. All precipitation experiments also increased the phosphate concentration 4-232 mg/L above the legal reuse limit. Images in Appendix B, Appendix Figure B.4 through Appendix Figure B.9, show images of the Precipitation 1, 4, and 6 results.

As a result of the minimal impact to the overall alkalinity and the large increase in phosphate concentrations further testing of precipitation was not conducted and the pretreatment option was ruled out.

4.3.2 Sand Filtration

Further investigation of sand filtration was decided upon after the particle size distribution results from Samples 1-3 were analyzed, and the maximum particle size from each one

could clog the polymeric membrane. This resulted in a need for a simple filter that could easily be installed, used, and maintained on a large scale on-site at the Biomakerij. This led to an investigation of sand filtration. The main goal of sand filtration as a pretreatment to the membrane was to remove any large particles that could clog the membranes. One concern prior to using the sand filter was additional ions being added to the water; however, each component of sand and rocks were thoroughly cleaned, and initial IC testing was done on Milli Q water to confirm no additional ions were being added. Figure 4.28 below shows the original particle size distribution before sand filtration, and the dashed line shows the samples after sand filtration. As you can see the dashed lines are significantly shifted to the right relative to the initial PSD showing that the particle sizes have significantly decreased.

Figure 4.29 shows the particle size distribution in the form of a boxplot of Sample 3, 4, and 6 as unsettled, settled, and sand filtered. In this plot it is easier to see how sand filtration shifted the overall particle size distribution by one degree of magnitude smaller. Unsettled Sample 3 has dominant particle sizes between 70-100 µm, which shifts to 2-5 µm after sand filtration. Unsettled Sample 4 has initial peak particle sizes around 40-80 µm and shifts to 3-8 µm after filtration. Sample 6 had less of an overall shift, but the initial peak from 20-70 µm with the maximum peak after sand filtration around 5-10 µm. Effectively showing that after sand filtration the bulk of particle size of all samples decreased by an order of magnitude. Figure 4.30 only has the boxplot of the sand filtered samples to see more variation in the particle size.

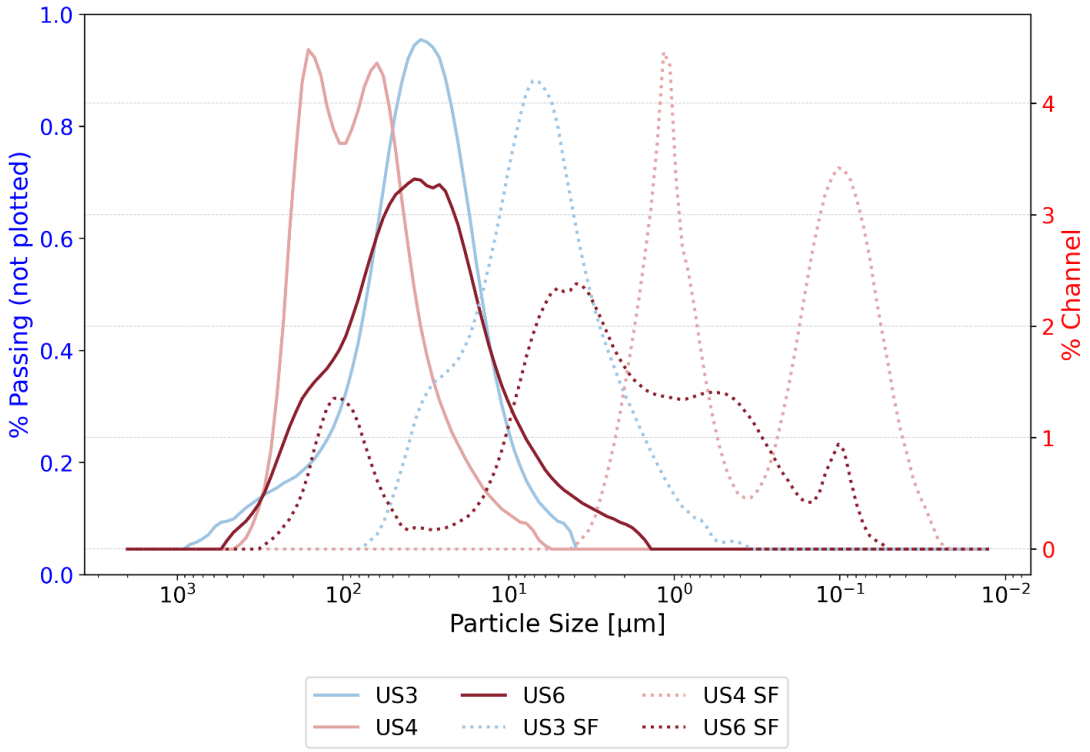

Figure 4.28 Particle Size Distribution of Samples Before and After Sand Filtration

Particle size distributions of Samples 3, 4, and 6 before, (US) unsettled samples and after (SF) sand filtration, showing the reduction of larger particles following filtration.

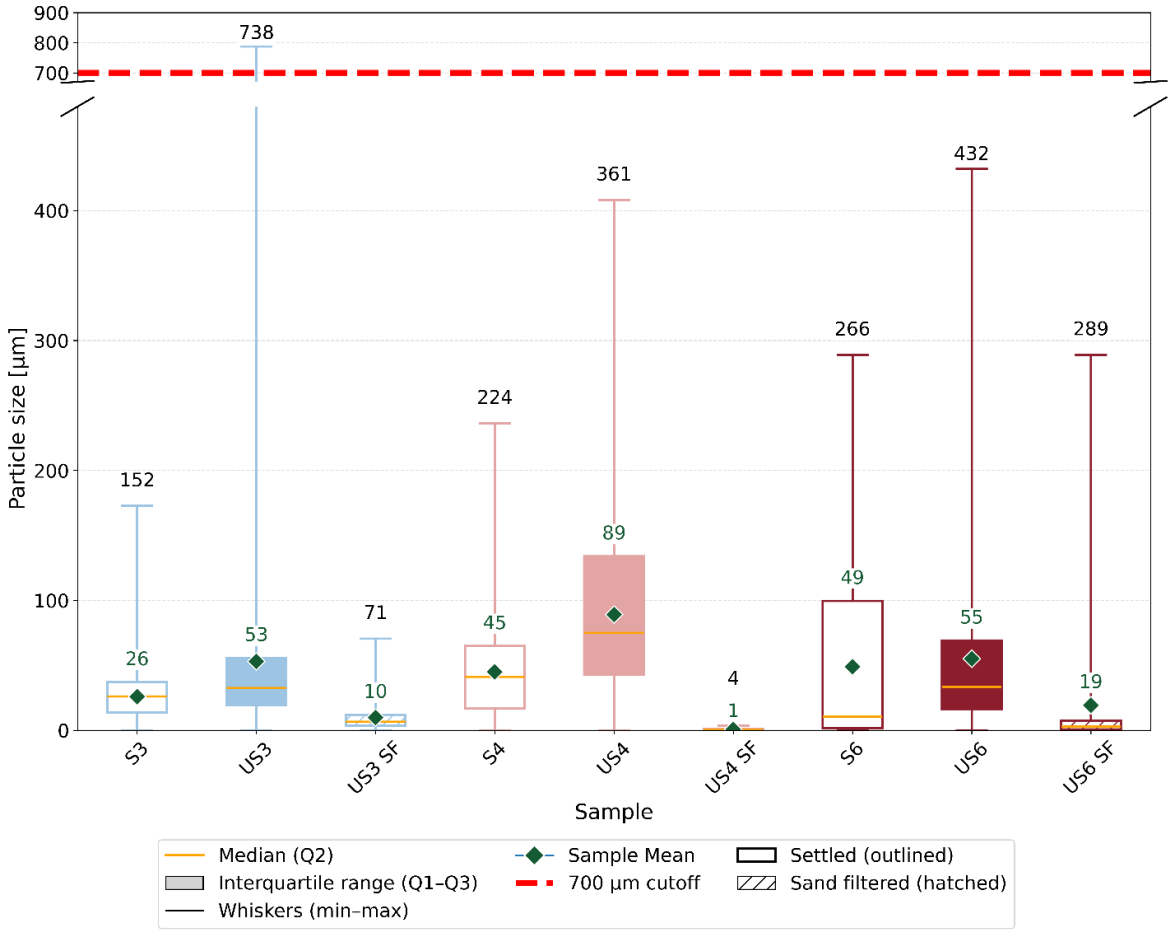

Figure 4.29 PSD Boxplot of Unsettled, Settled, and Sand Filtered Samples

Boxplot of particle size distribution (PSD) for unsettled (US), settled (S), and sand filtered samples, showing median, interquartile range, and extreme particle sizes relative to the 700 µm cutoff.

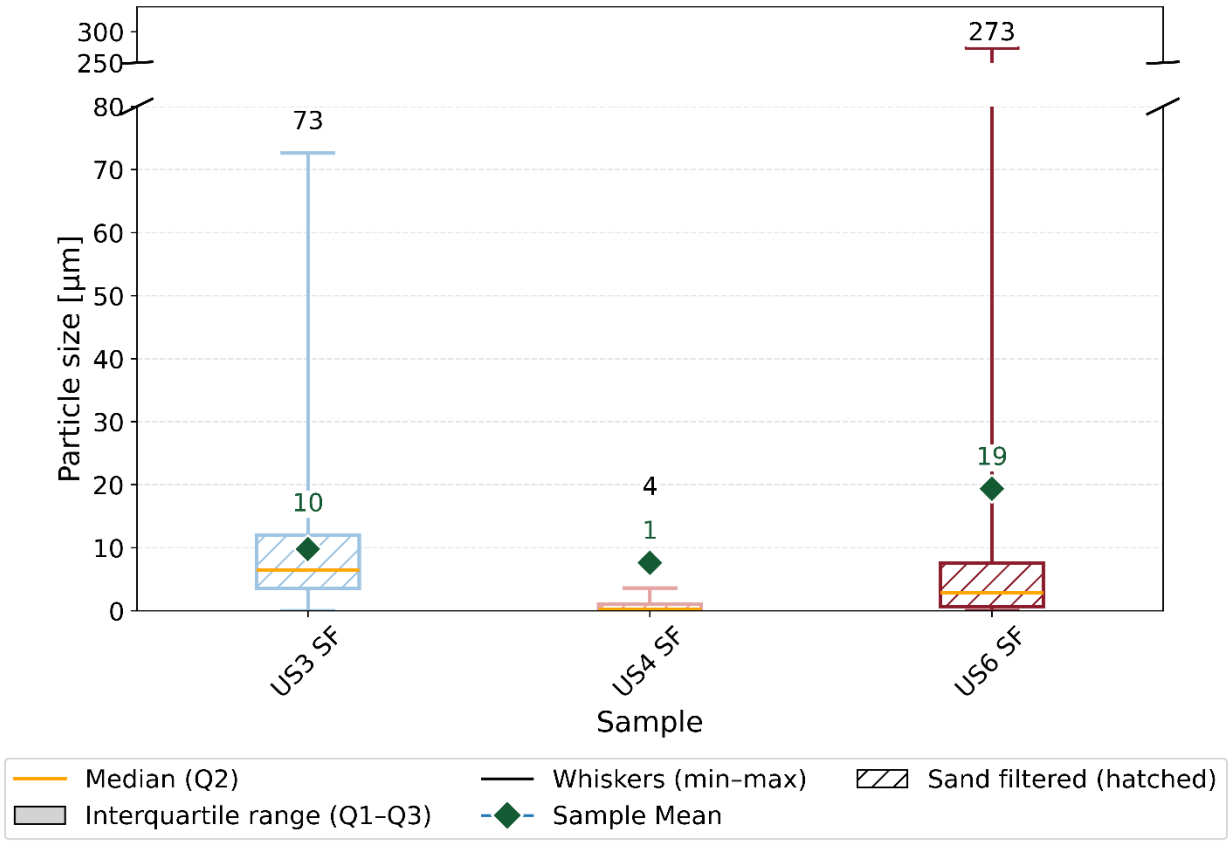

Figure 4.30 Boxplot of the Particle Size Distribution of Only the Sand Filtered Samples

Boxplot of particle size distribution (PSD) of only sand filtered Samples 3, 4, and 6, showing median, interquartile range, and extreme values for each sample.

Table 4.6 below shows the ion concentrations before and after sand filtrations which had positive impacts on sodium, potassium, magnesium, and calcium concentrations. The sulphate concentrations experienced both post and negative impacts. However, there was a very negative impact by the overall total nitrogen. Alkalinity also decreased by 41% for Sample 4 and 8% for Sample 3. Based on these results the benefits of not clogging the membranes outweigh the drawbacks to the increased total nitrogen concentrations, supporting the usage of the sand filter in the membrane experiments.

Table 4.6 Ion Concentration of Sand Filtered Samples

Ion	Initial Sample 4 Conc. [mg/L]	Sample 4 Conc. Post SF [mg/L]	Initial Sample 3 Conc. [mg/L]	Sample 3 Conc. Post SF [mg/L]	Legal Limit [mg/L]
Fluoride	0	0	0	0	1.5
Chloride	29	17	87	56	100
Nitrite	2	16	0	48	1
Bromide	5	3	5	5	N/A
Nitrate	1	3	1	6	10
Phosphate	0	0	2	0	1
Sulfate	149	89	138	142	100
Sodium	521	296	784	473	120
Ammonium	0	0	4	0	1.5
Potassium	56	25	43	33	N/A
Magnesium	61	8	32	10	N/A
Calcium	88	53	130	56	N/A

Ion concentrations of samples before and after sand filtration compared with the corresponding legal reuse limits [105,108].

5 Conclusion

As the water global water intensifies, identifying alternative water sources for agricultural irrigation is becoming increasingly important. One of the industries contributing significantly to this water demand is the brewery industry, which also produces large volumes of contaminated wastewater. To help fulfill this aim of wastewater reclamation for agricultural use, various technologies such as zeolites, activated carbon, multi-media filters, and membrane filtration, are being investigated as a tertiary treatment options. Based on previous studies, membrane treatment was selected as the optimal choice for this thesis because of its ability to produce high quality permeate, its relatively small special footprint, and its lower operating costs compared to other membrane systems.

The first research objective focused on characterizing the brewery wastewater and identifying the treatment requirements to meet legal reuse standards. Brewery wastewater typically exhibits high biological and chemical oxygen demand, total suspended solids (TSS), nutrients, *E. coli*, and sodium concentrations above the legal reuse limit. Once these key water quality performance characteristics were defined, the relevant legal limits for water reuse were identified, the removal efficiencies needed to reach the legal reuse limits, and the membrane characteristics likely to reach these limits.

Within membrane filtration, there are a wide range of treatment options based on the driving mechanism. For this thesis, pressure-driven membranes were selected as the most suitable driving mechanism. Out of the available pressure-driven membranes, nanofiltration was chosen for its balance between cost and production of permeate with sufficient reuse water quality.

These wastewater characteristics were compared to the site-specific results and common system behaviors. This also included reflecting on the previous pilot project's shortcomings and evaluating whether the new technologic improvements of nanofiltration membranes could address those issues.

The second objective examined how different membrane characteristics influence the contaminant removal and fouling behavior. Nano filtration membranes vary by geometry, material, pore size, surface coating, which all influence flux and removal efficiency of contaminants. One of the main challenges of membrane treatment which inhibit the ability of the membrane is fouling. The four main fouling mechanisms were identified and assessed to understand how membrane characteristics influence fouling potential by understanding the influence of fouling on membrane exclusion mechanisms.

Pore size and molecular weight cut-off (MWCO) were found to have the greatest impact on the removal of BOD, COD, TSS, and *E. coli* by using the steric hindrance exclusion

mechanism. While, elevated ion concentrations are more influenced by other exclusion mechanisms like Donnan exclusion, electrostatic interactions, and less hydrophilic interactions, which greatly depend on the membrane's surface charge, material, and coating.

Building on the identification of key membrane properties and fouling mechanisms, the third research objective focused on evaluating how specific membrane characteristics influence the treatment of brewery wastewater. Two distinct nanofiltration membranes were selected to represent contrasting geometries and materials, allowing for a comparative assessment of their behavior influence on exclusion mechanisms, fouling potential, and permeate production, under similar operating conditions.

The first membrane selected was the Inopor 0.9 nm tubular ceramic membrane, which was chosen to reflect typical membrane behavior because of its conventional geometry and low fouling propensity. It was expected to produce a smaller permeate volume but have a higher removal efficiency of chemical and biological contaminants and be less influenced by fouling. Its robust material also allows for more aggressive chemical cleaning, and its large internal diameter helps prevent complete blockage during overflow events. The produced permeate was expected to meet reuse standards, except for potential ion concentration issues.

The second membrane chosen for testing was the NX dNF80 polymeric membrane with a MWCO of 800 Da. This new design of a polymeric nanofiltration membrane is intended for direct industrial wastewater treatment. Its larger pore size compared to the ceramic membrane suggested a lower removal of chemical and biological contaminants. However, its surface area is 30 times that of the ceramic membrane, so a much higher permeate volume was expected. The polymeric membrane with a smaller MWCO was not selected because the high particle concentration of the brewery wastewater already poses a higher fouling propensity than the ceramic tubular membrane, so the larger pore size was chosen to help reduce the fouling propensity of the membrane to still be able to produce a permeate. Similar to the ceramic membrane, the polymeric membrane was expected to produce a permeate that met most reuse regulations, but with potential concerns about potential monovalent ion concentrations in the permeate.

Together, these two membranes provided complementary perspectives on how material composition, pore size, and geometry affect the trade-off between flux, removal efficiency, and fouling propensity of brewery wastewater nanofiltration.

The fourth research objective examined how these two membranes performed under the defined operating conditions and to what extent their treated permeates met reuse

standards. While several membrane characteristics varied between membranes, such as material, geometry, pore size, the results provided insight into how these combined properties influence the treatment efficiency and fouling behavior.

Overall, the ceramic membrane achieved higher removal of organic and biological contaminants, likely due to its smaller pore size and more hydrophilic surface, producing a permeate that met Class A biological reuse standards for nearly all experiments, and almost all chemical limits with the exception of nitrate, sulfate, and sodium. Conversely, the polymeric membrane produced higher fluxes and had lower rejection of monovalent ions and *E. coli* but still produced a permeate that meets nearly all chemical and biological reuse regulations exceeding the concentrations of sodium, ammonium, and Class A biological reuse under 2 bar conditions.

When comparing operating conditions, direct filtration at 4 bar yielded the most favorable overall removal efficiencies, suggesting that higher pressures may have improved parameter removal. The implementation of sand filtration as a pretreatment may not improve the membrane removal efficiencies, however, it did result in a more stable flux and permeability for both membranes. Implementing sand filtration on-site is advised to extend the longevity of the membrane, prevent fiber blockages, and minimize fouling, especially during overflow events.

The overall cost comparison between the two membranes showed the €2,300 difference in membrane module cost, and the difference in cost per unit area, the annual energy costs were nearly identical differing by €1-30 per system pressure. The significant difference in cost was the system pressure with the 4 bar tests being double the cost of 2 bar tests. Both membranes therefore have distinct advantages and limitations, producing permeates of varying quality but with comparable energy requirements. The chemical membrane showed little evidence of fouling and responded well to chemical cleaning, confirming its potential suitability for longer-term operation.

To what extent could the application of nanofiltration as a tertiary treatment improve the potential of treated brewery wastewater for agricultural?

Based on these results, nanofiltration significantly improves the potential for reuse by producing a permeate nearly compliant with reuse standards with the exception of a few ions.

5.1 Final Recommendations and Future Research

5.1.1 General Recommendations for Nanofiltration of Brewery Wastewater

More Extensive Membrane Comparisons:

During this thesis only two membranes were tested with many differences between the membranes tested, including pore, geometry, material, surface area, etc. To better identify which property impacted the differences in treatment more of the membrane properties should be kept constant only varying one at a time. Specifically with a ceramic and polymeric membrane with similar pore sizes based on the results of this thesis. If the brewery wastewater being treated does not have any risks of large particles clogging the hollow fiber tubing, then the smaller pore size should be tested, to see if the ceramic membrane still has higher overall removal efficiencies.

Complete Risk Assessment:

A complete risk assessment following the guidelines presented in *Annexes to the Proposal for a Regulation of the European Parliament and of the Council on Minimum Requirements for Water Reuse* and *Water Reuse in the European Union: Risk Management Approach According to the Regulation* [106,171] This is necessary before the implementation of any water reuse system to prevent any health and safety risks from occurring. This further includes a biological assessment of the potential impact and the possible impact salt accumulation within the soil will have.

Performance of the Different Membranes for Non-Laboratory Scale:

More extensive water treatment tests should be conducted with both membranes using the same influent brewery wastewater sample. Including treatment tests with wastewater collected during an overflow period and testing for longer periods to see the long term impacts on membrane performance of fouling, cleaning efficiency, and material degradation. This needs to be used for a better understanding of membrane life span and the performance of the membranes over a variety of fluctuating influent water quality. This will also impact on the cost comparison to determine how often the membranes lifespans may be with the brewery wastewater used.

Additionally, the experiments conducted were done as a pilot scale and would not be implemented at full scale. In addition to the overall impact of treatment for longer periods, increasing the scale to on-site implementation could also impact on the hydraulic behavior, fouling, and maintenance needed [172].

Post-Treatment Analysis:

Due to brewery wastewater typically having high concentrations of some monovalent ions. A study should be conducted to assess the impact of ion exchange for sodium to determine if this will successfully reduce the concentration to the legal limit if the chemicals dosed cannot be reduced. Additionally, further research to identify which sodium-based chemical agents being used could be swapped with different agents that are more easily removed by nanofiltration.

Modelling Application:

This study focused mostly on the treatment of total daily capacity with dead-end treatment rather than recirculation. The removal efficiencies calculated during these experiments should be used to create a model to determine if the influent should be completely treated, partially treated and recirculated, or partially treated and dispose of the concentrate. This same model should determine if the concentrate is disposed of, how high are the concentrations of key quality parameters. Additionally, the model in Appendix E can be used to help provide a better cost assessment between the two membranes.

Analysis of Additional Operational Parameters:

During this thesis the only operational parameters altered between tests were the pressure and pretreatment of the influent. However, many other operational parameters can greatly influence the performance of membranes during nanofiltration such as temperature, pH, or cross-flow velocity [149,173,174]. Further experimentation should be done to determine if the operational parameters used during experimentation could have been further optimized.

More Extensive Laboratory Measurements:

Based on the high *E. coli* levels found in the influent brewery wastewater, all research regarding the reclamation of brewery wastewater should conduct a biological parameter analysis in a certified laboratory. Abiding by the biological reuse regulations are crucial for the health and safety of those implicated by the reuse, as well as encouragement for other wastewater reclamation. If one instance provides a negative impact to the general public, it could greatly inhibit the continuous research of wastewater reclamation.

In addition to further biological measurements needed, the influence of the water matrix on ion removal efficiency is not determined by the research in this thesis as only one sample is tested. When determining which membrane fits the system best more experimental tests with different influents should be done, and further ion measurements should be conducted with higher and lower detection limits, measured in triplicate to improve the accuracy of findings.

5.1.2 Site Specific Recommendations for Nanofiltration of Brewery Wastewater

Existing System Optimization:

Prior to the implementation of a membrane treatment system the MNR tanks should be drained, cleaned and upon starting the system the domestic and industrial tanks should be separated remain separated. Following this restart of the MNR system the wastewater in the equalization tank should have a biological analysis in a certified lab, and the removal efficiencies should then be compared to see which reuse class the water qualifies for. Samples of the membrane system should be measured weekly to abide by the reuse guidelines and assure that the permeate can be reused.

Additional recommendations for the MNR system to optimize compatibility with a membrane treatment system would be better maintaining the nitrification process within the tank and keeping iron chloride as the phosphate removal agent opposed to iron sulfate. Maintaining the nitrification process in the MNR system would help prevent the concentrations of ammonium and nitrate in the effluent from being above the legal reuse limit.

Implementation of the Membrane system:

When implementing the membrane treatment system, the effluent pond should be used as an equalization settling pond where the influent for the membrane treatment should be taken from the settled sample on the surface. This will help lessen the risk of clogging and prolong the membrane lifespan. In the current laboratory experiments, only recirculated feed was measured, therefor, the performance and fouling behavior under continuous feed conditions still need to be verified. Further cost comparison should also be conducted with the pumps likely used, the desired percentage of permeate recovery. Additional Modelling should also be conducted assessing if dead-end treatment of the complete capacity, partial treatment with concentrate recirculation, or partial treatment with concentrate disposal is best.

Membrane Recommendation:

Based on the results of this thesis, a specific membrane cannot be recommended as the ceramic and polymeric membranes both have pros and cons. The selection of which membrane will be dependent on which membrane characteristics are prioritized and the desired percentage of daily capacity desired as permeate. The ceramic membrane provides more reliability and resilience over time, confirmed Class A biological reuse, however the flux production requires a large quantity of modules requiring a larger spatial footprint and

cost in the worst case scenario [14,18,43]. The polymeric membrane produces a higher flux with a permeate of similar reuse quality with less modules and spatial footprint, but has a greater fouling propensity, requires pretreatment for robustness, and maintenance needed as well as greater cost in the best case scenario [15,18,129,136,138]. Further comparison is also recommended with a polymeric membrane, a smaller pore size similar to the ceramic membrane to see how that affects the removal efficiencies and if fiber clogging is observed [12].

6 References

[1] R.C. van Leerdam, J.H. Rook, L. Riemer, N.G.F.M. van der Aa. Water availability for drinking water production until 2030 – bottlenecks and solutions. 2023.

[2] Hannah Ritchie, Max Roser. Water Use and Stress 2018. https://ourworldindata.org/water-use-stress.

[3] Jan Conway. Beer production worldwide from 1998 to 2023 (in billion hectares). 2024.

[4] Soliman R, Hamza RA, Iorhemen OT. Biofilm-based hybrid systems for enhanced brewery wastewater treatment – A review. Journal of Water Process Engineering 2024;58:104763. https://doi.org/10.1016/j.jwpe.2023.104763.

[5] Shumbe T, Angassa K, Tessema I, Tibebu S, Abewaa M, Getu T. Performance evaluation of a brewery wastewater treatment plant: A case of Heineken Brewery, Addis Ababa, Ethiopia. Heliyon 2024;10:e40719. https://doi.org/10.1016/j.heliyon.2024.e40719.

[6] Qin R. The characteristics of beer industrial wastewater and its influence on the environment. IOP Conf Ser Earth Environ Sci 2018;170:1–5. https://doi.org/10.1088/1755-1315/170/3/032068.

[7] Akinnawo SO. Eutrophication: Causes, consequences, physical, chemical and biological techniques for mitigation strategies. Environmental Challenges 2023;12:100733. https://doi.org/10.1016/j.envc.2023.100733.

[8] Gebeyehu A, Shebeshe N, Kloos H, Belay S. Suitability of nutrients removal from brewery wastewater using a hydroponic technology with Typha latifolia. BMC Biotechnol 2018;18:74. https://doi.org/10.1186/s12896-018-0484-4.

[9] Poór-Pócsi E, Lindeboom R, Kim JE, Hofman J. Factsheet-Metabolic Network Reactor (MNR). 2021.

[10] Roest M. Inzicht in de Metabolic Network Reactors. 2023.

[11] Ashraf A, Ramamurthy R, Rene ER. Wastewater treatment and resource recovery technologies in the brewery industry: Current trends and emerging practices. Sustainable Energy Technologies and Assessments 2021;47:101432. https://doi.org/10.1016/j.seta.2021.101432.

[12] Meshksar M, Roostaee T, Rahimpour MR. Membrane technology for brewery wastewater treatment. Current Trends and Future Developments on (Bio-)

Membranes, Elsevier; 2020, p. 289–303. https://doi.org/10.1016/B978-0-12-816823-3.00010-1.

[13] Simate GS, Cluett J, Iyuke SE, Musapatika ET, Ndlovu S, Walubita LF, et al. The treatment of brewery wastewater for reuse: State of the art. Desalination 2011;273:235–47. https://doi.org/10.1016/j.desal.2011.02.035.

[14] Jianjun Qin, Kiran A. Kekre, Chen JP, Wang LK, Yang L, Zheng Y-M, et al. Membrane and Desalination Technologies. In: Lawrence K. Wang, Jiaping Paul Chen, Yung-Tse Hung, Nazih K. Shammas, editors. Membrane and Desalination Technologies, Humana Press; 2011, p. 237–556. https://doi.org/10.1007/978-1-59745-278-6.

[15] Van Der Bruggen B, Vandecasteele C, Van Gestel T, Doyen W, Leysen R. A review of pressure-driven membrane processes in wastewater treatment and drinking water production. Environmental Progress 2003;22:46–56. https://doi.org/10.1002/ep.670220116.

[16] Liu C. Advances in Membrane Technologies for Drinking Water Purification. Comprehensive Water Quality and Purification, Elsevier; 2014, p. 75–97. https://doi.org/10.1016/B978-0-12-382182-9.00030-X.

[17] Pérez M-Á, Gallego S, Palacio L, Hernández A, Prádanos P, Carmona FJ. Saline Retention and Permeability of Nanofiltration Membranes Versus Resistance and Capacitance as Obtained from Impedance Spectroscopy under a Concentration Gradient. Membranes (Basel) 2023;13:608. https://doi.org/10.3390/membranes13060608.

[18] Crittenden JC., R. RHodes Trussell, David W. Hand, Kerry J. Howe, George Tchobanoglous. MWH's water treatment : principles and design. Third, John Wiley & Sons; 2012, p. 727–818.

[19] Alhussaini MA, Souza-Chaves BM, Felix V, Achilli A. Comparative analysis of reverse osmosis and nanofiltration for the removal of dissolved contaminants in water reuse applications. Desalination 2024;586:117822. https://doi.org/10.1016/j.desal.2024.117822.

[20] Benjamin M, Lawler D, Wiesner M. Water Quality Engineering - Chapter 15 "Membrane Processes." Water Quality Engineering. First Edition, John Wiley & Sons, Inc.; 2013, p. 731–846.

[21] Schaep J, Van der Bruggen B, Uytterhoeven S, Croux R, Vandecasteele C, Wilms D, et al. Removal of hardness from groundwater by nanofiltration. Desalination 1998;119:295–301. https://doi.org/10.1016/S0011-9164(98)00172-6.

[22] Panwattanakul S, Kasikun K, Musikavong C, Sinyoung S. Reduction Of Chloride In Raw Water By Nanofiltration And Reverse Osmosis. IOP Conf Ser Mater Sci Eng 2021;1163:012026. https://doi.org/10.1088/1757-899X/1163/1/012026.

[23] Ozcan A, Perego C, Salvalaglio M, Parrinello M, Yazaydin O. Concentration gradient driven molecular dynamics: a new method for simulations of membrane permeation and separation. Chem Sci 2017;8:3858–65. https://doi.org/10.1039/C6SC04978H.

[24] Laqbaqbi M, Eljaddi T, Khayet M. Membrane distillation for the treatment and recovery of nutrients and colored compounds from wastewaters: fundamentals, modeling, and applications. Nutrients and Colored Compounds in Wastewater, Elsevier; 2025, p. 157–85. https://doi.org/10.1016/B978-0-443-21701-2.00011-8.

[25] Van der Bruggen B. Advances in electrodialysis for water treatment. Advances in Membrane Technologies for Water Treatment, Elsevier; 2015, p. 185–203. https://doi.org/10.1016/B978-1-78242-121-4.00006-X.

[26] Liu X, Shan Y, Zhang S, Kong Q, Pang H. Application of metal organic framework in wastewater treatment. Green Energy & Environment 2023;8:698–721. https://doi.org/10.1016/j.gee.2022.03.005.

[27] Pandey P, Chauhan RS. Membranes for gas separation. Prog Polym Sci 2001;26:853–93. https://doi.org/10.1016/S0079-6700(01)00009-0.

[28] Hwang K-J, Hsu Y-L, Tung K-L. Effect of particle size on the performance of cross-flow microfiltration. Advanced Powder Technology 2006;17:189–206. https://doi.org/10.1163/156855206775992292.

[29] Saavedra A, Valdés H, Velásquez J, Hernández S. Comparative Analysis of Donnan Steric Partitioning Pore Model and Dielectric Exclusion Applied to the Fractionation of Aqueous Saline Solutions through Nanofiltration. ChemEngineering 2024;8:39. https://doi.org/10.3390/chemengineering8020039.

[30] Mohammad AW, Ali N. Understanding the steric and charge contributions in NF membranes using increasing MWCO polyamide membranes. Desalination 2002;147:205–12. https://doi.org/10.1016/S0011-9164(02)00535-0.

[31] Bellona C, Drewes JE, Xu P, Amy G. Factors affecting the rejection of organic solutes during NF/RO treatment—a literature review. Water Res 2004;38:2795–809. https://doi.org/10.1016/j.watres.2004.03.034.

[32] Jonkers WA, Cornelissen ER, de Vos WM. Hollow fiber nanofiltration: From lab-scale research to full-scale applications. J Memb Sci 2023;669:121234. https://doi.org/10.1016/j.memsci.2022.121234.

[33] Abdel-Fatah MA. Nanofiltration systems and applications in wastewater treatment: Review article. Ain Shams Engineering Journal 2018;9:3077–92. https://doi.org/10.1016/j.asej.2018.08.001.

[34] Labhasetwar PK, Yadav A. Membrane Based Point-of-Use Drinking Water Treatment Systems. IWA Publishing; 2023. https://doi.org/10.2166/9781789062724.

[35] Chew TL, Anbealagan LD, Yeong YF, Ng QH, Shuit SH. Development of mixed matrix membranes for gas separations. Handbook of Nanotechnology Applications: Environment, Energy, Agriculture and Medicine 2020:195–218. https://doi.org/10.1016/B978-0-12-821506-7.00008-9.

[36] Veríssimo S, Peinemann K-V, Bordado J. New composite hollow fiber membrane for nanofiltration. Desalination 2005;184:1–11. https://doi.org/10.1016/j.desal.2005.03.069.

[37] Ji J, Liu F, Hashim NA, Abed MRM, Li K. Poly(vinylidene fluoride) (PVDF) membranes for fluid separation. React Funct Polym 2015;86:134–53. https://doi.org/10.1016/j.reactfunctpolym.2014.09.023.

[38] Zhang S, Wang K, Rietveld LC, Heijman SGJ. Fouling removal in ceramic ultrafiltration membrane via catalyst modification with Fenton-like backwash. J Memb Sci 2025;734:124411. https://doi.org/10.1016/J.MEMSCI.2025.124411.

[39] Liu Z, Zhu X, Liang P, Zhang X, Kimura K, Huang X. Distinction between polymeric and ceramic membrane in AnMBR treating municipal wastewater: In terms of irremovable fouling. J Memb Sci 2019;588:117229. https://doi.org/10.1016/j.memsci.2019.117229.

[40] Fujioka T, Khan SJ, McDonald JA, Nghiem LD. Nanofiltration of trace organic chemicals: A comparison between ceramic and polymeric membranes. Sep Purif Technol 2014;136:258–64. https://doi.org/10.1016/j.seppur.2014.08.039.

[41] Braeken L, Van der Bruggen B, Vandecasteele C. Regeneration of brewery waste water using nanofiltration. Water Res 2004;38:3075–82. https://doi.org/10.1016/j.watres.2004.03.028.

[42] Li M-S, Fu Z-J, Li Z, Liu M-L, Sun S-P. Breaking barriers in membrane separation: Power of functional coatings. Sep Purif Technol 2025;360:131173. https://doi.org/10.1016/j.seppur.2024.131173.

[43] Xue YL, Zhang R, Cao B, Li P. Tubular membranes and modules. Hollow Fiber Membranes, Elsevier; 2021, p. 431–48. https://doi.org/10.1016/B978-0-12-821876-1.00011-1.

[44] Imbrogno A, Calvo JI, Breida M, Schwaiger R, Schäfer AI. Molecular weight cut off (MWCO) determination in ultra- and nanofiltration: Review of methods and implications on organic matter removal. Sep Purif Technol 2025;354:128612. https://doi.org/10.1016/j.seppur.2024.128612.

[45] Peeters JMM, Boom JP, Mulder MHV, Strathmann H. Retention measurements of nanofiltration membranes with electrolyte solutions. J Memb Sci 1998;145:199–209. https://doi.org/10.1016/S0376-7388(98)00079-9.

[46] Bandini S, Vezzani D. Nanofiltration modeling: the role of dielectric exclusion in membrane characterization. Chem Eng Sci 2003;58:3303–26. https://doi.org/10.1016/S0009-2509(03)00212-4.

[47] Li Q, Elimelech M. Synergistic effects in combined fouling of a loose nanofiltration membrane by colloidal materials and natural organic matter. J Memb Sci 2006;278:72–82. https://doi.org/10.1016/j.memsci.2005.10.045.

[48] Wan Ikhsan SN, Yusof N, Mat Nawi NI, Bilad MR, Shamsuddin N, Aziz F, et al. Halloysite Nanotube-Ferrihydrite Incorporated Polyethersulfone Mixed Matrix Membrane: Effect of Nanocomposite Loading on the Antifouling Performance. Polymers (Basel) 2021;13:441. https://doi.org/10.3390/polym13030441.

[49] Guo W, Ngo H-H, Li J. A mini-review on membrane fouling. Bioresour Technol 2012;122:27–34. https://doi.org/10.1016/j.biortech.2012.04.089.

[50] Pasquet PL, Villain-Gambier M, Ziegler-Devin I, Julien-David D, Trébouet D. Valorization of phenolic compounds from brewery wastewater: Performances assessment of ultrafiltration and nanofiltration process with application of HPLC coupled with antioxidant analysis tool. Chemical Engineering Journal 2023;476:146696. https://doi.org/10.1016/j.cej.2023.146696.

[51] Tien C, Ramarao B V. Revisiting the laws of filtration: An assessment of their use in identifying particle retention mechanisms in filtration. J Memb Sci 2011;383:17–25. https://doi.org/10.1016/j.memsci.2011.07.019.

[52] Satyannarayana KV V., Lakshmi Sandhya Rani S, Mathaji CB, Vinoth Kumar R. Fouling Mechanisms in Nanofiltration Membranes, 2023, p. 197–215. https://doi.org/10.1007/978-981-19-5315-6_11.

[53] Guo W, Ngo H-H, Li J. A mini-review on membrane fouling. Bioresour Technol 2012;122:27–34. https://doi.org/10.1016/j.biortech.2012.04.089.

[54] Al-Ahmad M, Abdul Aleem FA, Mutiri A, Ubaisy A. Biofuoling in RO membrane systems Part 1: Fundamentals and control. Desalination 2000;132:173–9. https://doi.org/10.1016/S0011-9164(00)00146-6.

[55] Nguyen T, Roddick F, Fan L. Biofouling of Water Treatment Membranes: A Review of the Underlying Causes, Monitoring Techniques and Control Measures. Membranes (Basel) 2012;2:804–40. https://doi.org/10.3390/membranes2040804.

[56] Li H, Chen V. Membrane Fouling and Cleaning in Food and Bioprocessing. Membrane Technology, Elsevier; 2010, p. 213–54. https://doi.org/10.1016/B978-1-85617-632-3.00010-0.

[57] Telgmann U, Horn H, Morgenroth E. Influence of growth history on sloughing and erosion from biofilms. Water Res 2004;38:3671–84. https://doi.org/10.1016/j.watres.2004.05.020.

[58] Burman I, Sinha A. Impact Assessment of Mixed Liquor Suspended Solids from Polyurethane Media Effluent on Ceramic Membrane Fouling in Anaerobic Hybrid Membrane Bioreactor. Journal of Environmental Engineering 2022;148. https://doi.org/10.1061/(ASCE)EE.1943-7870.0001956.

[59] Li H, Chen V. Membrane Fouling and Cleaning in Food and Bioprocessing. Membrane Technology, Elsevier; 2010, p. 213–54. https://doi.org/10.1016/B978-1-85617-632-3.00010-0.

[60] Yaroshchuk AE. Dielectric exclusion of ions from membranes. Adv Colloid Interface Sci 2000;85:193–230. https://doi.org/10.1016/S0001-8686(99)00021-4.

[61] Götz G, Geißen S-U, Ahrens A, Reimann S. Adjustment of the wastewater matrix for optimization of membrane systems applied for water reuse in breweries. J Memb Sci 2014;465:68–77. https://doi.org/10.1016/j.memsci.2014.04.014.

[62] Li Y, Zhu G, Wang Y, Chai Y, Liu C. Preparation, mechanism and applications of oriented MFI zeolite membranes: A review. Microporous and Mesoporous Materials 2021;312:110790. https://doi.org/10.1016/j.micromeso.2020.110790.

[63] Kumari S, Chowdhry J, Kumar M, Chandra Garg M. Zeolites in wastewater treatment: A comprehensive review on scientometric analysis, adsorption mechanisms, and future prospects. Environ Res 2024;260:119782. https://doi.org/10.1016/j.envres.2024.119782.

[64] Papaevangelou V, Bakalakou KA, Tsilinikos J, Akratos CS. Testing Zeolite and Palygorskite as a Potential Medium for Ammonium Recovery and Brewery Wastewater Treatment. Water (Basel) 2023;15:4069. https://doi.org/10.3390/w15234069.

[65] Baerlocher C, McCusker L, Olson D. ATLAS OF ZEOLITE FRAMEWORK TYPES. 6th Edition. Amsterdam: 2007.

[66] Wong CF, Saif UM, Chow KL, Wong JTF, Chen XW, Liang Y, et al. Applications of charcoal, activated charcoal, and biochar in aquaculture – A review. Science of the Total Environment 2024;929. https://doi.org/10.1016/j.scitotenv.2024.172574.

[67] Crittenden JC. MWH's water treatment : principles and design - Chapter 15 "Adsorption," John Wiley & Sons; 2012, p. 1901.

[68] Ahmad A, Azam T. Water Purification Technologies. Bottled and Packaged Water, vol. Volume 4, Elsevier; 2019, p. 83–120. https://doi.org/10.1016/B978-0-12-815272-0.00004-0.

[69] Bidira F, Al-Senani GM, Bekele EA, Garomsa FS, Vigneshwaran S, Al-Qahtani SD, et al. Synergistic pollutant removal from brewery wastewater using electrocoagulation-assisted pumpkin seed-activated carbon. Process Safety and Environmental Protection 2025;200:107429. https://doi.org/10.1016/J.PSEP.2025.107429.

[70] Bagus I, Gunam W, Eva F, Natalia L, Wayan Arnata I. Combination of filter media to reduce total suspended solids, biochemical and chemical oxygen demand in wastewater using installation of horizontal roughing filter Cenny Putnarubun Politeknik Perikanan Negeri Tual, Indonesia. Tual state Fisheries Polytechnic. vol. 6. 2016.

[71] L. Huisman, W.E. Wood FICE. Slow Sand Filtration. 1974.

[72] Woodard & Curran Inc. Methods for Treating Wastewaters from Industry. Industrial Waste Treatment Handbook, Elsevier; 2006, p. 149–334. https://doi.org/10.1016/B978-075067963-3/50009-6.

[73] Xyla AG, Giannimaras EK, Koutsoukos PG. The precipitation of calcium carbonate in aqueous solutions. Colloids and Surfaces 1991;53:241–55. https://doi.org/10.1016/0166-6622(91)80140-J.

[74] Al-Harahsheh M, Batiha M, Kraishan S, Al-Zoubi H. Precipitation treatment of effluent acidic wastewater from phosphate-containing fertilizer industry: Characterization of solid and liquid products. Sep Purif Technol 2014;123:190–9. https://doi.org/10.1016/j.seppur.2013.12.027.

[75] Diro K, Angassa K, Gebremeskel T, Abewaa M, Mengistu A. Assessment of the water footprint of the brewery industry: The case of Heineken, Addis Ababa, Ethiopia. Results in Engineering 2024;24:102928. https://doi.org/10.1016/j.rineng.2024.102928.

[76] Santonja GG, Karlis P, Stubdrup KR, Brinkmann T. Best Available Techniques (BAT) Reference Document for the Food, Drink and Milk Industries. 2010.

[77] Adugna DB, Ante AA, Aschale M, Maja MM. Characterization of physicochemical and bacteriological properties of Harar Brewery wastewater and its suitability for irrigation. Environmental Challenges 2024;16:100967. https://doi.org/10.1016/j.envc.2024.100967.

[78] Fillaudeau L, Blanpain-Avet P, Daufin G. Water, wastewater and waste management in brewing industries. J Clean Prod 2006;14:463–71. https://doi.org/10.1016/j.jclepro.2005.01.002.

[79] Enitan AM, Adeyemo J, Kumari SK, Swalaha FM, Bux F. Characterization of brewery wastewater composition. International Journal of Environmental and Ecological Engineering 2015;9:1073–6. https://doi.org/10.51415/10321/2992.

[80] Nowicki S, deLaurent ZR, de Villiers EP, Githinji G, Charles KJ. The utility of Escherichia coli as a contamination indicator for rural drinking water: Evidence from whole genome sequencing. PLoS One 2021;16:e0245910. https://doi.org/10.1371/journal.pone.0245910.

[81] Khan FM, Gupta R. Escherichia coli (E. coli) as an Indicator of Fecal Contamination in Groundwater: A Review, 2020, p. 225–35. https://doi.org/10.1007/978-3-030-45263-6_21.

[82] Khan FM, Gupta R. Escherichia coli (E. coli) as an Indicator of Fecal Contamination in Groundwater: A Review, 2020, p. 225–35. https://doi.org/10.1007/978-3-030-45263-6_21.

[83] Epa U. E. coli (Escherichia coli). n.d.

[84] World Health Organization. Diarrhoeal disease. Https://WwwWhoInt/News-Room/Fact-Sheets/Detail/Diarrhoeal-Disease 2024.

[85] Anwar N, Rahaman MdS. Membrane desalination processes for water recovery from pre-treated brewery wastewater: Performance and fouling. Sep Purif Technol 2020;252:117420. https://doi.org/10.1016/j.seppur.2020.117420.

[86] Mabasa NC, Jones CLW, Laing M. The use of treated brewery effluent for salt tolerant crop irrigation. Agric Water Manag 2021;245:106590. https://doi.org/10.1016/j.agwat.2020.106590.

[87] Taylor RP, Jones CLW, Laing M, Dames J. The potential use of treated brewery effluent as a water and nutrient source in irrigated crop production. Water Resour Ind 2018;19:47–60. https://doi.org/10.1016/j.wri.2018.02.001.

[88] Sou/Dakouré MY, Mermoud A, Yacouba H, Boivin P. Impacts of irrigation with industrial treated wastewater on soil properties. Geoderma 2013;200–201:31–9. https://doi.org/10.1016/j.geoderma.2013.02.008.

[89] Kaushik A, Nisha R, Jagjeeta K, Kaushik CP. Impact of long and short term irrigation of a sodic soil with distillery effluent in combination with bioamendments. Bioresour Technol 2005;96:1860–6. https://doi.org/10.1016/j.biortech.2005.01.031.

[90] Kramer FC, Shang R, Rietveld LC, Heijman SJG. Influence of pH, multivalent counter ions, and membrane fouling on phosphate retention during ceramic nanofiltration. Sep Purif Technol 2019;227:115675. https://doi.org/10.1016/j.seppur.2019.115675.

[91] Jafarinejad S, Esfahani MR. A Review on the Nanofiltration Process for Treating Wastewaters from the Petroleum Industry. Separations 2021;8:206. https://doi.org/10.3390/separations8110206.

[92] Mahvi AH, Malakootian M, Fatehizadeh A, Ehrampoush MH. Nitrate removal from aqueous solutions by nanofiltration. Desalination Water Treat 2011;29:326–30. https://doi.org/10.5004/dwt.2011.1743.

[93] Sugali CS, Sajja C, G. NS, Sundergopal S. Application of nanofiltration membrane process for the treatment of laundry wastewater. Water Pract Technol 2025;20:324–39. https://doi.org/10.2166/wpt.2025.003.

[94] Cabrera SM, Winnubst L, Richter H, Voigt I, McCutcheon J, Nijmeijer A. Performance evaluation of an industrial ceramic nanofiltration unit for wastewater treatment in oil production. Water Res 2022;220:118593. https://doi.org/10.1016/j.watres.2022.118593.

[95] Chemical-free drinking water production-Next-gen water treatment demonstrated-Case study: Hollow Fiber Nanofiltration (HFNF) membranes in chemical free drinking water treatment set-up with Vitens. n.d.

[96] Yitbarek M, Abdeta K, Beyene A, Astatkie H, Dadi D, Desalew G, et al. Experimental evaluation of sorptive removal of fluoride from drinking water using natural and brewery waste diatomite. Process Safety and Environmental Protection 2019;128:95–106. https://doi.org/10.1016/j.psep.2019.05.052.

[97] Kettunen R, Keskitalo P. Combination of membrane technology and limestone filtration to control drinking water quality. Desalination 2000;131:271–83. https://doi.org/10.1016/S0011-9164(00)90025-0.

[98] Lhassani A. Selective demineralization of water by nanofiltration Application to the defluorination of brackish water. Water Res 2001;35:3260–4. https://doi.org/10.1016/S0043-1354(01)00020-3.

[99] Popova A, Rattanakom R, Yu Z-Q, Li Z, Nakagawa K, Fujioka T. Evaluating the potential of nanofiltration membranes for removing ammonium, nitrate, and nitrite in drinking water sources. Water Res 2023;244:120484. https://doi.org/10.1016/j.watres.2023.120484.

[100] Hurtado CF, Cancino-Madariaga B, Torrejón C, Villegas PP. Separation of nitrite and nitrate from water in aquaculture by nanofiltration membrane. Desalination Water Treat 2016;57:26050–62. https://doi.org/10.1080/19443994.2016.1160440.

[101] Choi S, Yun Z, Hong S, Ahn K. The effect of co-existing ions and surface characteristics of nanomembranes on the removal of nitrate and fluoride. Desalination 2001;133:53–64. https://doi.org/10.1016/S0011-9164(01)00082-0.

[102] Ian Kurniawan. Removal of the Most Probable Number of coli from Hospital Wastewater Using Nanofiltration Membranes. Science Get Journal 2025;2:40–52. https://doi.org/10.69855/science.v2i3.168.

[103] Arsene TK, Tian M, Zhang Y. High-performance nanofiltration membranes enhanced by bis(4-aminophenyl) phenylphosphonate for improved thermal stability and antibacterial properties. Sep Purif Technol 2025;376:134095. https://doi.org/10.1016/j.seppur.2025.134095.

[104] Kumar Y, Khalangre A, Suhag R, Cassano A. Applications of Reverse Osmosis and Nanofiltration Membrane Process in Wine and Beer Industry. Membranes (Basel) 2025;15:140. https://doi.org/10.3390/membranes15050140.

[105] L. Alcalde-Sanz, Gawlik BM. Minimum quality requirements for water reuse in agricultural irrigation and aquifer recharge Towards a legal instrument on water reuse at EU level. 2017. https://doi.org/10.2760/887727.

[106] European Commission. European Commission Annexes to the “Proposal for a Regulation of the European Parliament and of the Council on minimum requirements for water reuse.” Brussels: 2018.

[107] Singh R, Bhadouria R, Singh P, Kumar A, Pandey S, Singh VK. Nanofiltration technology for removal of pathogens present in drinking water. Waterborne Pathogens, Elsevier; 2020, p. 463–89. https://doi.org/10.1016/B978-0-12-818783-8.00021-9.

[108] F.A. Swartjes, H.H.J.L. van den Berg, F. Biemans, D.J van der Gaag, R. de Jonge, R.C. van Leerdam, et al. Assessment framework for the use of municipal wastewater in agriculture. Phase 1: Legal framework and food safety. 2023.

[109] Johnson TL, McQuarrie JP, Shaw AR. INTEGRATED FIXED-FILM ACTIVATED SLUDGE (IFAS): THE NEW CHOICE FOR NITROGEN REMOVAL UPGRADES IN THE UNITED STATES. Proceedings of the Water Environment Federation 2004;2004:296–318. https://doi.org/10.2175/193864704784147214.

[110] Slade AH, Thorn GJS, Dennis MA. The relationship between BOD:N ratio and wastewater treatability in a nitrogen-fixing wastewater treatment system. Water Science and Technology 2011;63:627–32. https://doi.org/10.2166/wst.2011.215.

[111] Martikainen PJ. Heterotrophic nitrification – An eternal mystery in the nitrogen cycle. Soil Biol Biochem 2022;168:108611. https://doi.org/10.1016/j.soilbio.2022.108611.

[112] Verma S, Kuila A, Jacob S. Role of Biofilms in Waste Water Treatment. Appl Biochem Biotechnol 2023;195:5618–42. https://doi.org/10.1007/s12010-022-04163-5.

[113] Hwang JH, Cicek N, Oleszkiewicz JA. Achieving biofilm control in a membrane biofilm reactor removing total nitrogen. Water Res 2010;44:2283–91. https://doi.org/10.1016/j.watres.2009.12.022.

[114] Chang Y-J, Chang Y-T, Chen H-J. A method for controlling hydrogen sulfide in water by adding solid phase oxygen. Bioresour Technol 2007;98:478–83. https://doi.org/10.1016/j.biortech.2005.11.031.

[115] Das J, Lens PNL. Resilience of hollow fibre membrane bioreactors for treating H2S under steady state and transient conditions. Chemosphere 2022;307:136142. https://doi.org/10.1016/j.chemosphere.2022.136142.

[116] Nailwal BC, Salvi J, Chotalia P, Goswami N, Muhmood L, Kar S, et al. Enhanced H2S decomposition using membrane reactor. Int J Hydrogen Energy 2024;70:251–61. https://doi.org/10.1016/j.ijhydene.2024.05.195.

[117] UK Health Security Agency. UK_Hydrogen_sulfide. 2025.

[118] Mees van Someren. Optimal conditions for the efficient functioning of the Biomakerij Advisory report. Berkel-Enschot: 2023.

[119] Kentie N. Adviesrapport De stikstofverwijdering binnen een MNR-waterzuivering. 2025.

[120] Tchobanoglous George, Burton FL., Stensel HDavid. Wastewater engineering : treatment and reuse, Metcalf & Eddy. McGraw-Hill; 2004.

[121] Garcia F, Ciceron D, Saboni A, Alexandrova S. Nitrate ions elimination from drinking water by nanofiltration: Membrane choice. Sep Purif Technol 2006;52:196–200. https://doi.org/10.1016/j.seppur.2006.03.023.

[122] Fang Y, Duranceau S. Study of the Effect of Nanoparticles and Surface Morphology on Reverse Osmosis and Nanofiltration Membrane Productivity. Membranes (Basel) 2013;3:196–225. https://doi.org/10.3390/membranes3030196.

[123] Wang Y, Ju L, Xu F, Tian L, Jia R, Song W, et al. Effect of a nanofiltration combined process on the treatment of high-hardness and micropolluted water. Environ Res 2020;182:109063. https://doi.org/10.1016/j.envres.2019.109063.

[124] Vogel D, Simon A, Alturki AA, Bilitewski B, Price WE, Nghiem LD. Effects of fouling and scaling on the retention of trace organic contaminants by a nanofiltration membrane: The role of cake-enhanced concentration polarisation. Sep Purif Technol 2010;73:256–63. https://doi.org/10.1016/j.seppur.2010.04.010.

[125] Liu W, Wang X-M, Li D, Gao Y, Wang K, Huang X. Dominant Mechanism of Nanofiltration for Chloride/Sulfate Ion Separation in High Salinity Solutions: The Quantification of Pore Size-Influenced Dielectric Exclusion. Environ Sci Technol 2025;59:5848–55. https://doi.org/10.1021/acs.est.5c00277.

[126] Tian M, Hui H, Ma T, Zhao G, Zarak M, You X, et al. A novel nanofiltration membrane with a sacrificial chlorine-resistant nanofilm: Design and characterization of tailored membrane pores and surface charge. Desalination 2022;538:115896. https://doi.org/10.1016/j.desal.2022.115896.

[127] Liu M, Yu F, Niu L, Chi H. Advances in nanofiltration membrane pore size adjustment techniques: A review. Environmental Functional Materials 2025. https://doi.org/10.1016/j.efmat.2025.02.002.

[128] Gryta M. Alkaline scaling in the membrane distillation process. Desalination 2008;228:128–34. https://doi.org/10.1016/j.desal.2007.10.004.

[129] Ophorst M, Grooth J de, Heijman SGJ, Vaudevire EMH, Jafari M. Operation and performance analysis of direct hollow fiber nanofiltration: A pilot study at IJsselmeer. Sep Purif Technol 2024;349:127786. https://doi.org/10.1016/j.seppur.2024.127786.

[130] Zsirai T, Qiblawey H, Buzatu P, Al-Marri M, Judd SJ. Cleaning of ceramic membranes for produced water filtration. J Pet Sci Eng 2018;166:283–9. https://doi.org/10.1016/j.petrol.2018.03.036.

[131] Xiao H, Huang C, Wei H, Zhong M, Chen Z, Xie P, et al. In-situ atomic hydrogen generation: A key to elevating membrane cleaning via citric acid-modified Fenton-like system. Chemical Engineering Journal 2024;498:155547. https://doi.org/10.1016/j.cej.2024.155547.

[132] Li Y, Xu Y, Rietveld LC, Heijman SGJ. Calcium carbonate precoating/acid cleaning method for fouling control in ceramic nanofiltration membranes. Sep Purif Technol 2025;356:130002. https://doi.org/10.1016/j.seppur.2024.130002.

[133] Jonkers WA, Cornelissen ER, de Vos WM. Hollow fiber nanofiltration: From lab-scale research to full-scale applications. J Memb Sci 2023;669:121234. https://doi.org/10.1016/j.memsci.2022.121234.

[134] EES. dNF Process Design Manual Stage N Feed & Bleed. 2023.

[135] Rutten SB, Junker MA, Leal LH, de Vos WM, Lammertink RGH, de Grooth J. Influence of dominant salts on the removal of trace micropollutants by hollow fiber nanofiltration membranes. J Memb Sci 2023;678:121625. https://doi.org/10.1016/j.memsci.2023.121625.

[136] Jarvis P, Carra I, Jafari M, Judd SJ. Ceramic vs polymeric membrane implementation for potable water treatment. Water Res 2022;215:118269. https://doi.org/10.1016/j.watres.2022.118269.

[137] Dong Y, Wu H, Yang F, Gray S. Cost and efficiency perspectives of ceramic membranes for water treatment. Water Res 2022;220:118629. https://doi.org/10.1016/j.watres.2022.118629.

[138] Jonkers WA, Cornelissen ER, de Vos WM. Hollow fiber nanofiltration: From lab-scale research to full-scale applications. J Memb Sci 2023;669:121234. https://doi.org/10.1016/j.memsci.2022.121234.

[139] Alhussaini MA, Souza-Chaves BM, Felix V, Achilli A. Comparative analysis of reverse osmosis and nanofiltration for the removal of dissolved contaminants in water reuse applications. Desalination 2024;586:117822. https://doi.org/10.1016/j.desal.2024.117822.

[140] Miller DJ, Kasemset S, Paul DR, Freeman BD. Comparison of membrane fouling at constant flux and constant transmembrane pressure conditions. J Memb Sci 2014;454:505–15. https://doi.org/10.1016/j.memsci.2013.12.027.

[141] NX Filtration B. V. MP025 modules & MexplorerTM pilot. 2023.

[142] Woo YC, Lee JJ, Oh JS, Jang HJ, Kim HS. Effect of chemical cleaning conditions on the flux recovery of fouled membrane. Desalination Water Treat 2013;51:5268–74. https://doi.org/10.1080/19443994.2013.768754.

[143] Baker J, Bernard D, Christensen S, Sale M, Freda J, Heltcher K, et al. Biological effects of changes in surface water acid-base chemistry. Oak Ridge, TN (United States): 1990. https://doi.org/10.2172/7255574.

[144] Mohammadian E, Hadavimoghaddam F, Kheirollahi M, Jafari M, Chenlu X, Liu B. Probing Solubility and pH of CO2 in aqueous solutions: Implications for CO2 injection into oceans. Journal of CO2 Utilization 2023;71:102463. https://doi.org/10.1016/j.jcou.2023.102463.

[145] Mahvi AH, Talaeipour M, Nouri J, Hassani AH, Tadi RA. Evaluation of removing monovalent and divalent ions of brackish water in Qom Province using membrane processes of nanofiltration, reverse osmosis and hybrid system. Desalination Water Treat 2021;209:16–23. https://doi.org/10.5004/dwt.2021.26485.

[146] Schäfer AI, Fane AG, Waite TD. Cost factors and chemical pretreatment effects in the membrane filtration of waters containing natural organic matter. Water Res 2001;35:1509–17. https://doi.org/10.1016/S0043-1354(00)00418-8.

[147] Zhu A, Long F, Wang X, Zhu W, Ma J. The negative rejection of H+ in NF of carbonate solution and its influences on membrane performance. Chemosphere 2007;67:1558–65. https://doi.org/10.1016/j.chemosphere.2006.11.065.

[148] Reig M, Licon E, Gibert O, Yaroshchuk A, Cortina JL. Rejection of ammonium and nitrate from sodium chloride solutions by nanofiltration: Effect of dominant-salt concentration on the trace-ion rejection. Chemical Engineering Journal 2016;303:401–8. https://doi.org/10.1016/j.cej.2016.06.025.

[149] Luo J, Wan Y. Effects of pH and salt on nanofiltration—a critical review. J Memb Sci 2013;438:18–28. https://doi.org/10.1016/j.memsci.2013.03.029.

[150] Hilal N, Kochkodan V, Al Abdulgader H, Mandale S, Al-Jlil SA. A combined ion exchange–nanofiltration process for water desalination: I. sulphate–chloride ion-exchange in saline solutions. Desalination 2015;363:44–50. https://doi.org/10.1016/j.desal.2014.11.016.

[151] Ho C-C, Zydney AL. A Combined Pore Blockage and Cake Filtration Model for Protein Fouling during Microfiltration. J Colloid Interface Sci 2000;232:389–99. https://doi.org/10.1006/jcis.2000.7231.

[152] AlSawaftah N, Abuwatfa W, Darwish N, Husseini G. A Comprehensive Review on Membrane Fouling: Mathematical Modelling, Prediction, Diagnosis, and Mitigation. Water (Basel) 2021;13:1327. https://doi.org/10.3390/w13091327.

[153] Zhou F, Wang D, Hu J, Zhang Y, Tan BK, Lin S. Control Measurements of Escherichia coli Biofilm: A Review. Foods 2022;11:2469. https://doi.org/10.3390/foods11162469.

[154] Du X, Shi Y, Jegatheesan V, Haq IU. A Review on the Mechanism, Impacts and Control Methods of Membrane Fouling in MBR System. Membranes (Basel) 2020;10:24. https://doi.org/10.3390/membranes10020024.

[155] Atkinson S. NX Filtration's hollow-fibre NF technology makes peat water from Indonesia's Mesjid River safe to drink. Membrane Technology 2021;2021:7–9. https://doi.org/10.1016/S0958-2118(21)00045-8.

[156] Pérez-González A, Ibáñez R, Gómez P, Urtiaga AM, Ortiz I, Irabien JA. Nanofiltration separation of polyvalent and monovalent anions in desalination brines. J Memb Sci 2015;473:16–27. https://doi.org/10.1016/j.memsci.2014.08.045.

[157] KOCH AL, HIGGINS ML, DOYLE RJ. Surface Tension-like Forces Determine Bacterial Shapes: Streptococcus faecium. Microbiology (N Y) 1981;123:151–61. https://doi.org/10.1099/00221287-123-1-151.

[158] Salinas-Almaguer S, Mell M, Almendro-Vedia VG, Calero M, Robledo-Sánchez KCM, Ruiz-Suarez C, et al. Membrane rigidity regulates E. coli proliferation rates. Sci Rep 2022;12:933. https://doi.org/10.1038/s41598-022-04970-0.

[159] Arumugham T, Kaleekkal NJ, Gopal S, Nambikkattu J, K R, Aboulella AM, et al. Recent developments in porous ceramic membranes for wastewater treatment and desalination: A review. J Environ Manage 2021;293:112925. https://doi.org/10.1016/j.jenvman.2021.112925.

[160] Hu K, Dickson JM. Nanofiltration membrane performance on fluoride removal from water. J Memb Sci 2006;279:529–38. https://doi.org/10.1016/j.memsci.2005.12.047.

[161] Listiarini K, Tor JT, Sun DD, Leckie JO. Hybrid coagulation–nanofiltration membrane for removal of bromate and humic acid in water. J Memb Sci 2010;365:154–9. https://doi.org/10.1016/j.memsci.2010.08.048.

[162] Firdaus AAF, Slamet A, Yuniarto A, Said NI. Removal of total phosphate and sulfate from industrial wastewater by recirculating flow in nanofiltration. IOP Conf Ser Earth Environ Sci 2024;1307:012020. https://doi.org/10.1088/1755-1315/1307/1/012020.

[163] Rashki P, piri H, Khamari E. Effect of potassium fertilization on roselle yield and yield components as well as IWUE under deficit irrigation regimes. South African Journal of Botany 2022;148:21–32. https://doi.org/10.1016/j.sajb.2022.03.048.

[164] Smith C, Profile S, Oster JD, Smith CJ, Sposito G. Potassium and magnesium in irrigation water quality assessment ARTICLE IN PRESS G Model Potassium and magnesium in irrigation water quality assessment. Agric Water Manag 2014. https://doi.org/10.1016/agwat.2014.09.003.

[165] Ford DM, Glandt ED. Steric hindrance at the entrances to small pores. J Memb Sci 1995;107:47–57. https://doi.org/10.1016/0376-7388(95)00101-H.

[166] Pieper R, Zhang Q, Clark DJ, Huang S-T, Suh M-J, Braisted JC, et al. Characterizing the Escherichia coli O157:H7 Proteome Including Protein Associations with Higher Order Assemblies. PLoS One 2011;6:e26554. https://doi.org/10.1371/journal.pone.0026554.

[167] Schäfer AI, Fane AG, Waite TD. Cost factors and chemical pretreatment effects in the membrane filtration of waters containing natural organic matter. Water Res 2001;35:1509–17. https://doi.org/10.1016/S0043-1354(00)00418-8.

[168] Bargeman G. Creating saturated sodium chloride solutions through osmotically assisted reverse osmosis. Sep Purif Technol 2022;293:121113. https://doi.org/10.1016/j.seppur.2022.121113.

[169] Overstappen NL. Energy prices in the Netherlands 2025. https://www.overstappen.nl/energie/compare-energy/energy-prices-netherlands/ (accessed October 11, 2025).

[170] Satyannarayana KVV, Sandhya Rani SL, Baranidharan S, Kumar RV. Indigenous bentonite based tubular ceramic microfiltration membrane: Elaboration,

characterization, and evaluation of environmental impacts using life cycle techniques. Ceram Int 2022;48:28843–55. https://doi.org/10.1016/j.ceramint.2022.03.156.

[171] Minella M, Bianco A, Valter P, Editors M. Water Reuse and Unconventional Water Resources A Multidisciplinary Perspective. Lecture Notes in Chemistry, vol. 113, Cham, Switzerland: Springer Nature Switzerland AG; n.d.

[172] Jonkers WA, Cornelissen ER, de Vos WM. Hollow fiber nanofiltration: From lab-scale research to full-scale applications. J Memb Sci 2023;669:121234. https://doi.org/10.1016/j.memsci.2022.121234.

[173] Tonova K, Lazarova M, Dencheva-Zarkova M, Paniovska S, Tsibranska I, Stanoev V, et al. Separation of glucose, other reducing sugars and phenolics from natural extract by nanofiltration: Effect of pressure and cross-flow velocity. Chemical Engineering Research and Design 2020;162:107–16. https://doi.org/10.1016/j.cherd.2020.07.030.

[174] Roy Y, Warsinger DM, Lienhard JH. Effect of temperature on ion transport in nanofiltration membranes: Diffusion, convection and electromigration. Desalination 2017;420:241–57. https://doi.org/10.1016/j.desal.2017.07.020.

Appendix A. Additional Water Quality Results

Appendix Table A.1 Complete Chemical Water Quality of all Samples

Ion	Unit	Sample 1	Sample 2	Sample 3	Sample 4	Sample 5	Sample 6
Fluoride	[mg/L]	0	0	0	0	0	4
Chloride	[mg/L]	49	75	87	29	27	34
Nitrite	[mg/L]	1	0	0	2	1	4
Bromide	[mg/L]	5	4	5	5	5	5
Nitrate	[mg/L]	1	1	1	1	1	4
Phosphate	[mg/L]	0	1	1	0	0	5
Sulfate	[mg/L]	226	238	138	149	147	10
Sodium	[mg/L]	529	762	722	525	525	462
Ammonium	[mg/L]	3	29	4	0	0	19
Potassium	[mg/L]	25	42	43	56	56	35
Magnesium	[mg/L]	19	29	32	61	61	20
Calcium	[mg/L]	65	118	130	88	89	134
TOC	[mg/L]	39	30	49	35	33	38
Alkalinity	[meq/L]	69	61	65	77	80	25
% Alkalinity from hardness	[% meq/L]	7%	14%	14%	12%	12%	33%

Error! Reference source not found. provides the water quality average from each sample within a week of collection. There was little to no chemical variability between settled and unsettled samples, so these values are an average of everything.

Sample Images:

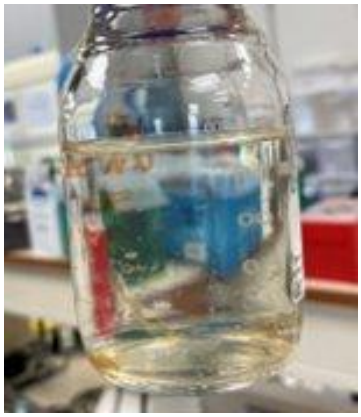

Appendix Figure A.1 Sample 1

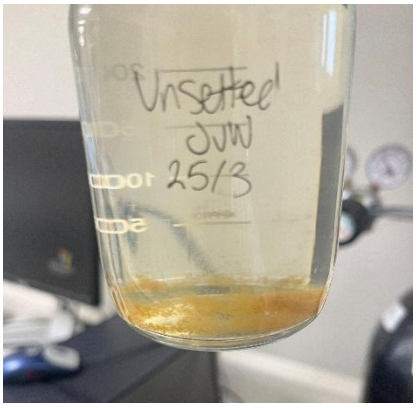

Appendix Figure A.2 Sample 2

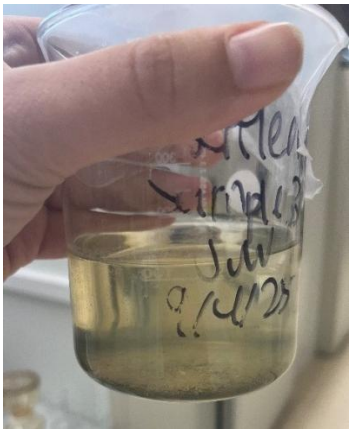

Appendix Figure A.3 Sample 3

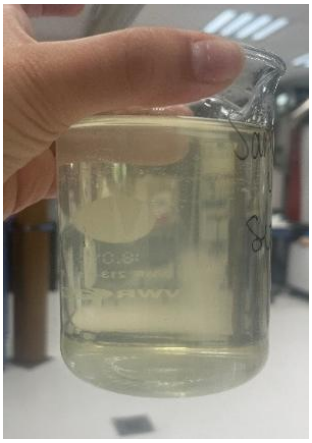

Appendix Figure A.4 Sample 4

Appendix Figure A.5 Sample 5

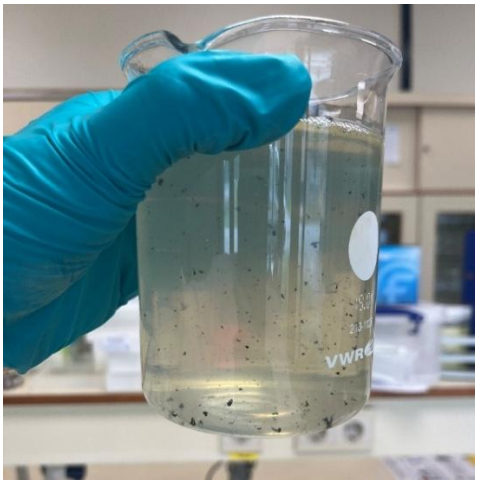

Appendix Figure A.6 Sample 6

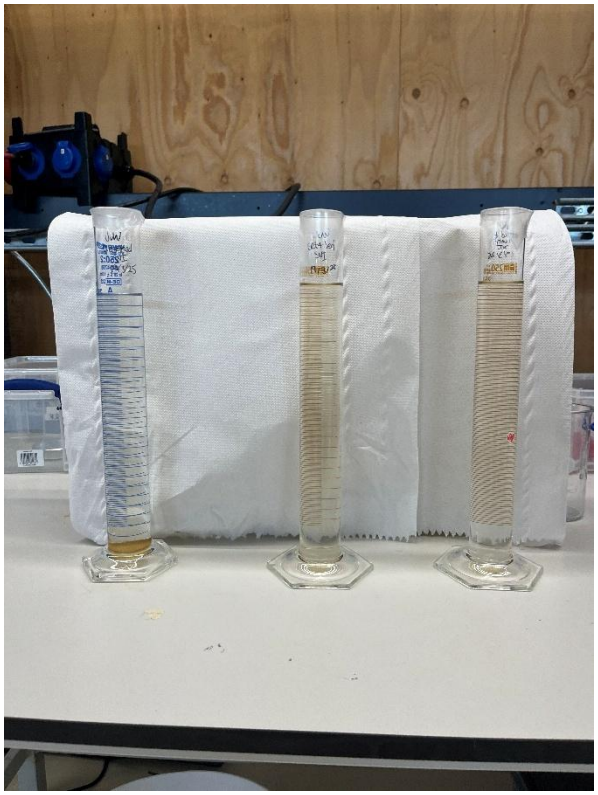

Appendix Figure A.7 Initial SVI Testing of Sample 1

The first sample was measured using an SVI test, the sample was allowed to settle, measurements were taken after 30 minutes and a week, showing no change between the measurements and still having inconclusive results. The first graduated cylinder is the unsettled Sample1, While the second and third graduated cylinders are settled Sample 1.

Appendix B. Further Results From Experiments

Ceramic Membrane Permeate:

Appendix Figure B.1 Ceramic Membrane Permeate alongside Concentrate

Polymeric Membrane Permeate:

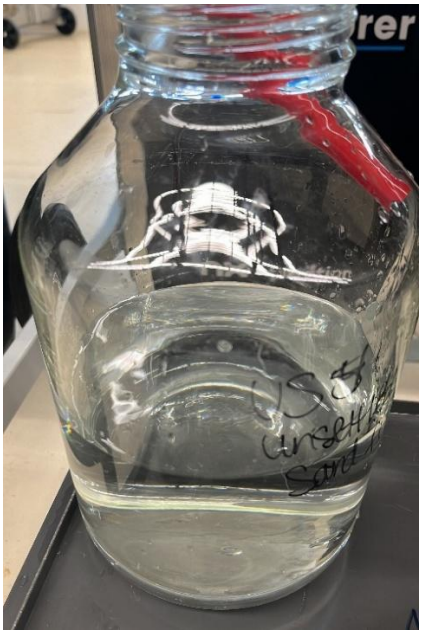

Appendix Figure B.2 Polymeric Membrane Permeate

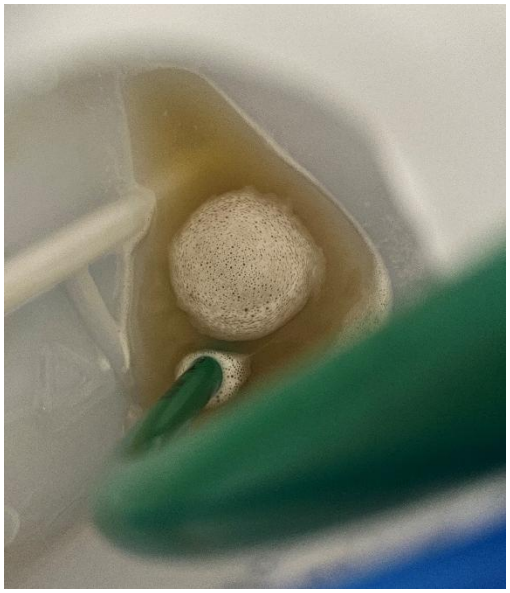

Appendix Figure B.3 The Remaining Feed from Polymeric Fouling Test 1

Precipitation Experiment Figures:

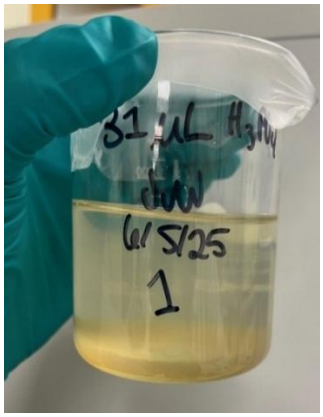

Appendix Figure B.4 Precipitation 2.1 Front

Appendix Figure B.5 Precipitation 2.1 Bottom

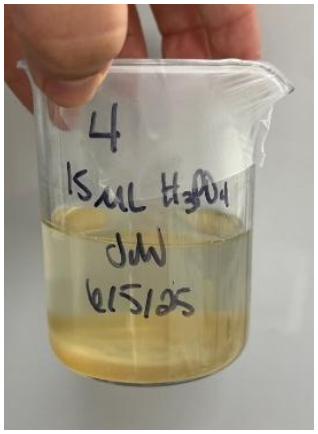

Appendix Figure B.6 Precipitation 2.4 Front

Appendix Figure B.7 Precipitation 2.4 Bottom

Appendix Figure B.8 Precipitation 2.6 Front

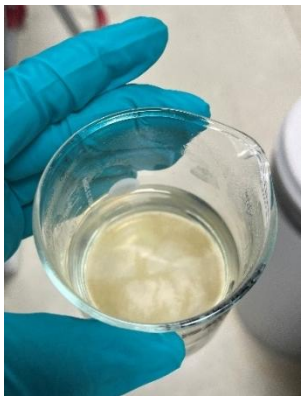

Appendix Figure B.9 Precipitation 2.6 Top

Appendix C. Wastewater Source Background

MNR Equalization Tank:

Appendix Figure C.1 MNR Equalization Tank When Fully Functional

Appendix Figure C.2 MNR Equalization Tank During Overflow 1

Appendix Figure C.3 MNR Equalization Tank During Overflow 2

Appendix Figure C.4 Rotary Drum Iron Scaling

Appendix D. Experimental Setups

Experimental Setups:

Appendix Figure D.1 Ceramic Membrane Experimental Setup

Appendix Figure D.2 Polymeric Membrane Experimental Setup

Polymeric Membrane Cleaning Procedure:

The recommended manufacturer cleaning procedure for the polymeric membrane is seen in **Error! Reference source not found.** from the membrane's manual [134]. Similar to the c eramic membrane, the chemical cleaning agent will be determined from the results of the water quality measurements.

Appendix Table D.1 Polymeric Membrane Cleaning Procedure [134]

Chemical	Type of fouling	Cleaning solution	Recommended concentration
Oxidizing agent	Biofouling Protein	NaOCl H_2O_2	100-250 ppm at pH >10
Acid	Inorganic salts Polymers	HCl HNO_3	pH 1
Complex formers Equilibrium shift	Inorganic salts Humic substances	EDTA Citric acid	0.5 wt%
Reducer	Ferric/ Manganese	Citric Acid Oxalic acid Ascorbic acid	0.5 wt%
Caustic	Biofouling Silica scaling	NaOH	pH 13

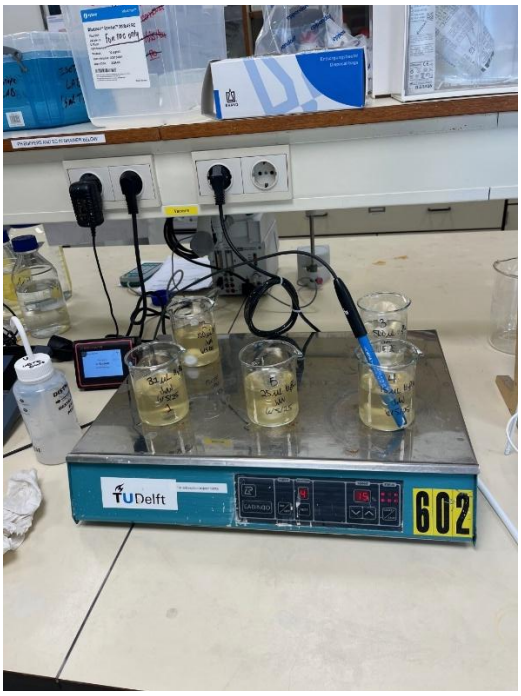

Appendix Figure D.3 Precipitation Experimental Setup

Appendix Figure D.4 Sand Filtration Experimental Setup

Appendix E. Differential Equation Model Predicting Concentrate Concentration Under Varying Conditions

The model was created to estimate the final concentrations of chemical water quality parameters in the concentrate based on whether the concentrate is recirculated or not at the different pressures using the measured removal rates. Equation E.1 is the equation for a no recirculation mass balance to determine the final concentration [18,20]. While equation E.2, is a mass balance for unsteady state systems, due to the removal of the permeate volume in the influent.

$$\mathrm{C}_c = C_f \frac{1 - rS_i}{1 - r} \qquad (E.1)$$

$$\frac{dC}{dt} = -\frac{Q_p}{V}(1 - S_i)C \qquad (E.2)$$

- C_f is the feed concentration [mg/L]
- C_c is the concentrate concentration [mg/L]
- C is the initial concentration
- r is the recovery rations of $\frac{Q_p}{Qf}$
- $S_i$sieving coefficient $\frac{C_p}{Cf}$
- Q_p is the permeate volumetric flow [L/s]
- $V\ is\ the\ volume\ of\ the\ mixed\ tank\ [L]$
- $t\ is\ time\ [s]$

	No recirculation / Dead-end Treatment					
Ceramic	100% of Capacity Treated		75% of Capacity Treated		50% of Capacity Treated	
Ion	2 bar	4 bar	2 bar	4 bar	2 bar	4 bar
Flouride (mg/L)	0.174407319	0.11205	0.185645664	0.175863702	0.184380804	0.177827745
Chloride (mg/L)	23.69627385	25.09529266	27.95801956	27.89857419	28.25737057	65.1660685
Nitrite (mg/L)	0.64525045	0.534375465	1.596523185	1.521586699	1.649276496	1.64766027
Bromide (mg/L)	4.433838158	4.466269813	5.193638245	5.15141727	5.239928263	6.25085844
Nitrate (mg/L)	9.839258413	9.958855053	11.57057243	11.48102536	11.67772522	17.40012135
Phosphate (mg/L)	0.490014549	0.442785059	0.569490314	0.557696656	0.572864139	0.559991882
Sulfate (mg/L)	80.69322638	39.415064	145.2524845	135.2478123	148.0384413	464.9364995
Sodium (mg/L)	204.905805	204.905805	496.7239864	478.6928065	515.2346778	6289.675576
Ammonia (mg/L)	0.02471	0.023937107	0.082564889	0.078877452	0.086210243	0.083615338
Potassium (mg/L)	18.66437205	10.34603564	24.06710085	22.52101021	24.41120081	36.96751746
Magnesium (mg/L)	13.08158551	13.71372908	18.20358657	17.97922733	18.52822985	31.50366826
Calcium (mg/L)	53.3830981	45.17055888	56.12615365	54.75982	56.13522908	190.4264395
TOC (mg/L)	3.912386623	2.22159933	4.54257458	4.257231355	4.536542633	4.907147291
Alkalinity (meq/L)	16.33609672	16.33609672	73.21526821	69.70075596	76.82324351	143.8311506

Appendix Figure E.1 Ceramic Membrane Model Final Concentrations with no Recirculation

	Recirculation Concentrate + Bypass Concentration					
Ceramic	100% of Capacity Treated		75% of Capacity Treated		50% of Capacity Treated	
Ion	2 bar	4 bar	2 bar	4 bar	2 bar	4 bar
Flouride (mg/L)	0.186050761	0.182596656	0.186447278	0.183617576	0.186548076	0.184649976
Chloride (mg/L)	28.11311509	28.19141615	28.26228106	28.23753466	28.3003512	28.28380431
Nitrite (mg/L)	1.632607861	1.62674504	1.664718367	1.642110668	1.673061112	1.65776934
Bromide (mg/L)	5.22127191	5.223083986	5.247879859	5.23431507	5.254668961	5.245594557
Nitrate (mg/L)	11.63356121	11.64024236	11.69417382	11.66519526	11.70964152	11.69025537
Phosphate (mg/L)	0.572378824	0.569750834	0.575163659	0.571619555	0.575874014	0.573500575
Sulfate (mg/L)	147.6689469	145.4748056	149.8743609	146.9583824	150.4440105	148.4725305
Sodium (mg/L)	507.7856105	507.7856105	517.6424149	512.0774281	520.2025336	516.4424132
Ammonia (mg/L)	0.084778914	0.084738372	0.08671619	0.085589816	0.087221501	0.086458543
Potassium (mg/L)	24.26515002	23.81341211	24.45309173	24.00482908	24.50120441	24.19934827
Magnesium (mg/L)	18.39239446	18.42720854	18.5697205	18.49634439	18.61522291	18.56600096
Calcium (mg/L)	56.22490721	55.76452632	56.32178866	55.92099152	56.34640424	56.07833722
TOC (mg/L)	4.565476527	4.472870029	4.587559923	4.505066892	4.593192749	4.537730639
Alkalinity (meq/L)	75.40545289	75.40545289	77.29919935	76.22742566	77.79453555	77.06751608

Appendix Figure E.2 Ceramic Membrane Model Final Concentrations With Recirculation

Polymeric						
Ion	2 bar	4 bar	2 bar	4 bar	2 bar	4 bar
Flouride (mg/L)	0.042134617	0.030531838	0.073849811	0.069339557	0.088241335	0.064378613
Chloride (mg/L)	115.5865755	118.105069	117.1773448	117.771668	117.8731464	4243.892025
Nitrite (mg/L)	0.3485	0.3485	0.455819729	0.4825382	0.521053879	0.412821338
Bromide (mg/L)	3.412623143	3.514868361	3.4283022	3.45985928	3.437290866	6.016679834
Nitrate (mg/L)	1.378881183	1.455191133	1.422214021	1.513674093	1.480199806	1.641474732
Phosphate (mg/L)	1.205318118	0.986690229	2.32849884	2.104621736	2.775138035	2.910090858
Sulfate (mg/L)	3.35172983	2.121068042	19.36290428	13.27760566	23.90253694	37.12952663
Sodium (mg/L)	416.7118928	397.384218	446.3479135	423.6947802	451.2222092	55132.39877
Ammonia (mg/L)	19.28145196	18.50746904	20.6908532	73.79368362	49.82666845	133.4680286
Potassium (mg/L)	32.42626002	30.61378759	35.115555	33.03896427	35.55545497	359.5396363
Magnesium (mg/L)	15.41454656	12.90068226	19.64873747	17.40013272	20.83551891	99.63713484
Calcium (mg/L)	63.59362831	53.97157707	78.98537915	64.09791906	79.78766732	1464.726587
TOC (mg/L)	76.23056929	83.13183327	50.95607337	63.08156151	44.3928676	959.7114712
Alkalinity (meq/L)	16.17800001	16.17800001	22.19624828	20.21740604	23.99804646	140.3515539

Appendix Figure E.3 Polymeric Model Final Concentrations with no Recirculation

Polymeric						
Ion	2 bar	4 bar	2 bar	4 bar	2 bar	4 bar
Flouride (mg/L)	0.082802129	0.076904136	0.084622988	0.079924658	0.08652573	0.083192152
Chloride (mg/L)	117.5910869	117.8312278	117.697401	117.8777407	117.8039076	117.9242903
Nitrite (mg/L)	0.485167892	0.490727416	0.491723917	0.495995269	0.498459551	0.501377448
Bromide (mg/L)	3.432370086	3.45433909	3.433422346	3.449882888	3.434475251	3.445438168
Nitrate (mg/L)	1.4335356	1.499086411	1.436409313	1.48521515	1.439294571	1.471598241
Phosphate (mg/L)	2.647855697	2.410169786	2.711388775	2.520491477	2.778045651	2.641397238
Sulfate (mg/L)	24.08920477	19.91774805	24.92466126	21.44013952	25.82015002	23.21451585
Sodium (mg/L)	454.1623757	434.6503583	456.0967452	441.1796359	458.047663	447.9080696
Ammonia (mg/L)	21.06264392	-25.1067121	21.15456841	-54.9165655	21.24729879	293.1603186
Potassium (mg/L)	35.82644643	34.06172334	36.00121176	34.64830882	36.17769051	35.2554518
Magnesium (mg/L)	20.80224673	18.9394522	21.0627651	19.59891698	21.32989146	20.30596317
Calcium (mg/L)	83.16154046	72.56427254	84.11574823	75.72629204	85.09210762	79.17643956
TOC (mg/L)	45.90770916	77.39228489	43.50713531	61.20513409	41.34514394	50.61801388
Alkalinity (meq/L)	23.85279115	21.98379107	24.21590418	22.7436282	24.59024352	23.55787108

Appendix Figure E.4 Polymeric Model Final Concentrations with Recirculation